AWARD NUMBER: W81XWH-15-1-0574

TITLE: Long-Term Followup of the Delayed Effects of Acute Radiation Exposure in Primates

PRINCIPAL INVESTIGATOR: J. Mark Cline, DVM, PhD

CONTRACTING ORGANIZATION: Wake Forest University Health Sciences
Winston-Salem, NC 27157-0001

REPORT DATE: OCT 2018

TYPE OF REPORT: Annual

PREPARED FOR: U.S. Army Medical Research and Materiel Command
Fort Detrick, Maryland 21702-5012

DISTRIBUTION STATEMENT: Approved for Public Release;
Distribution Unlimited

The views, opinions and/or findings contained in this report are those of the author(s) and should not be construed as an official Department of the Army position, policy or decision unless so designated by other documentation.

REPORT DOCUMENTATION PAGE

Form Approved
OMB No. 0704-0188

Public reporting burden for this collection of information is estimated to average 1 hour per response, including the time for reviewing instructions, searching existing data sources, gathering and maintaining the data needed, and completing and reviewing this collection of information. Send comments regarding this burden estimate or any other aspect of this collection of information, including suggestions for reducing this burden to Department of Defense, Washington Headquarters Services, Directorate for Information Operations and Reports (0704-0188), 1215 Jefferson Davis Highway, Suite 1204, Arlington, VA 22202-4302. Respondents should be aware that notwithstanding any other provision of law, no person shall be subject to any penalty for failing to comply with a collection of information if it does not display a currently valid OMB control number. **PLEASE DO NOT RETURN YOUR FORM TO THE ABOVE ADDRESS.**

1. REPORT DATE *(DD-MM-YYYY)*	**2. REPORT TYPE**	**3. DATES COVERED** *(From -To)*
OCT 2018	Annual	30SEP2017 - 29SEP2018

4. TITLE AND SUBTITLE
Long-Term Followup of the Delayed Effects of Acute Radiation Exposure in Primates

5a. CONTRACT NUMBER
PR141508

5b. GRANT NUMBER
W81XWH-15-1-0574

5c. PROGRAM ELEMENT NUMBER

6. AUTHOR(S)
J Mark Cline, DVM, PhD, DACVP
Professor of Pathology/Comparative Medicine,
Radiation Oncology and Translational Sciences

EMAIL: jmcline@wakehealth.edu

5d. PROJECT NUMBER

5e. TASK NUMBER

5f. WORK UNIT NUMBER

7. PERFORMING ORGANIZATION NAME(S) AND ADDRESS(ES)
Wake Forest School of Medicine
Medical Center Boulevard
Winston-Salem, NC 27157

8. PERFORMING ORGANIZATION REPORT NUMBER

9. SPONSORING / MONITORING AGENCY NAME(S) AND ADDRESS(ES)
U.S. Army Medical Research and
Materiel Command
Fort Detrick, Maryland 21702-5012

10. SPONSOR/MONITOR'S ACRONYM(S)

11. SPONSOR/MONITOR'S REPORT NUMBER(S)

12. DISTRIBUTION / AVAILABILITY STATEMENT
Approved for Public Release; Distribution Unlimited

13. SUPPLEMENTARY NOTES

14. ABSTRACT This program studies the mechanisms and consequences of delayed effects of acute radiation exposure (DEARE) in non-human primates (NHP), with complementary mechanistic and therapeutic studies in mice. The program consists of 4 projects, focused on: 1. Type 2 diabetes mellitus (T2DM); 2. Radiation-induced heart disease (RIHD); 3. Chronic immune impairment; and 4. Genomics and transcriptomics. Major findings include peripheral microvascular and bioenergetic abnormalities in NHP with T2DM; restrictive myocardial fibrosis in RIHD; dose and age-dependent immuen impairment; and ongoing sequencing work which will inform us regarding the molecular pathogenesis of T2DM, RIHD, and immune impairment in the context of DEARE.

15. SUBJECT TERMS Radiation; delayed effects; late effects; heart; immune system; type 2 diabetes mellitus; genomics; transcriptomics; *Mus musculus*; *Macaca mulatta*.

16. SECURITY CLASSIFICATION OF:			**17. LIMITATION OF ABSTRACT**	**18. NUMBER OF PAGES**	**19a. NAME OF RESPONSIBLE PERSON**
a. REPORT	**b. ABSTRACT**	**c. THIS PAGE**			**19b. TELEPHONE NUMBER** *(include area code)*
U	U	U	UU	105	USAMRMC

Standard Form 298 (Rev. 8-98)
Prescribed by ANSI Std. Z39.18

TABLE OF CONTENTS

1. INTRODUCTION: Narrative that briefly (one paragraph) describes the subject, purpose and scope of the research.

The **subject** of this research is the phenomenon of Delayed Effects of Acute Radiation Exposure (DEARE). The **purpose** and overarching goal of this program is to explore our recent clinically relevant observations of DEARE in a unique cohort of non-human primates (NHP), termed the Radiation Survivor Cohort (RSC), and a smaller more controlled group of NHP exposed to radiation prospectively, termed the Prospective Radiation Cohort (PRC), with complementary studies in mouse models to explore growth factor therapeutics and genomic consequences. The **scope** of this work consists of 4 projects making use of these unique NHP resources: 1. Studies of type 2 diabetes mellitus (T2DM); 2. Radiation-induced heart disease (RIHD); 3. Chronic immune impairment with restriction of the antigenic response repertoire; and 4. Genomic and transcriptomic studies which will inform us regarding the molecular pathogenesis of T2DM, RIHD, and immune impairment in the context of DEARE. Work during the first three years of this program has proceeded as planned, with slight logistical modifications but no major changes or delays.

2. KEYWORDS: Provide a brief list of keywords (limit to 20 words).

Radiation; delayed effects; late effects; heart; immune system; type 2 diabetes mellitus; genomics; transcriptomics; *Mus musculus*; *Macaca mulatta*.

3. ACCOMPLISHMENTS:

What were the major goals of the project?

Major goals are listed below by project, including relevant dates and percentage completion as indicated.

Core Primate Studies (Cline)

SA1: Provide NHP Investigative Platform

Major Task 1:	Regulatory Approval (months 1-6)
Milestone:	Local Institutional Animal Care and Use Committee (IACUC) and DOD Animal Care and Use Review Office (ACURO) approvals in place (100%)
Major Task 2:	Access to Long Term Radiation Survivor Cohort (months 1-6)
Milestone:	Scheduling and meetings in progress (75%)
	Sample collections have begun, in support of all projects (planned for months 6-60; 60% complete)
Major Task 3:	Acquisition of Prospective Cohort (months 1-6)
Milestone:	Animals arrived at Wake Forest 2/9/16 (100% completed).
Major Task 4:	Irradiation and Study of Prospective Cohort
Milestone:	Irradiations planned for quarter 4 (100% completed)

SA2: Promote Synergy and Productivity

Major Task 5:	Data management/tracking, group interactions (months 1-6)
Milestones:	Data management (100% completed for years 1 and 2)
	Establish monthly web meetings (100% complete)
	Annual strategic retreat to be scheduled (100% complete for year 1)
	Publications (months 6-60; 40% complete in the context of 5 year plan, cardiac, metabolic and genomic papers submitted and accepted; abstracts presented at the annual Radiation Research Society Meeting and other meetings)

SA3: Facilitate Translation and Therapeutic/Preventive approaches

Major Task 6:	Strategize towards clinical implementation and future funding
Milestones:	Promote new grant submissions (months 36-60; 30% complete)
	Progress update at end of year 2 (100% complete)

Project 1: Diabetes (Kavanagh)

SA1: Document the time course of IR-mediated reduced insulin sensitivity

Major Task 1: PRC - Prospective Cohort
Milestones: Create a longitudinal clinical profile of diabetes mellitus (DM) risk with irradiation (15% achieved in context of 5 year plan)
Local IACUC approval (100% achieved)
ACURO Approval (100% Achieved)

Major Task 2: RSC - Radiation Survivor Cohort
Milestones: Generate comparable clinical data in monkeys with DM as DEARE to compare with the earlier prospectively irradiated monkeys (90% achieved in context of 5-year plan)

SA2: Examine IR-related increases in oxidation of tissue proteins over time

Major Task 3: Redox Proteomics of prospective and long-term irradiated tissue
Milestones: Compare and contrast early and late changes in redox proteomics following irradiation in mice and monkeys. Verify the role of Akt protein in DM. Identify individual or protein clusters with long-term modifications following irradiation. (65% achieved in context of 5-year plan)

SA3: Track extracellular matrix (ECM) remodeling, including fibrosis, in muscle and adipose depots after irradiation

Major Task 4: ECM characterization and magnetic resonance imaging (MRI).
Milestones: Characterize tissue changes in both prospective and long-term IR monkeys and relate these to in vivo insulin sensitivity assessments. Validate the utility of MR imaging to detect qualitative tissue changes (40% achieved in context of 5-year plan)

SA4: Evaluate therapeutic agents that reduce fibrosis and restore fat expansion to mitigate metabolic changes with IR.

Major Task 5: Mouse intervention study
Milestones: Prevent metabolic disease development in IR mice with interventions. Demonstrate reductions in protein modifications and/or tissue remodeling with treatment (60% achieved in context of 5-year plan).

Project 2 – Radiation-Induced Heart Disease (Register)

We proposed 3 inter-related Specific Aims across the 5 Year Grant Period.

SA 1: Determine the Effects of Total Body Irradiation on NHP Cardiac Structure and Function.

Major Task 1: Novel cardiac MRI approaches will be used to evaluate myocardial tissue fibrosis, a key component of RIHD, in order to follow changes in myocardial phenotypes in animals across time. Additional structural and functional cardiac phenotypes to be assessed by echocardiography/MRI include left ventricular (LV) mass, posterior and interventricular wall thickness, right ventricular thickness, and aortic wall thickness. Functional parameters will include systolic and diastolic function, ejection fraction, aortic stiffness/pulse wave velocity, wall motion, and electrocardiography. Grid tag mapping will be also used to assess strain and LV volume.
Scheduled Dates: Months 6-48
Milestones: Percent completion: 55% in the context of 5 year plan
Detailed cardiac ultrasound (US) evaluations have been conducted and images acquired on the RSC (year 01, year 02, GE instrument) at baseline, 20 weeks (March 2017), 1 year (October 2017) and will be obtained at the 2 year timepoint in coming weeks (October 2018) post exposure in the PRC. Echocardiographic image analysis was conducted using the scanner for images collected in the PRC at Baseline. New US image analysis software (TOMTEC) was installed and Drs. Register, Michalson, and staff were trained in its use. The PRC 20 week and 1 year cardiac US images were evaluated using this analysis package. Data from baseline which was collected and measured on the GE instrument were validated for reproducibility by repeat reads using the TOMTEC software. M Mode measurements were assessed on the GE US instrument with plans to move analyses to the TOMTEC. Cardiac MRI image analysis is underway and extensive MR phenotype data has been collected in the PRC. Tissue collections from subjects going to necropsy continue.

SA 2: Identify Novel Molecular Biomarkers of Cardiovascular Injury and RIHD

Major Task 2: Identify and evaluate emerging serum markers of cardiac damage implicated in cardiomyocyte death (microRNAs such as miR133a) and extracellular matrix remodeling (type I and III collagen propeptides and degradation products). Circulating miRNA levels and serum extracellular matrix turnover biomarkers will be evaluated in relation to structural and functional phenotypes and histologic and biomolecular features of myocardial tissues and differentially expressed myocardial mRNA and miRNA which will be identified through expression profiling of heart tissues obtained at necropsy.
Scheduled Dates: Months 6-48
Milestones: Percent completion: 20%
RSC: blood samples obtained and processed; PRC: baseline and immediate post-radiation blood samples were collected, processed, and archived for future biochemical analyses. Ongoing blood collections are underway.

SA 3: Determine the Efficacy of Candidate Mitigating Agents on RIHD.

Major Task 3: Assessment of Mitigating Agents. We propose to retrospectively and prospectively assess cardiac and coronary artery injury in NHP in studies of mitigating agents, using animals in the de novo cohort, the long-term cohort, and from prospective studies of growth factors (e.g. HGH), superoxide dismutase mimetics, and novel therapeutics (e.g.

platelet analogs). We will use the pathologic and biomarker approaches noted above, including in vivo assessments. These results will be critical to our understanding of RIHD. The preliminary data suggests that the changes in the heart based on the radiation dose are significantly greater that would have been predicted from prior murine studies.
Scheduled Dates: Months 6-48
Milestones: Percent completion: 40% complete in the context of a 5 year plan plan (assessed effects of a mitigating agent (superoxide dismutase analogue, hexyl MnSOD) on myocardial gene expression, (manuscript in development), performed histologic staining of coronary arteries in available hearts and completed assessments of atherosclerotic lesion size, collected cardiac tissues from a Project 1 mouse study and cardiac tissue from rhesus monkeys, planning for ECM and other biomarkers in the radiation survivor cohort; other evaluations are under way). Myocardium from the RSC has been phenotyped for atherosclerosis and is being organized for preparation for RNAseq.

Goals for the 3rd annual reporting period related to completing 24 month cardiac echo and MRI imaging, ongoing collection and blood processing of samples in the RSC and PRC, continuing analysis of data from the cardiac ultrasound and MRI images from the PRC, and ongoing analysis of tissues in hand from studies in the RSC including immunohistochemical analyses of myocardial cellular subtypes. Two manuscripts are in development.

Project 3 – Immune Recovery (Duke Consortium – Chen & Sempowski)

SA 1: Define the roles of thymopoiesis and peripheral expansion in overall T cell reconstitution after radiation-induced injury based on radiation dose.

Major Task 1: NHP Studies (5% complete in context of 5 year plan, first analysis in progress)
Milestones:

1.1. Phenotypic analyses in long-term cohort (60 months, 60% complete)
1.2. sjTREC in long-term cohort (60 months, 60% complete)
1.3. Phenotypic analyses in prospective cohort (60 months, 60% complete)
1.4. sjTREC in prospective cohort (60 months, 60% complete)
1.5. Determine primary immune response to influenza vaccine (36 months, 5% complete)
1.6. Determine primary and recall immune response to influenza vaccines (60 months, 0% complete)

Major Task 2: Murine Studies
Milestones:

2.1. Local IACUC Approval (3 months, 100% complete)
2.2. Determine the roles of thymopoiesis and peripheral expansion in overall T cell recovery in the classic radiation injury model (18 months, 100% complete)
2.3. Determine the roles of thymopoiesis and peripheral expansion in overall T cell recovery in the second radiation injury model (7-24 months, 30% complete)

SA 2: Determine if therapeutic agents identified in our previous studies are able to promote or accelerate overall T cell immunity after radiation injury.

Major Task 3: HGH Mouse Studies
Milestones:

3.1. Determine the effect of HGH on phenotypic T cell reconstitution (25-36 months, 0% complete)
3.2. Determine the effect of HGH on functional T cell recovery (37-48 months, 0% complete)
3.3. Determine the mechanism by which HGH promote T cell reconstitution (49-60 months, 0% complete)

Major Task 4: IGF-1 Mouse Studies
Milestones:

4.1. Determine the effect of IGF-1 on phenotypic T cell reconstitution (25-36 months, 0% complete)
4.2. Determine the effect of IGF-1 on functional T cell recovery (37-48 months, 0% complete)
4.3. Determine the mechanism by which IGF-1 promote T cell reconstitution (49-60 months, 0% complete)

Project 4 - Genomic Sequencing and Stem Cell Lines (Duke Consortium – Dave)

Aim1: Define the genetic mutations and gene expression signatures induced by DEARE

Major Task 1: Exome Sequencing
Milestones:
DNA Sample extraction (months 1-36) - 100% complete
Exome analyisis (months 13-60) - 40% complete
Major Task 2: Transcriptome Sequencing
RNAseq (months 6-48) - 40% complete
RANseq analysis (months 12-60) - 40% complete

Aim 2: Determine the molecular basis of lymphoid immunodeficiency induced by DEARE.

Major Task 1: Generate iPSCs
Milestones: iPSC from controls complete 30% complete
Milestones: iPSC from genetic variants 10% complete

Major Task 2: Differentiate iPSCs into lymphoid lineages
Milestone(s) Achieved: B cell characterization 30% complete
Milestone(s) Achieved: T cell characterization 30% complete

What was accomplished under these goals?

Core Primate Studies (Cline)

1) Major activities:

Protocol approvals for all animal studies; establishment of subcontracts and accounts; development of a meeting schedule; review of goals and plans with all investigators; hiring/allocation of effort for personnel; acquisition of NHP subjects for the prospective cohort; pre-irradiation physical examinations, imaging, and blood sampling for all projects; total body irradiation.
Characteristics of our animal populations are briefly described below.

2) Specific objectives:

As per SOW. Regulatory approvals, establishment of meeting schedule, hiring, planning, animal acquisition, irradiation.

3) Results/key outcomes:

- All animal protocol approvals complete at local and ACURO level
- Subcontracts and accounts established
- Goals and plans reviewed with all investigators
- Monthly web conferences established and continuing
- Hiring/effort allocations made as planned
- Secure server folders established for data exchange
- NHP subjects acquired for PRC, irradiations completed and studies in progress
- Sampling and data acquisition on schedule

4) Other achievements:

Data presented at local and national meetings each year.

A brief overview and synopsis of major findings is presented below.

The Radiation Survivor Cohort (RSC)

The population of the RSC is shown graphically in Figure 1 (see next page). Briefly, this cohort consists of rhesus macaques (*Macaca mulatta*) irradiated as juveniles or adults, in the range of 3-8.5 Gy via single total body exposure, at a dose delivery of 60-80 cGy/min. The cohort is supported by the National Institute of Allergy and Infectious Disease (NIAID), which is leveraged by this DOD Focused Program award. Animals were acquired between 2007 and 2018 through an “adoption” strategy from multiple sites. The RSC currently consists of 105 irradiated animals and 30 controls. The population has a 4:1 male:female ratio. Animals are housed socially whenever possible, primarily in pens, and fed a custom-formulated “Typical American Diet”. All animals receive daily environmental enrichment and are part of a behavioral management program. Approximately one-third of the animals were given mitigating agents (e.g. antibiotics or growth factors) during the acute period of hematopoietic injury. This cohort is studied using a multidisciplinary approach to long-term morbidity/mortality. Notably, some animals are now 14 years out from irradiation (1/2 of their lifespan), providing a unique long-term view of DEARE.

Animals in the RSC undergo a regular schedule of medical care and assessment, including but not limited to:

Daily
- Twice-daily clinical observations
- Environmental enrichment

Monthly
- Physical exam
- Blood collection for experimental measures and archive
- Urine collection for experimental measures and archive
- Body weight

Semiannually
- Complete blood counts
- Clinical chemistry panels
- Testing for diabetes mellitus (hemoglobin A1c, glucose, with glucose tolerance testing and mimimal model testing on a subset)
- Anthropometrics (trunk length, waist diameter)

Annually
- Flow cytometry (blood, see Project 3)
- Bone marrow aspirate
- Echocardiography
- Computed tomography scan (whole body)
- Renal ultrasound
- Gastrointestinal endoscopy and biopsy
- Bronchoalveolar lavage
- Cranial MRI (subset, 3 year rotation)
- Ocular exam

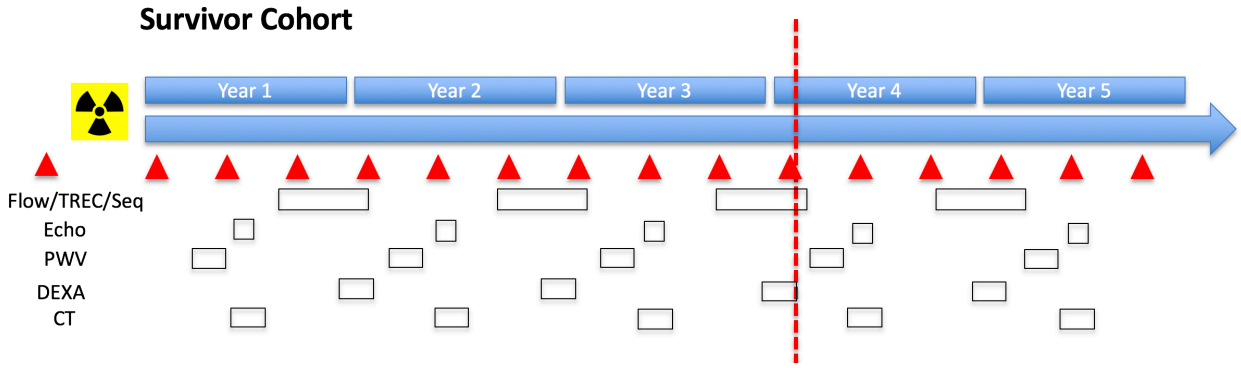

Figure 1: Diagram representing the annual schedule of clinical assessments in the RSC. The vertical red line indicates the current date. Red triangles indicate blood collection dates. Abbreviations: Flow = flow cytometric measurement of lymphocyte subets; TREC = T cell receptor excision circles; Seq = DNA and RNA sequencing collections from peripheral blood; Echo = echocardiography; PWV pulse wave velocity; DEXA = dual energy x-ray absorptiometry; CT = computed tomography.

All animals are given routine veterinary care, and we have established clinical criteria for identification and management of animals with health abnormalities. Major patterns of morbidity in the RSC are summarized in Table 1, below.

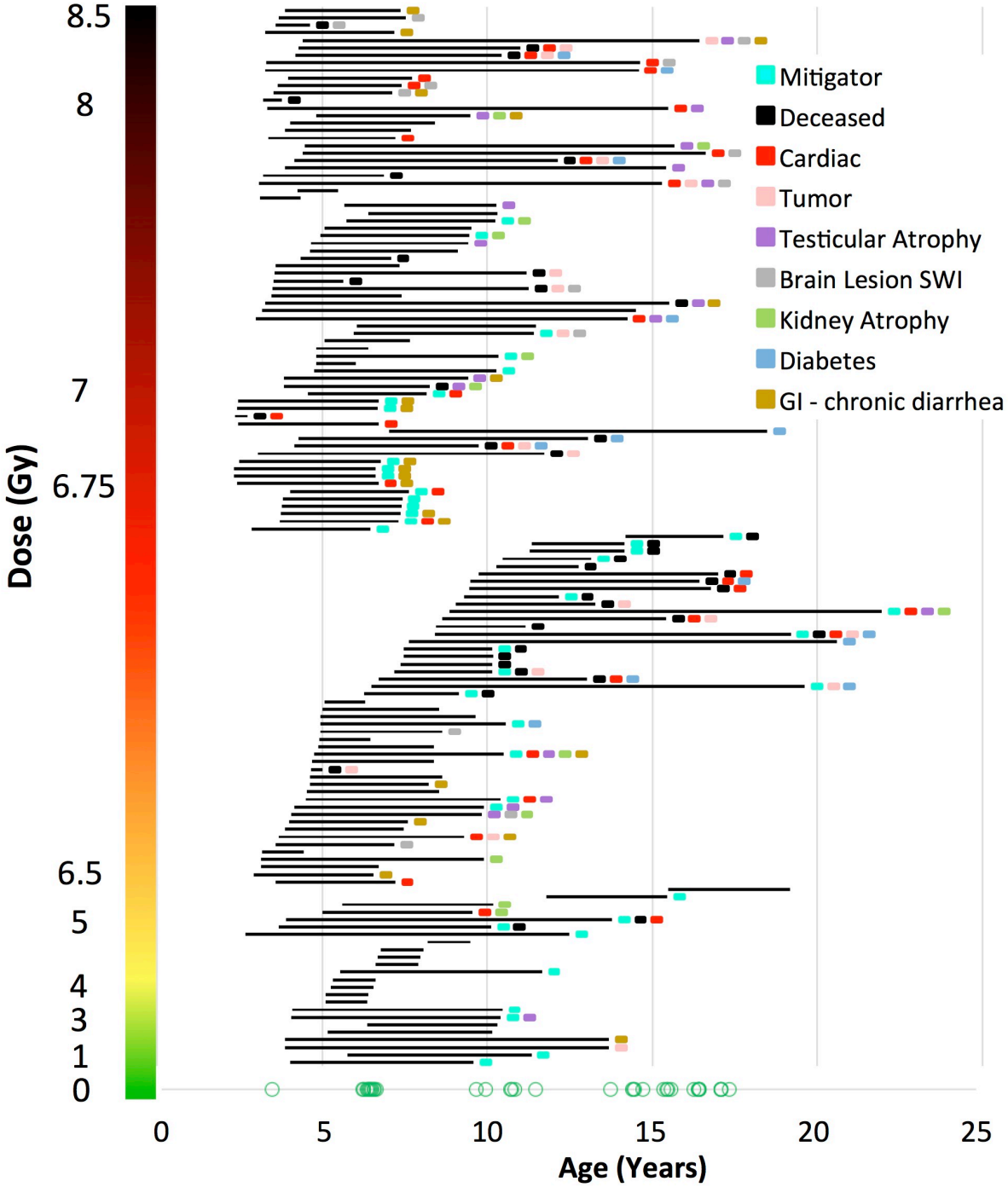

Figure 2: Age and dose distribution of the Radiation Survivor Cohort *(updated 10/18) Each horizontal bar represents a single animal; the left end of the bar is the age at which the animal was irradiated, and the right end of the bar is the animal's current age or age at time of death. Green circles represent the current age of non-irradiated controls. For rhesus monkeys, the typical age a puberty is 3.5 years; typical lifespan is 30 years.*

During the past year as part of the publication planning process we have characterized the radiation doses given to the RSC animals based on typical lethal dose for the acute hematopoietic syndrome. This classification scheme was based on a recent review of 15 studies encompassing over 1000 animals by MacVittie et al., (Health Phys 2015 109:342, PMID 26425897), and is represented below (Figure 3).

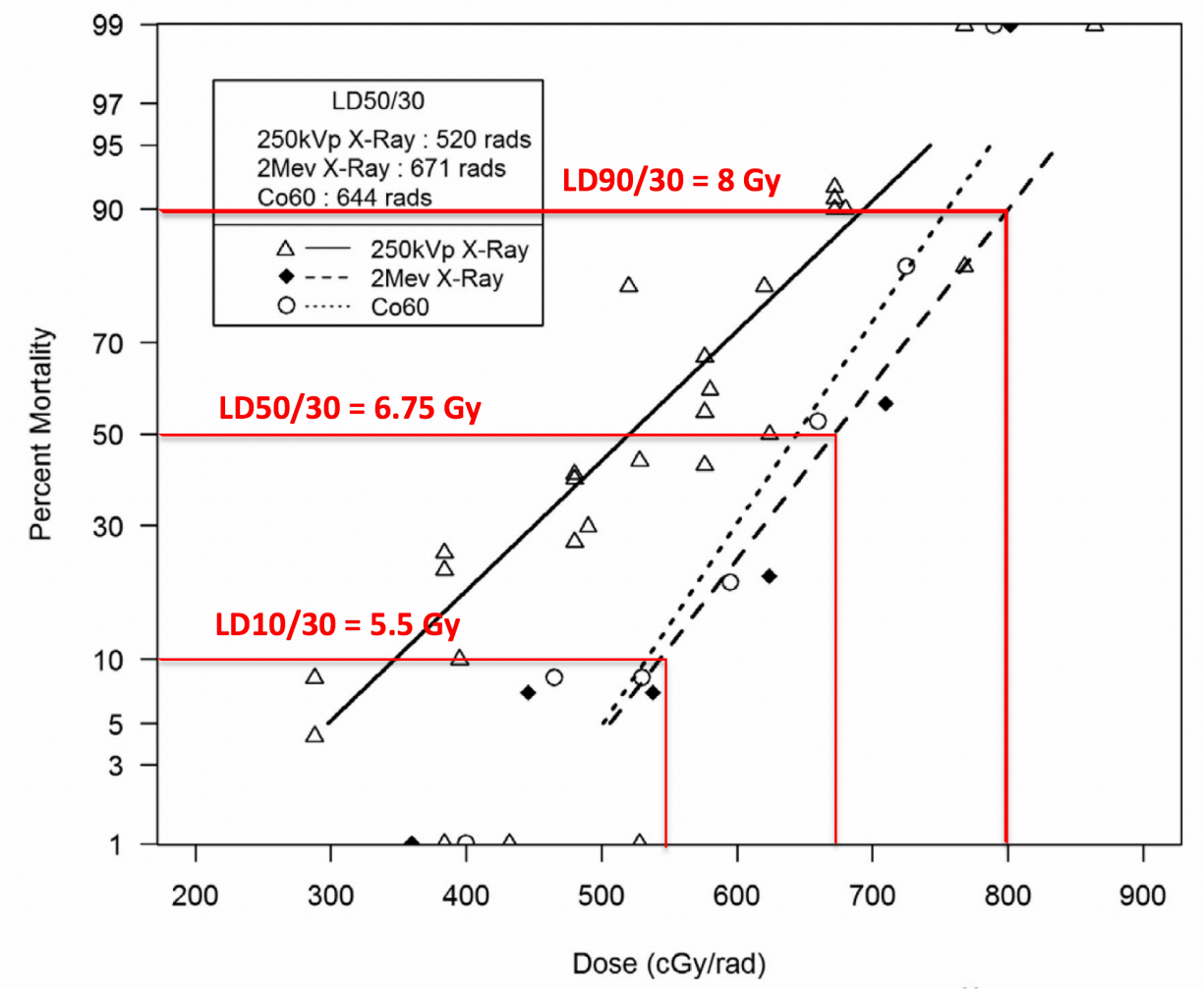

Figure 3: Four dose classes defined by historical LD10, LD 50, and LD90 doses. Modified from MacVittie et al., 2015.

Mortality

Four animals died in the RSC during the 2017-2018 reporting period including 3 irradiated animals and one control. Causes of mortality included cardiovascular disease (3 animals including the control), and chronic gastroenteritis. Overall mortality in the RSC has not differed from that of controls; these data do not differ substantially from those presented previously (data not shown).

Morbidity

Patterns of radiation associated morbidity are shown below in Table 1.

Table 1: Threshold-based determinations of morbidity in the long-term Radiation Survivor Cohort (updated 10/23/18).

Organ/Disease	Irradiated	Control	Criteria for Diagnosis
Diabetes	13.5% (19/141)	0% (0/38)	Hemoglobin A1c (HbA1c) >6.5% Three fasting blood glucose > 100 mg/dL Any non fasted blood glucose > 200 mg/dL
Kidney	22% (31/141)	7.9% (3/38)	BUN > 30 mg/dl or Cr > 1.1 mg/dl Loss of renal volume >50% Urolithiasis
Lung	6.3% (9/141)	5.2% (2/38)	Pulmonary consolidation on CT scan Bullous emphysema >25% of lung volume Hypoxia under sedation (SPO2 < 80% or requiring oxygenation) Respiratory rate >80 breaths per minute
GI	19% (26/134)	6% (2/35)	Any lesion on endoscopy Chronic diarrhea (severity code >2 for >5 days)
Skin	13.5% (19/141)	2.6% (1/38)	Persistent dermatitis, alopecia or loss of pigmentation
Heart/CV	29.1% (41/141)	13.1% (5/38)	Murmur detected on ausculation Valvular insufficiency on echocardiograph Mean arterial pressure >120 Stroke volume <5 mls/stroke & Cardiac output <0.5 L/min at >7 y
Brain (any lesion)	12% (17/141)	0% (0/38)	Y/N MRI lesions visible on SWI Neurologic abnormality on clinical exam
Eyes (cataracts)	12.8% (18/141)	0% (0/38)	Any lens opacity on annual slit-lamp exam
Behavior	33.3% (47/141)	31.6% (12/38)	Any behavioral abnormality requiring management (customized enrichment plan or medication)
Neoplasia	16% (23/141)	0% (0/38)	Any neoplastic disease (imaging or biopsy)
Testicular atrophy	21.5% (26/121)	5% (1/20)	Testis volume <10 ml each after 7 years of age; Vol = (p/6)(LxW^2)
Bone	10.6% (15/141)	0% (0/38)	Adult bone mineral content (BMC) < 274g Bone mineral density (BMD) < 0.373 g/cm^3 Gross abnormality on exam or CT scan
Obese **Underweight**	12% (17/141) 22% (31/141)	31.6% (12/38) 10.5% (4/38)	Obesity: Waist Circumference > 45 cm or Dexa Body Fat > 30% Underweight: Waist Circumference < 25 cm or Dexa Body Fat < 12.3% (Excluding animals under 7 yrs old)

Abbreviations: BUN = blood urea nitrogen; Cr = serum creatinine; CT = computed tomography; DEXA = dual emission x-ray absorptiometry; HbA1c = hemoglobin A1c; MRI = magnetic resonance imaging; NSD = no significan difference; SP02 = oxygen saturation.

During the past year we have undertaken a summary of diarrheal disease in the RSC, based on the prior 7 years of daily observation data. We view gastrointestinal disease as an important covariate to consider for disease outcomes in all projects. The results of this review are shown below. Our data show that brief/isolated bouts of diarrhea are seen in most control and irradiated animals, much as would be expected from any human or nonhuman primate population. However, those animals with chronic diarrhea occurring with a frequency of greater than 14% of the total time (conceptually “more than one day a week”), fell almost exclusively in the irradiated cohort, with a possible dose-dependent effect at >6.5 Gy and a weak statistically significant polynomial dose trend (Figure 4).

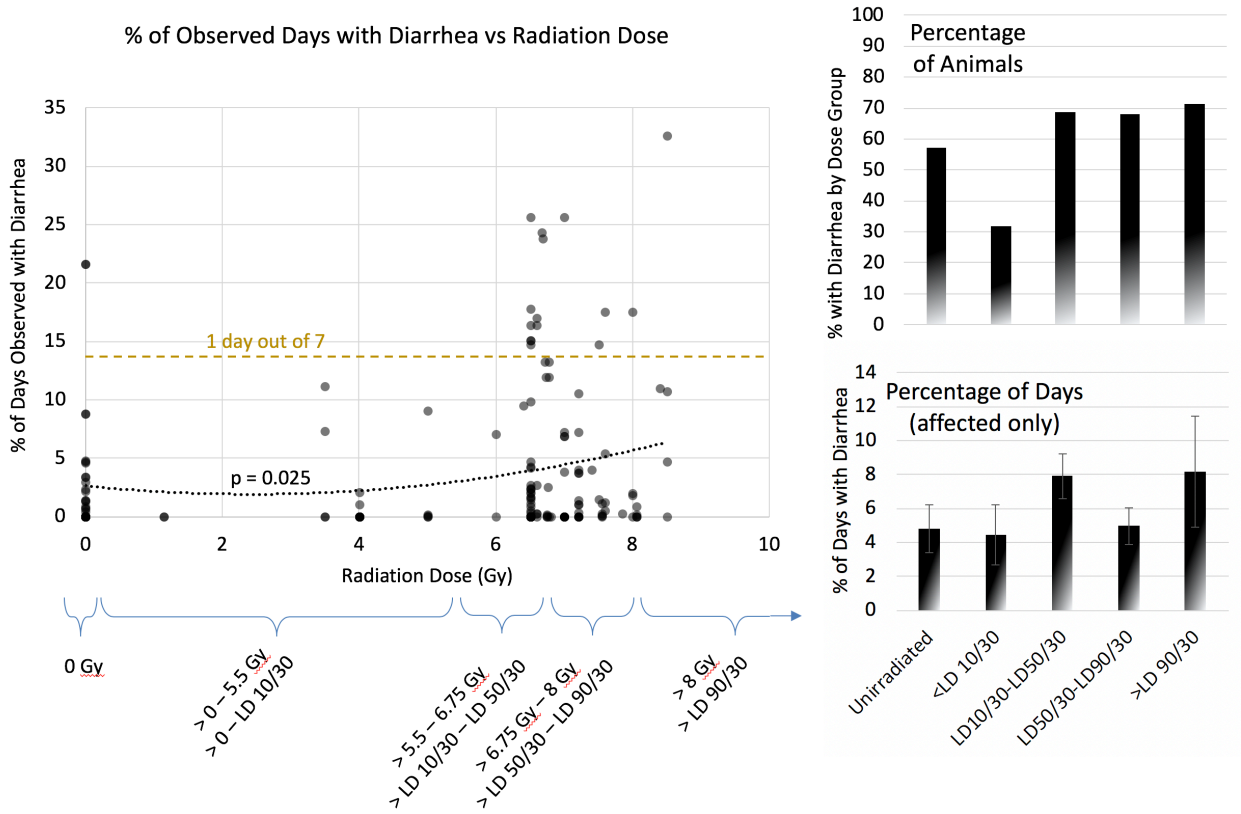

Figure 4: Diarrheal disease in the RSC. Over half of all animals had at least one episode of diarrheal disease in the past 7 years; the duration of diarrhea increased ad dose increased (p = 0.025)

The Prospective Radiation Cohort (PRC)

The study design for the PRC is shown below. These specific-pathogen-free animals were acquired and quarantined in year 1 and irradiated in October 2016. Imaging and sample collections are proceeding as per the program statement of work and the needs of the individual projects.

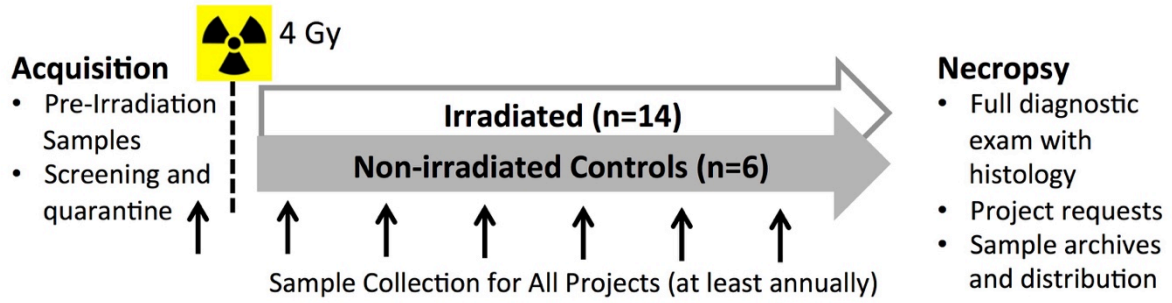

Figure 5: Study design for the Prospective Radiation Cohort (PRC).

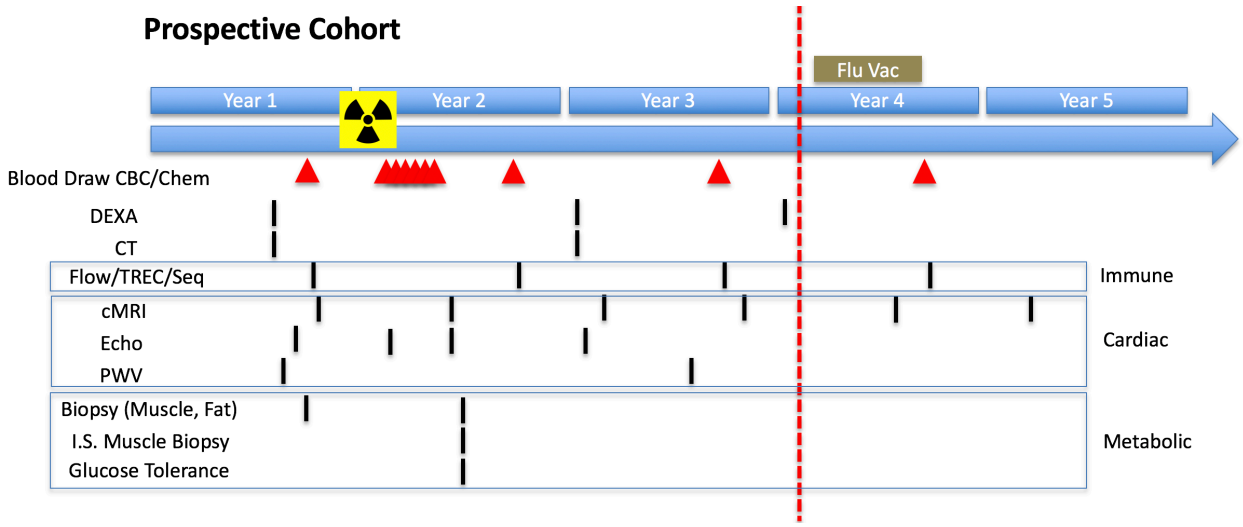

Figure 6: Diagram showing clinical assessments in the Prospective Cohort. The vertical red line indicates the current date. Red triangles indicate blood collection dates. Abbreviations: CBC = complete blood count; Chem = serum chemistry measurements; cMRI = cardiac magnetic resonance imaging; Echo = echocardiography; PWV = pulse wave velocity; I.S. = insulin stimulated.

Acute Effects in the Prospective Cohort

Irradiation exposures were done as planned, using a 6MV Varian Linear Accelerator and parallel opposed fields to maximize uniformity of dose delivery (total dose 4Gy).

As anticipated, total body irradiation (TBI) produced a rapid and profound hematopoietic injury resulting in lymphopenia, followed by neutropenia, thrombocytopenia and anemia. Eight irradiated animals required transfusions of irradiated blood. The pattern of acute hematopoietic injury is shown in figure 7.

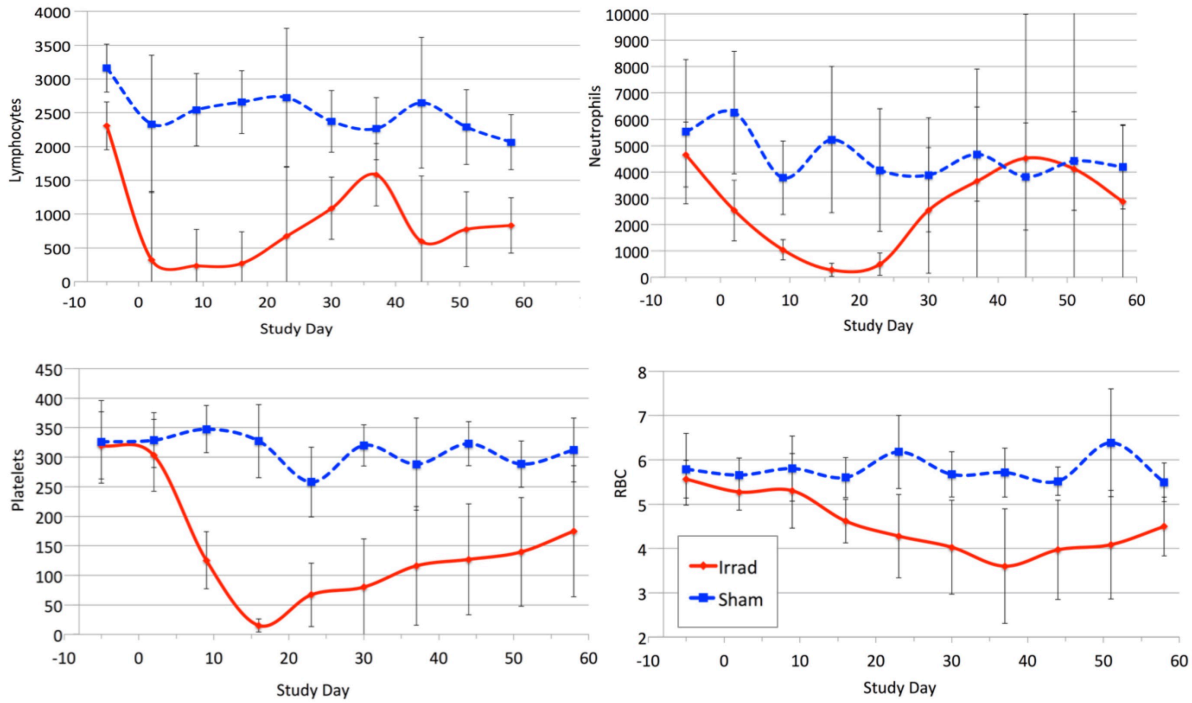

Figure 7: Longitudinal graphs of lymphocyte, neutrophil, platelet and red blood cell counts after 4 Gy TBI.

Three TBI exposed animals in the PRC reached pre-determined endpoints for experimental euthanasia (persistent thrombocytopenia or neutropenia, or evidence of infection such as fever unresponsive to antibiotic treatment). Two of these animals were diagnosed with *Spironucleus* infection, an unusual opportunistic protozoal pathogen of immunosuppressed primates, and one was diagnosed with a disseminated bacterial infection (*Klebsiella)*. All three animals were humanely euthanized and a complete post-mortem tissue collection was done, including terminal samples for Project outcomes. These findings were reported previously (Year 2 annual report)

Project 1. Diabetes (Kavanagh)

The overall goal of Project 1 is to identify pathways that track some radiation survivors on a path that results in dysregulated metabolism and increased risk for diabetes. Our studies (**Figures 1.1 and 1.2**) utilize a unique reverse translational flow whereby diabetes has been reported in survivors of radiation exposures, including our nonhuman primates, and we have designed studies to identify the time course, tissue targets, and interventional strategies that will combat diabetogenesis in at-risk individuals. In accordance with this continuum, this annual report is divided into sections that address major accomplishments within the sub-studies named the Radiation Survivor Cohort (RSC), the Prospective Radiation Cohort (PRC), and the Interventional Rodent Studies.

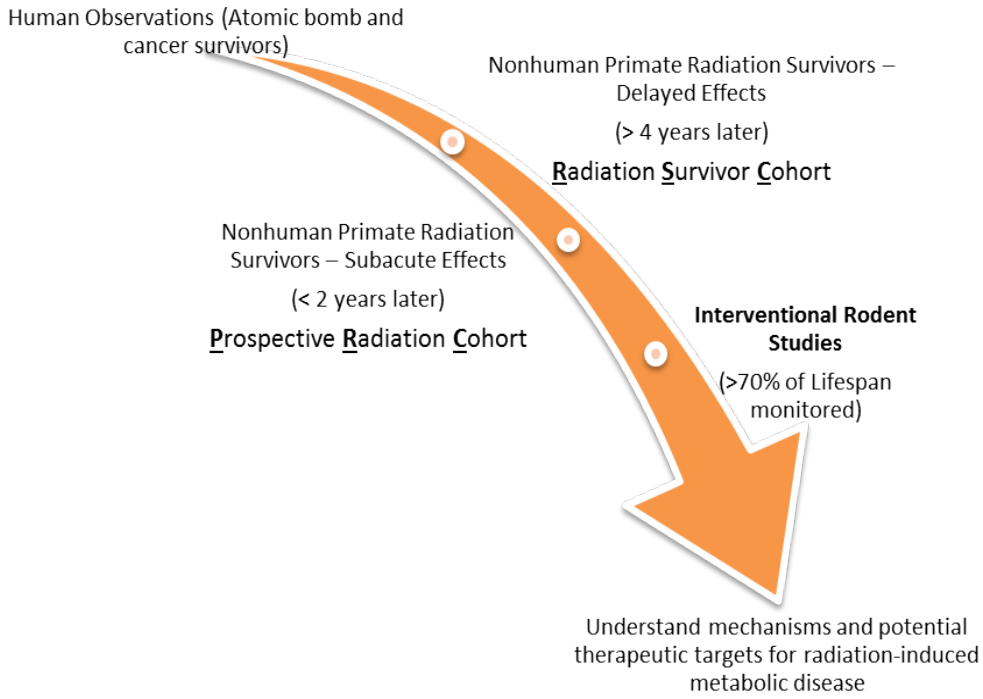

Figure 1.1: Studies reported on for Project 1.

A diagram of the monkey cohorts (RSC and PRC) and the assessment points are shown in **Figure 1.2**. We are halfway through the assessment period.

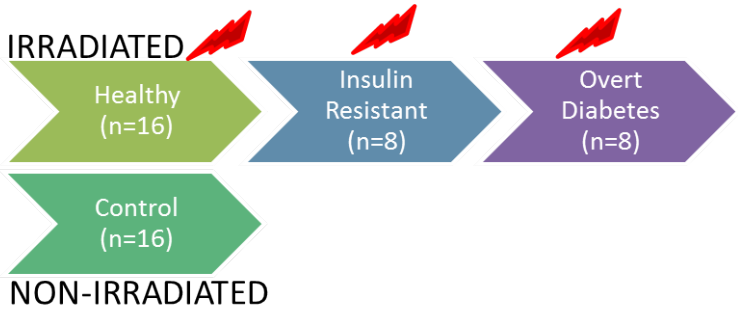

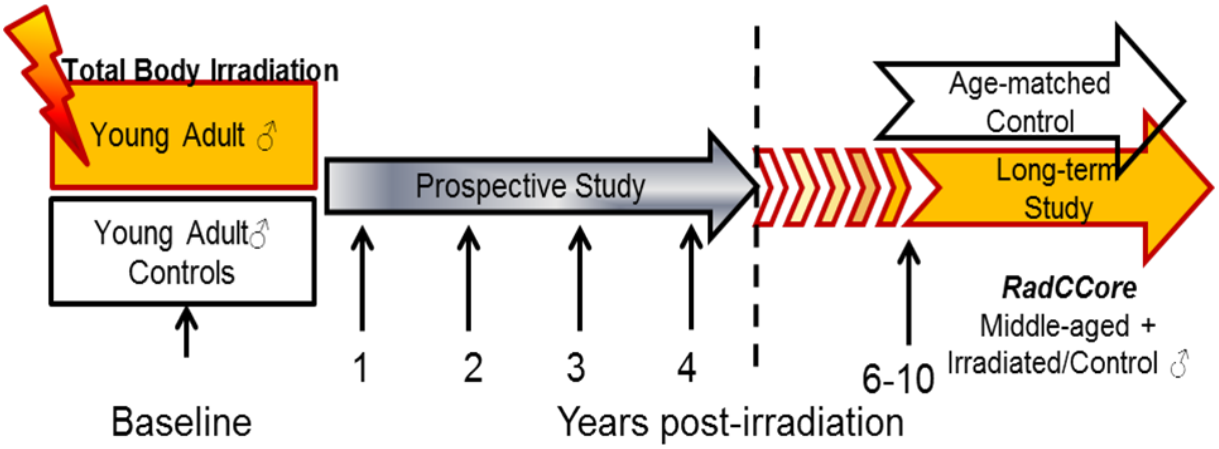

Figure 1.2. RSC monkey groups evaluated within Project 1 (top) and the overlap/continuum achieved with the PRC and RSC

1. **Radiation Survivor Cohort (RSC)**

Our prior published studies identified that skeletal muscle maintains an insulin resistant state years after radiation exposure, but animals exhibiting indicators of enhanced capillary perfusion were able to maintain normal overall glucose metabolism and prevent diabetes from developing. In the current year we have evaluated a new cohort of radiation survivors and age-matched control animals that have not been exposed for ongoing assessment. We have non-diabetic representatives so as to get information from animals that have not yet developed diabetes, or are intermediate in their metabolic response (**Figure 1.2**). The goal here was to discriminate changes seen with radiation from those that may have occurred secondarily to diabetes.

The demographics of the new animals (16 irradiated and 8 control) are shown in **Table 1.1**. Characteristics of the monkeys evaluated are shown in **Table 1.1**. As previously reported, irradiation reduces their size and waist circumference. Monkeys were also young and had lower systolic blood pressures. These typically 'healthy' phenotypes contrast with the significant reduction both at baseline and in response to insulin stimulation (**Figure 1.3**). This functional impairment of muscle was not related to structural changes as measured by histological assessment of major extracellular matrix proteins (**Table 1.2**). Fibrosis is a well-known consequence of radiation exposure and is observed in irradiated monkeys that have developed diabetes (1). Proteomics was performed to help determine cellular changes that could explain the observed insulin resistance in otherwise normal healthy monkeys that had prior radiation exposure.

Table 1.1. Summary demographics and study outcomes measured from RSC monkeys assessed in Project 1.

		CTL (n=8)	IRRAD (n=16)	p-value
Age	yrs	13.1 (0.90)	9.41 (0.72)	0.01
Age at Irradiation	yrs	N/A	4.56 (0.34)	-
Irradiation Dose	Gy	N/A	6.52 (0.33)	-
BW	kg	16.1 (1.90)	8.83 (0.61)	<0.001
Waist	cm	43.3 (9.66)	33.3 (1.52)	0.01
Systolic BP	mmHg	130 (4.94)	113 (4.65)	0.03
Diastolic BP	mmHg	72 (3.32)	67 (4.59)	0.45
Heart Rate	bpm	136 (9.20)	138 (5.00)	0.87
Fasting Glucose	mg/dL	65.2 (5.17)	81.2 (8.35)	0.20
Fasting Insulin	uIU/mL	39.4 (7.16)	39.8 (15.6)	0.99
HOMA	AU	6.57 (1.51)	8.69 (3.83)	0.75
AUC glucose	AU	7086 (598)	7317 (586)	0.80
AUC insulin	AU	3593 (712)	2914 (909)	0.22
A1c	%	4.55 (0.38)	4.68 (0.43)	0.93
Total Nitric Oxide	uM	19.9 (3.37)	26.0 (4.36)	0.35
Cyclic GMP	ng/mL	69.5 (29.5)	39.7 (6.75)	0.23

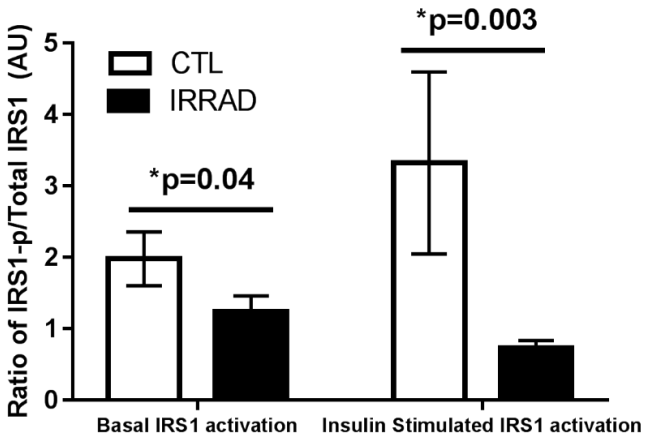

Figure 1.3. Prior irradiation exposure consistently reduces skeletal muscle's ability to respond to insulin administration. This deficiency is present in non-diabetic or otherwise 'healthy' survivors of radiation exposure.

Table 1.2. Non-diabetic irradiated monkeys do not have extracellular matrix changes apparent, suggesting that large changes in collagen 4 and loss of capillaries observed previously are the result of interaction of hyperglycemia and insulin resistance at the level of the myocyte.

		CTL (n=8)	IRRAD (n=16)	p-value
Trichrome staining	%	3.61 (0.66)	3.50 (0.42)	0.89
Collagen 1	%	12.4 (2.48)	17.2 (2.31)	0.20
Collagen 3	%	18.3 (4.06)	16.7 (3.32)	0.77
Collagen 4	%	25.2 (1.74)	26.9 (2.82)	0.67
Fibrinogen	%	14.6 (6.78)	12.4 (1.16)	0.40
Fiber area	um^2	9795 (1514)	8062 (649)	0.23
$CD31^{+ve}$ cells	$\#/mm^2$	0.013 (0.002)	0.015 (0.001)	0.14

In our proposal we aimed to do redox evaluations of skeletal muscle proteins. The rationale was that oxidative damage is a known pathway for radiation-related tissue damage and our collaborator has published that Akt was a specific target for this type of modification. Akt2 is a key step in insulin signaling, and is a required activation step for glucose transporters to be mobilized to the cell surface and glucose taken up from the circulation. We checked this lack of generalized oxidation with tissue staining for oxidative changes using the BP-1 ligand. Although we did not see overall differences in protein oxidation when evaluated as non-specific markers

(**Figures 1.4 and 1.5**), when a specific immunoprecipitation of our Akt2 protein was performed we do see a significant increase in sulfyl-modification in the irradiated monkey tissue (**Figure 1.6**). We are delighted to translate this in vitro finding published by our collaborator to corroborate with in vivo relevance.

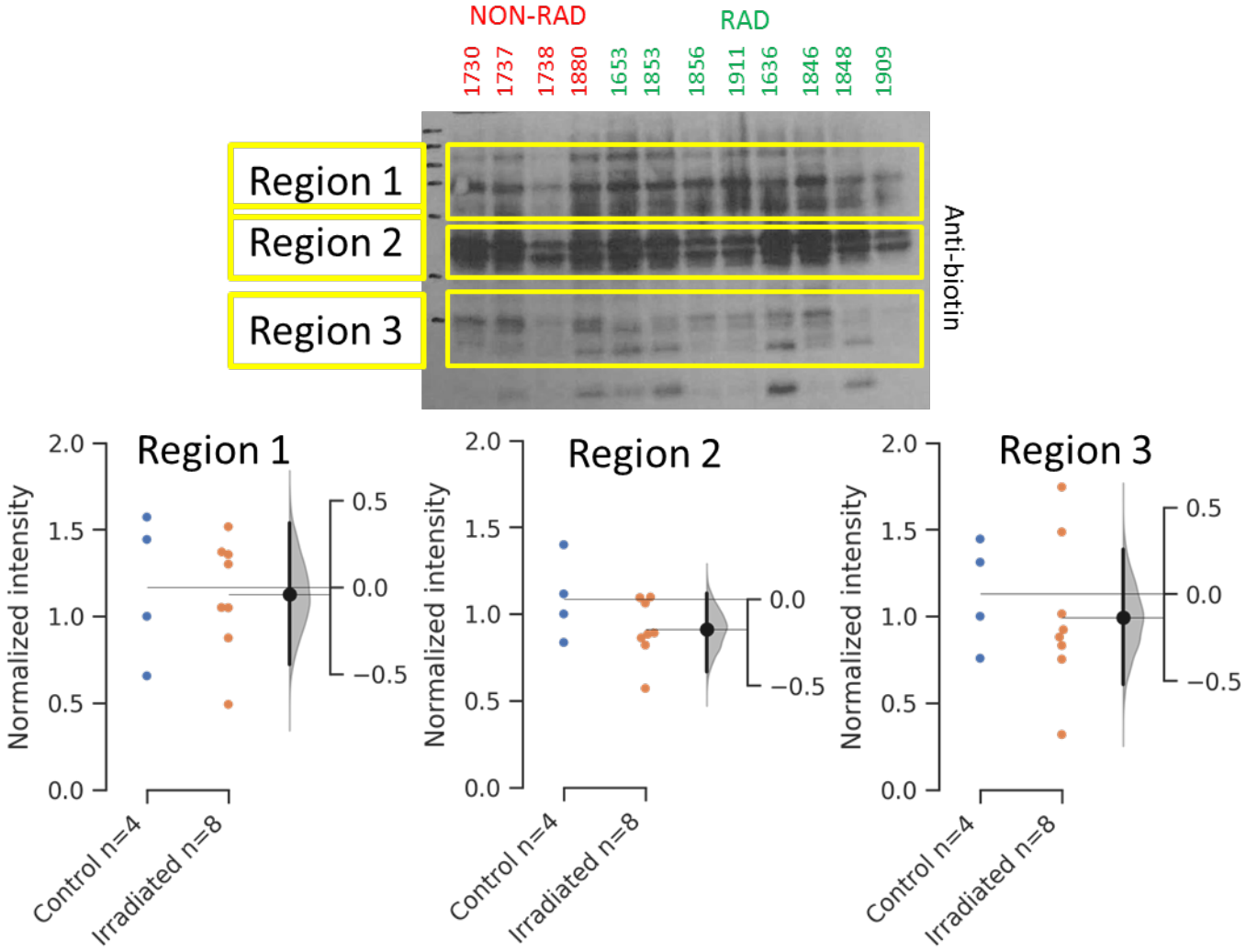

Figure 1.4. Generalized oxidation profile of proteins from the cytosol of skeletal muscle tissue of control (NON-RAD) versus irradiated (RAD) monkeys. No profile differences are observed across different groups of protein sizes.

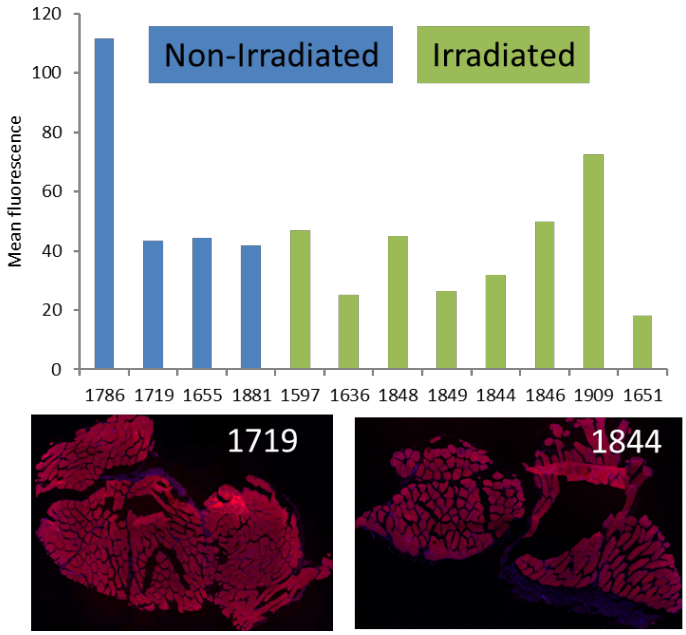

Figure 1.5. Immunohistochemistry of skeletal muscle stained with protein oxidation marker BP1 suggest that overall oxidation is not detectably different with prior radiation exposure.

Proteomics assessments have been completed in the RSC monkeys. This is aimed to provide more granular data about changes in myocellular function and identify pathways that differentiate why the tissues from irradiated individuals are less insulin responsive. Non-targeted proteomics were performed on tissues retrieved by muscle biopsies, and over 1300 proteins were annotated. In non-targeted proteomics, the results reflected the most abundant proteins in muscle, which are primarily reflecting muscle's contractile function

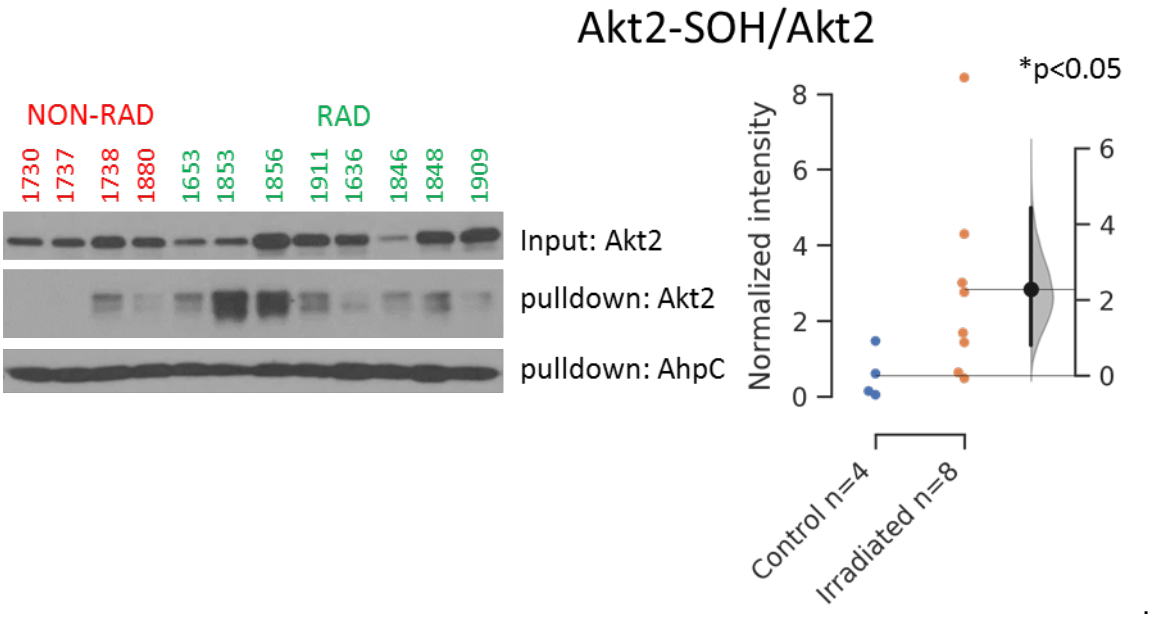

Figure 1.6. Specific oxidation of Akt2 is seen in skeletal muscle tissue of irradiated monkeys. The functional consequence of this modification is to reduce the ability to respond to insulin and remove glucose from the circulation. These data in concert with data presented in Figure 3 demonstrates that insulin action is reduced at 2 steps of the signaling pathway.

We see a lot of overlap in proteins between the groups but more proteins are upregulated in the irradiated group (**Figure 1.7**).

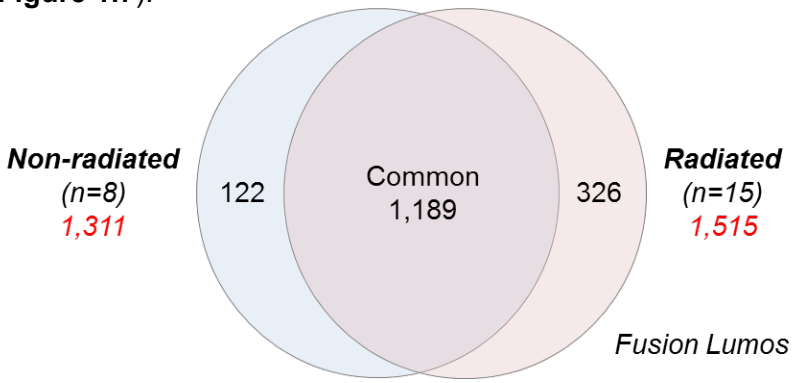

Figure 1.7. Venn diagram of proteome identity in the control and irradiated monkey skeletal muscle tissue.

Our first assessment was to evaluate for differences that were related to radiation exposure, not metabolic disease. Consistent with non-targeted proteomics we see that radiation exposure generally upregulated protein abundance. **Table 1.3** shows the top 30 upregulated proteins seen in irradiated tissues. Many are mitochondria related. We are checking Protein S100-A13 levels by immunoblotting as this shows a large difference that is highly significant.

Table 1.3. Proteomics results: Upregulated Proteins in Irradiated Muscle		*RAD/NON_RAD*	
Description	*Accession*	*Fold ratio*	*p-Value*
Glyoxylate reductase/hydroxypyruvate reductase	Q9UBQ7	11.200	0.00048
Mitochondrial carrier homolog 2	Q9Y6C9	9.067	0.05347
Protein S100-A13	Q99584	6.400	0.00082
Myosin light chain 5	Q02045	4.800	0.00472
Transmembrane emp24 domain-containing protein 2	Q15363	3.200	0.02743
Adenine phosphoribosyltransferase	P07741	3.200	0.07238
39S ribosomal protein L12, mitochondrial	P52815	3.200	0.01359
26S protease regulatory subunit 6A	P17980	2.933	0.05922
Peptidyl-prolyl cis-trans isomerase F, mitochondrial	P30405	2.933	0.09611
60S acidic ribosomal protein P0	P05388	2.667	0.04846
Dendritic cell-specific transmembrane protein	Q9H295	2.667	0.06050
Acylamino-acid-releasing enzyme	P13798	2.533	0.05030
60S ribosomal protein L38	P63173	2.533	0.06463
Isocitrate dehydrogenase [NAD] subunit alpha, mitochondrial	P50213	2.489	0.03605
LETM1 and EF-hand domain-containing protein 1, mitochondrial	O95202	2.400	0.09797
Succinate dehydrogenase [ubiquinone] cytochrome b small subunit, mitochondrial	O14521	2.347	0.03679
Microtubule-associated protein tau	P10636	2.333	0.06491
UTP--glucose-1-phosphate uridylyltransferase	Q16851	2.248	0.02557
Electron transfer flavoprotein-ubiquinone oxidoreductase, mitochondrial	Q16134	2.237	0.00434
Transaldolase	P37837	2.193	0.02646
Potassium-transporting ATPase alpha chain 1	P20648	2.133	0.08725
Heat shock protein HSP 90-alpha	P07900	2.116	0.02929
60S ribosomal protein L35	P42766	2.067	0.00285
Pyruvate dehydrogenase protein X component, mitochondrial	O00330	2.000	0.07838
CDGSH iron-sulfur domain-containing protein 2	Q8N5K1	1.956	0.05178
NADH dehydrogenase [ubiquinone] 1 beta subcomplex subunit 5, mitochondrial	O43674	1.813	0.02176
60S ribosomal protein L15	P61313	1.800	0.07784
Trifunctional enzyme subunit beta, mitochondrial	P55084	1.783	0.00809
NADH dehydrogenase [ubiquinone] iron-sulfur protein 6, mitochondrial	O75380	1.714	0.07699
Endothelial differentiation-related factor 1	O60869	1.707	0.01177

The proteins were subjected to pathway analysis and mitochondrial dysfunction is the largest pathway affected irradiation (**Figure 1.8**). We are doing sensitivity analysis on this pathway analysis by increasing the stringency of pathway inclusion and re-sampling with 8 controls and 8 irradiated monkeys to be sure the same pathways still become highlighted. We originally did a 1:2 control: case ratio as we know that variability is higher in irradiated animal's outcomes.

As mitochondrial function was the top hit on the pathway analyses, we did a survey of mitochondria-related proteins by immunoblotting. We saw no differences in abundance of these proteins, tabulated below (**Table 1.4**).

Table 1.4. Mitochondrial and redox significant proteins evaluated
VDAC
COX4
PRX-SO2/3
Periredoxin 3
Catalase
Superoxide dismutase 2
Pink-1
Fission related protein 1 (FIS1)
SIRT3* - results suggest Sirt3 may be reduced with irradiation

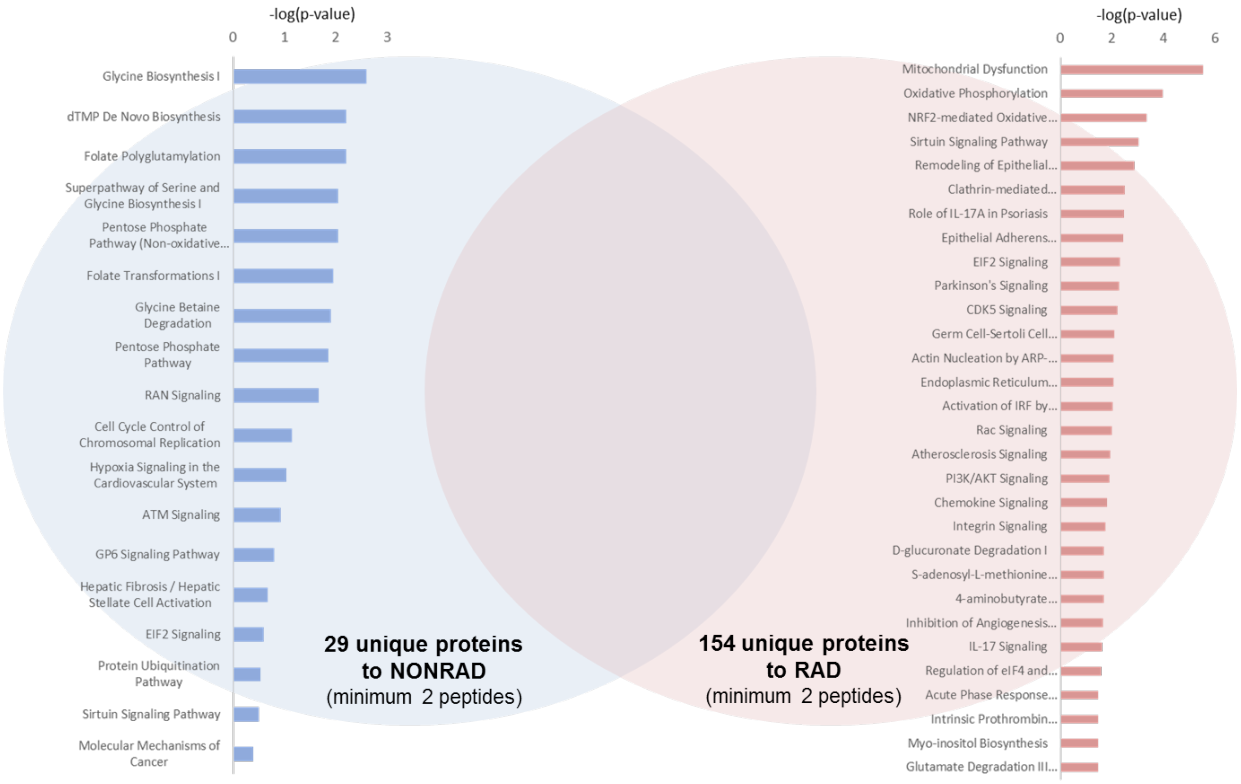

Figure 1.8. Top canonical pathways from unique proteins identified in non-irradiated or irradiated skeletal muscle

These data are in process of being written up for publication. We believe that characterization of the insulin resistance and proteomics profiling will lead to new targets for therapy.

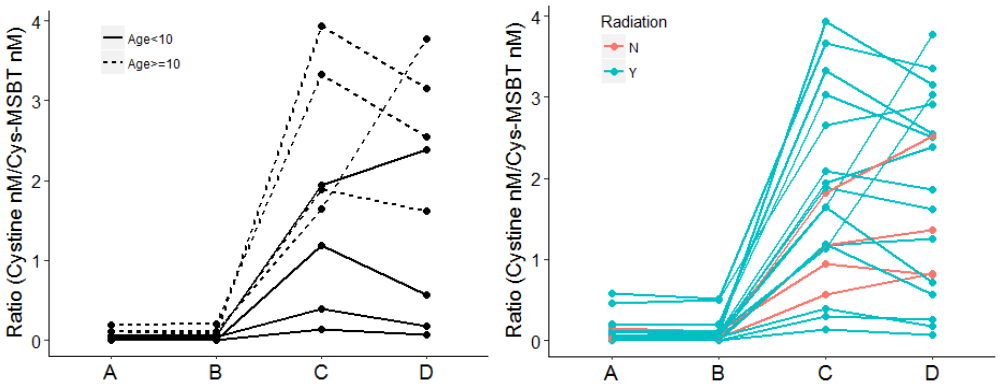

Figure 1.9. Comparisons of collection buffers for redox proteomic detections (left) and differences observed by the age of the individual (right).
A: EDTA anticoagulated blood only
B: EDTA + BHT and DTPA preservatives
C: EDTA + 10mM MSBT and 1mM BP1
D: EDTA + BHT, DTPA, MSBT and BP1

We have a number of related project outcomes that have also arisen from assessment of these survivor monkeys. We have initiated some methods development for how to best extract proteins for proteomics analysis. We compared 4 different conditions for biosample collections, prior to proteomics analysis. Addition of BP1 significantly protects protein oxidation status and thus improves detection ability. We also noted that aged animals (> 10 years) had greater levels of oxidation as compared to younger animals. We are continuing to work on this methodological study as a scholarly contribution to proteomics protocol development.

2. Prospective Radiation Cohort

Twenty monkeys were stratified into a radiation exposed (RAD) and control (CTL) based on bodyweight and cardiovascular risk factors. We are nearing the 2-year post-irradiation time point in this study. We have some evaluations at 6 and 12 months and are planning a complete set of evaluations at 2 years. To date we have noted that irradiation 'stunts' the growth of these animals as has previously been reported (**Figure 1.10 Left**). As in the section 1 describing the Radiation Survivor Cohort, despite these smaller less-obese animals, we are seeing a shift towards reduced glycemic control (**Figure 1.10 Right**). We believe these trends will continue such that statistical significance will be attained at 2 years.

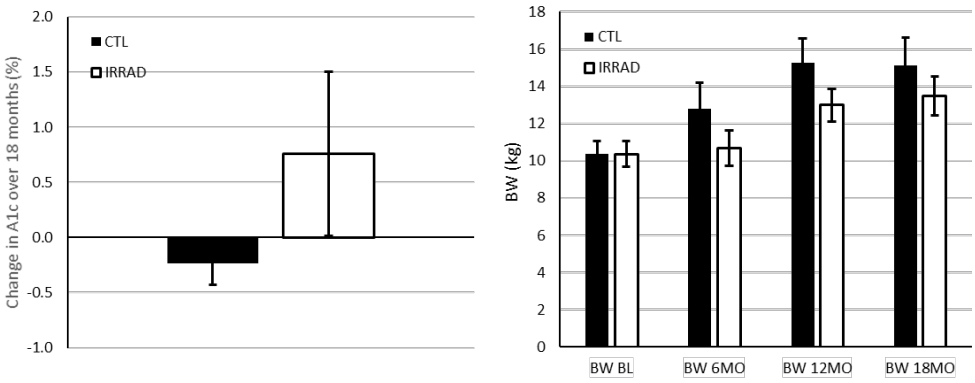

Figure 1.10. Bodyweight change over time (Left) and change from baseline A1c (=average blood glucose; Right) over 18 months of study.

A change in A1c values of 0.5% is a clinical benchmark for intervention efficiency so the change seen in irradiated monkeys is biologically significant. We have one animal diagnosed as overtly diabetic, which is the youngest known case of diabetes in a rhesus macaque that we are aware of. We would like to stress that this change over the last year of study has completely reversed from the prior year's report, where control monkeys had greater insulin resistance, A1c and blood glucose values. This identifies a critical period for diabetes as a delayed effect of radiation exposure evaluation as the period after 12-months post-exposure.

Also consistent with the data presented above for the radiation survivor cohort is a reduction in skeletal muscle insulin signaling at both baseline and significantly (p=0.03) after insulin infusion (**Figure 1.11**)

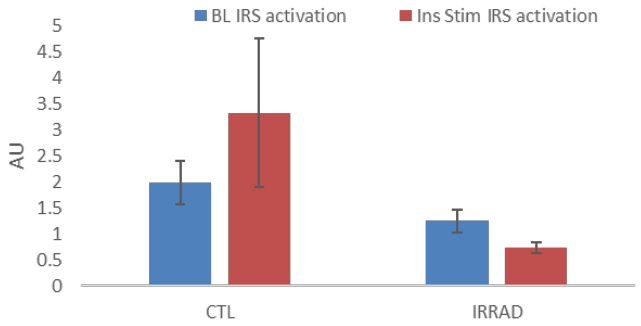

Figure 1.11. Insulin receptor substrate 1 (IRS1) activation at baseline and after insulin stimulation is lower in irradiated monkey skeletal muscle. Tissues evaluated at 6 months, and will be repeated at 24-months post-exposure.

At 6 months of study we performed glucose tolerance testing (presented in last year's annual report). This measures the integration of pancreatic responses, insulin-stimulated and insulin-independent glucose-stimulated disposal of a dextrose bolus. We are planning insulin tolerance testing at 24 months as this will facilitate repetition of the data in Figure 1.11 and more directly quantitate the ability of insulin to effect glucose disposal. We believe that deficits will be measurable in the irradiated animals as compared to control.

As fibrosis is a common pathway for radiation-related tissue dysfunction, we have assessed collagen 1 deposition at 6-months post-exposure in this new cohort. Table 2 shows data from

the radiation survivor cohort, and exposed monkeys had non-significantly higher skeletal muscle fibrosis. In this new cohort, we have the benefit of having a baseline estimate. Over 6 months of study, control animals actually decreased collagen staining by 4% while irradiated monkeys increased their collagen staining by 4%. Histological evaluation will be repeated at 24 months with this divergence expected to increase further and reach statistical significance.

3. Interventional Rodent Studies

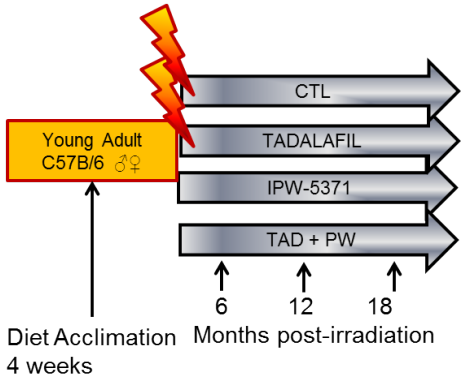

Figure 1.12. Rodent study overview.

In our first annual report we demonstrated that we had validated a rodent model of sub-lethal irradiation that creates insulin resistance. This model and resultant phenotype are being written up for publication with the addition of the positive multisystemic effects of an unrelated intervention aimed to improve protein quality control. We have taken that model and have completed a 12-month interventional study designed to evaluate potential countermeasures to abrogate radiation-induced insulin resistance (**Figure 1.12**). In this study we are evaluating the effects of inhibiting fibrotic signaling (Transforming Growth Factor beta [TGFb receptor inhibition; IPW-5371 by Innovation Pathways). Briefly, the rationale for this intervention is the observation in the RSC that TGFb was increased with radiation (Fanning et al., AJP 2017) and we see an accumulation of collagen subtypes in the muscle tissue. Fibrosis is a well-recognized outcome of radiation exposure and is increasingly important in multiple chronic disease conditions such as heart failure and liver diseases. A related compound in this drug class is already in Phase 2 clinical trials for pulmonary fibrosis, and IPW-5371 has published efficacy in reducing lung fibrosis following radiation in mice. We are also evaluating Tadalafil, a phosphodiesterase-5 inhibitor, marketed as Cialis. This drug has been chosen for emerging evidence that it can enhance perfusion, specifically in skeletal muscle. To date, 3 small clinical trials have demonstrated efficacy and preclinical studies have shown it to reduce heart fibrosis and extracellular matrix accumulation in the context of hyperglycemia. These compounds are studied as single agents and in combination after sub-lethal irradiation.

The IPW-5371 and Tadalafil are administered to the study mice by compounding them in the Western diet being used to drive insulin resistance and obesity. Mice are fed once daily and drug was introduced 2 weeks after irradiation, mimicking what might be possible in the clinical situation. The drug interventions have had no effect on food consumption and weight gain to date. Due to the Western diet, all groups are considered obese. In our prior annual report we summarized the following:

- Drug agents had no effect on bodyweight or food consumption.

- Sudden death was observed only in males exposed to agents in combination (Tadalafil and IPW-5371). Differences in survival were statistically significant.
- We have not seen a consistent improvement in physical function or metabolic testing as a result of drug therapy.

In this current year's body of work, we have pursued further investigation into the importance of the significant drug interaction (negative) and benefits of our intervention on fatty liver phenotype.

IPW-5371 was initially administered as 30mg/kg/d based on prior efficacy for prevention of post-radiation lung fibrosis. At this dose we saw unexpected adverse effects with deaths all in males and 89% of them in the combination treatment group. One death occurred in the IPW-5371 single agent group. The dose was reduced to 10mg/kg/d from 6 to 12 months of study and no further deaths have been observed. The cause of death appears to be great vessel rupture and death with hemorrhage observed in body cavities. As drugs of this class are currently in clinical use, it highly relevant to the population that is prescribed Tadalafil. We know Tadalafil also has some anti-fibrotic effects, so we hypothesize that the combination of drugs has limited the required amount of extracellular collagen to be deposited at vulnerable sites such as the heart base and aorta. These outflow tracts are subject to high oscillations in pressure and require enough structural integrity to move ejected blood down to the abdomen and brain. Sudden death by vascular accident is an important side effect as it is difficult to predict or quantitate risk. The mechanisms behind why a sex difference in risk exists (males affected) are unknown. We completed an evaluating the same drug combination (Tadalafil + IPW-5371) in non-irradiated male mice to evaluate if radiation-related changes in inflammation and fibrotic signaling are required for this serious side effect to manifest. Non-irradiated mice were actually more susceptible to this adverse side effect and died even more rapidly (**Figure 1.13**). We believe that this is all a result of the anti-fibrotic effects of our therapeutic countermeasures – and the pro-fibrotic effects of radiation exposure resulted in some protection.

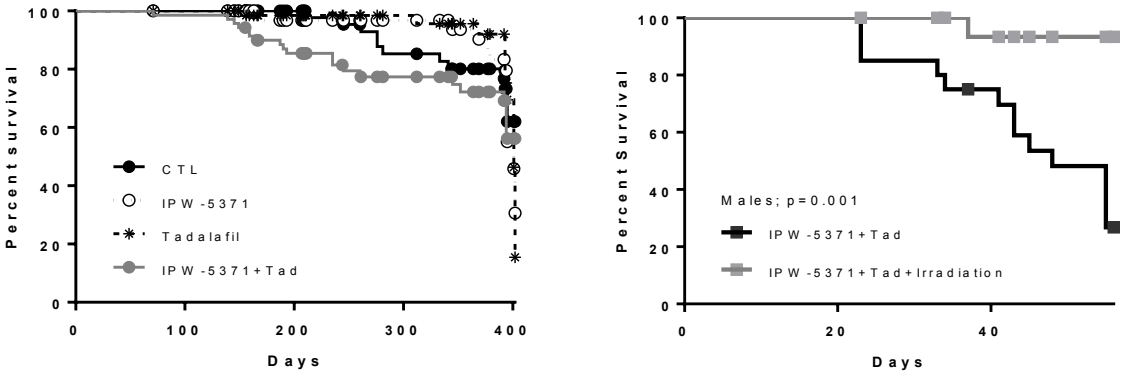

Figure 1.13. Left: Survival curve showing significant reduction in survival in mice receiving both IPW-5371 and Tadalafil at 30mg/kg/d and 5mg/kg/d respectively. The grey marked survival curve was significantly different (p=0.02). Right: Survival curve of mice receiving the same drug combination in the absence of irradiation, showing that this combination is lethal in an even more significant way in non-irradiated mice.

We checked drug levels of IPW-5371 in plasma and in lung tissue to see if a pharmacokinetic interaction could explain the significant mortality observed in the mice receiving IPW-5371 and Tadalafil in combination. IPW-5371 is a potent anti-fibrotic agent, so this was the compound focused on. We find that dosing in combination did not increase bioavailability of IPW-5371 in

plasma or in tissues (**Figure 1.14**). Plasma levels were not linear by dose in the plasma, but were in tissue concentrations.

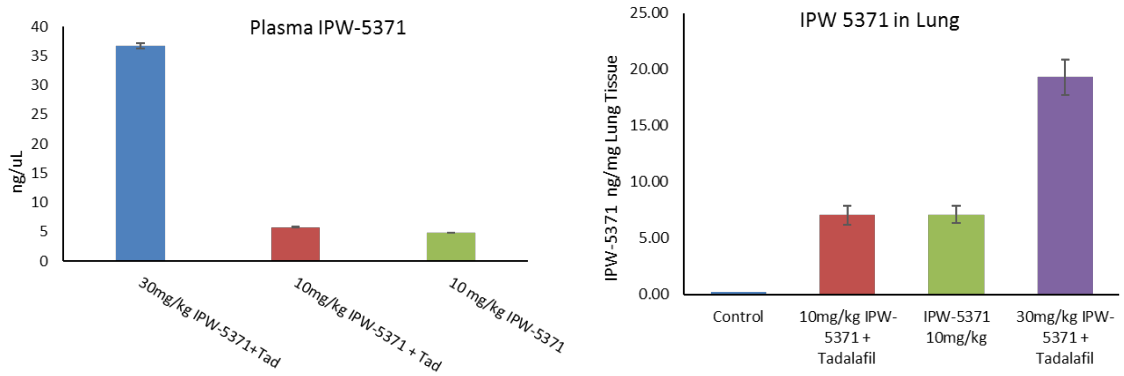

Figure 1.14. Left: Plasma IPW-5371 anti-fibrotic agent concentrations. Right: Lung tissue concentrations of IPW-5371 at the same time point. No change in IPW-5371 bioavailability is seen with co-administration with Tadalafil.

We believe that this story will be of great interest to pharmacologists. Second generation TGFbeta receptor 1 inhibitors have been generated and we will advise in our publication that their safety profile should include great vessel integrity and be monitored as an outcome.

Our next focus for this evaluation of anti-fibrotic agent IPW-5371 and angiogenic agent, Tadalafil will be effects on fatty liver. This is a disease of great public health significance with no effect therapies currently in place. We see a clear benefit of IPW-5371 therapy on both fat and fibrosis content of the liver. This is a very important finding as it has not yet been shown that targeting fibrosis can lead to changes in ectopic adipose tissue mass. We see at 6 months, a reduction in fat and fibrosis is seen in mice receiving IPW-5371 alone or in combination. At 12 months, we see improvements in all treated mice which we believe is in part therapeutic efficiency and in part an effect of survivorship. Many mice that were euthanized earlier in study appeared to be removed due to weight loss and fatty liver.

Data presented below is from 6-months post-irradiation. We completed blinded histopathological scoring for non-alcoholic steatohepatitis, which includes components of steatosis, hepatocyte ballooning, and inflammation (**Figure 1.15**). These scores were robustly supported by biochemically measured neutral lipid content (**Figure 1.16**) and histologically quantitated fibrosis area (**Figure 1.17**). In all cases the treatment effect of IPW-5371 (by factorial ANOVA), p-values were < 0.05.

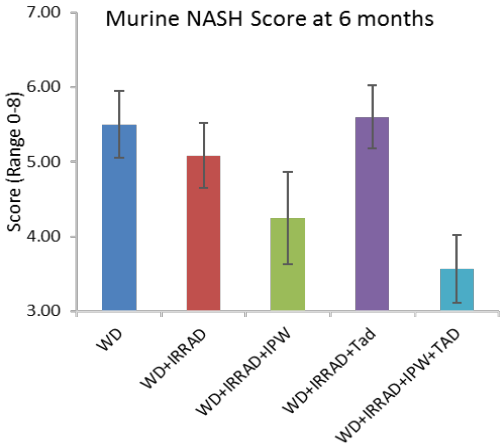

Figure 1.15. Non-alcoholic liver disease (NASH) scores for mice receiving anti-fibrotic IPW-5371 and perfusion-promoting Tadalafil post-irradiation. IPW-5371 exposure significantly improved the histological appearance of the liver.

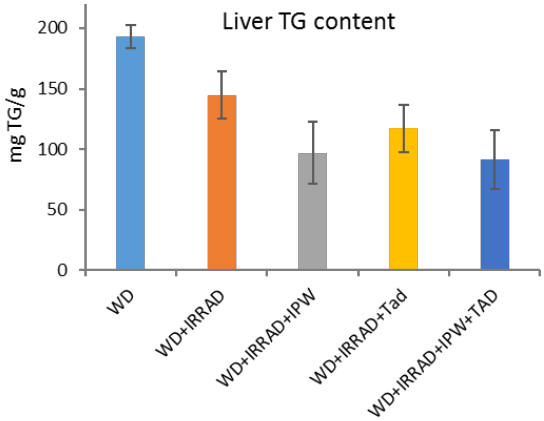

Figure 1.16. Liver triglyceride (TG) content in mice. Anti-fibrotic therapy reduced liver fact accumulation.

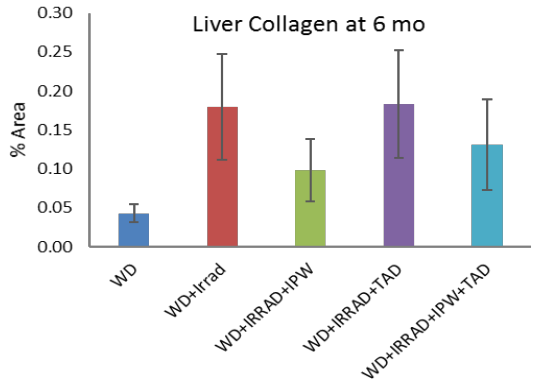

Figure 1.17. Collagen content of the liver, measured by Masson's trichrome staining, is significantly increased with irradiation but attenuated by administration of IPW-5371 as expected.

To confirm the anti-fibrotic actions at the cellular level, we used lung tissue to immunoblot for activated SMAD which is directly downstream of TGFb receptor activation (**Figure 1.18**). These data are from 12 month samples but in concordance with the fibrosis data, suggest there is an anti-fibrotic effect in place. We are corroborating these data with measures in skeletal muscle and liver at 6 months to demonstrate a generalized and persistent reduction in TGFb signaling. Representative histological sections stained for collagen by Masson's Trichrome are shown in in Figure 1.19, demonstrating the significant improvement in fat droplet frequency and blue fibrosis apparent in the liver parenchyma.

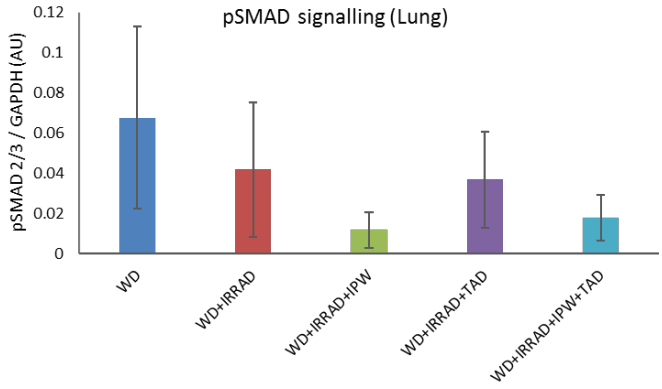

Figure 1.18. TGFb signal transduction activity in lung tissue of mice treated with IPW-5371 (TGFb receptor 1 inhibitor) and Tadalafil alone or in combination for 12 months. Reduced signaling is present in mice exposed to IPW-5371.

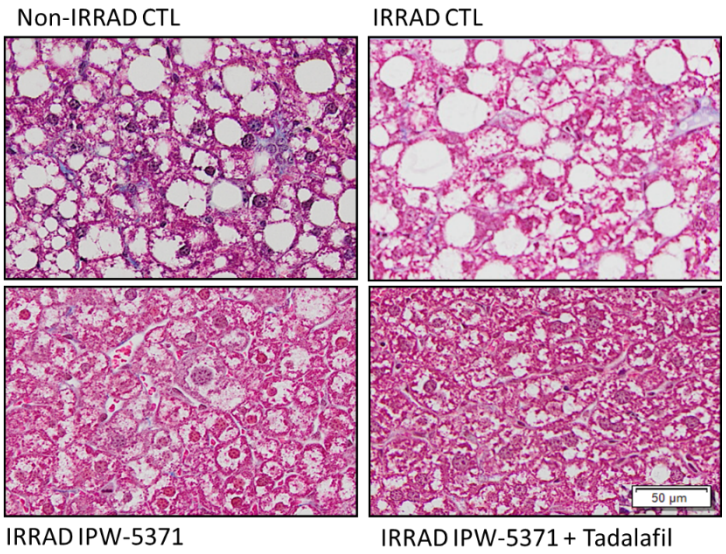

Figure 1.19. Representative liver histology from control and IPW-5371 receiving mice (a TGFb receptor 1 inhibitor). Slides are stained for collagen (blue) and demonstrate that TGFb inhibition leads to reduction in both lipid accumulation and fibrosis. Magnification is 20x

Our strategy will be to first report these 2 stories, improvements in fatty liver disease and dangerous interactions with Tadalafil, and potentially other agents in these classes of drugs.

In collaboration with Dr. Greg Sempowski's laboratory, we have been assessing the immune recovery of these mice. Again we see a clear signal for changes resulting of IPW-5371 exposure. We observed increased cellularity of the spleen and thymus at 6 months (**Figure 1.20**). Most cells that were increased were CD3+ve lymphocytes. Cell sorting is complete and these effects will be interpreted by the Duke

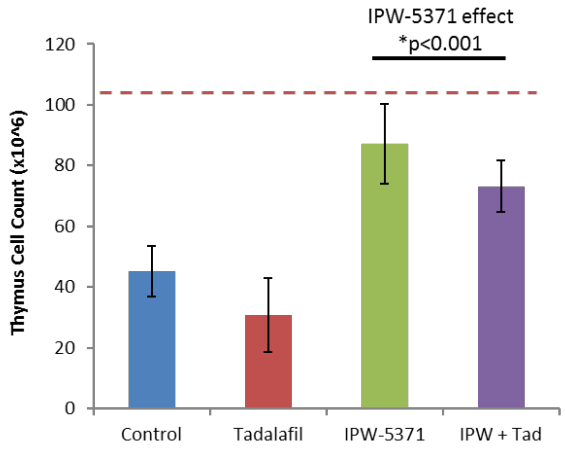

Figure 1.20. Thymic cellularity is significantly improved post-irradiation in mice treated with anti-fibrosis agent IPW-537. The dotted line represents the average cellularity of age- and diet-fed matched control mice that were not irradiated.

4) Other Achievements:

Nothing to Report

Project 2 – Radiation/Heart Disease (Register)

1) Major Activities

a) Collection and processing of blood samples in the prospective cohort during the subacute post-radiation phase for planned serum and plasma biomarker analyses.

b) Monitoring and surveillance of animals in the prospective cohort

c) Continued discussions with Duke investigators on cross-project technical collaboration on cell collections, processing, and data analysis.

d) PBMC preparations and monocyte isolations and sorting from selected monkeys in the PRC and RSC.

e) Biomarkers: Cardiac biomarkers: Acquired instrumentation (Siemens ADVIA Centaur CP Analyzer) for onsite assessments of troponin I, BNP, and other targets. Staff trained in the use of instrument by WF Clinical Chemistry staff. Submitted internal grant application for performing setup and validation of biomarkers in NHP on the instrument. Grant was funded, initiated July 1, 2018. Visited with a miRNA analytical group (*Chromologic LLC*, Monrovia CA) to discuss capabilities and optimal approaches to analysis of miRNA in the work proposed for specific aims 2 and 3.

f) Cardiac tissue analyses: Processing of myocardial and coronary artery tissue blocks (RSC, & past Project with mitigator) for assessment of coronary artery atherosclerosis (CAA) using VVG stain, stained sections were all scanned into a digital format for analysis using Visiopharm software, for which we developed new protocols for semi-automated atherosclerosis assessments. Measurements have been completed on available subjects (see results below) and data analysis is underway.

g) Cardiac Ultrasound Analysis Software: Cardiac Image Analysis software system (TOMTEC) is being used for customized output to accommodate the smaller NHP heart sizes.

h) Cardiac Ultrasound Data collected from the PRC 1 Year studies have been collected and evaluated. Additional modification to the data processing and output from the TOMTEC system is ongoing. Ultrasound images from the past 2 years in the RSC are being analyzed and are 100% completed.

j) Cardiac MRI studies on the 16 PRC monkeys were scheduled and are ½ way completed for the 2 year timepoint. Analyses of the images from baseline and the first year have been partially completed.

k) Monthly DOD Conference calls

l) New grant application submitted to the 2018 Peer Reviewed Medical Research Program for a Discovery Award to expand this work into a new area (epigenetic regulation through DNA methylation). The proposal is entitled “Effects of Ionizing Radiation (IR) on Myocardial DNA Methylation Profiles in Relation to Cardiomyopathy in a Nonhuman Primate Model”.

2) Specific objectives

Collections of samples, US, and cMRI images from the prospective cohort as described above. Planning for next cardiac imaging and biomarker assessments.

3) Results/key outcomes

Echocardiography: Baseline, 5 month, and 12 month follow-up echocardiographic measures have been evaluated, the 12 month data are shown in Table 2.1 with table definitions described in Table 2.2, selected outcomes are shown in Figures 2.1 and 2.2. Significant differences in body surface area (BSA) were observed between groups (Figure 2.1), as there was weight loss in some of the irradiated NHP post radiation, whereas the control group gained weight. After recovery the irradiated group began to gain weight, and associated BSA, in parallel with the controls. There were no significant differences between groups in any of the baseline echocardiographic measures of CV structure or function (not shown). Over the first 5 months following TBI, no significant changes over time or differences between groups were observed in fractional shortening, ejection fraction, cardiac output, aorta/left atrium ratio, or M mode measures of chamber size. Early diastolic filling of the left ventricle did not change over time and was not different between groups, but TBI monkeys experienced a significant increase in the late filling velocity across the mitral valve, and the E/A ratio showed a non-significant trend towards a reduction, which would be indicative of impairment on LV relaxation, though the numbers technically appear to be within the normal range. Mitral valve late filling velocity in the TBI group returned to levels comparable to controls at 1 year. Analyses of structural parameters (LV PW and IVS wall thicknesses and internal diameters suggest no significant differences between TBI and Control over the 1st year. Figure 2.2 illustrates changes in LVOT-AV VTI stroke volume and cardiac output, both of which increased over time in the Control group but was relatively constant in the irradiated group.

Table 2.1 Echocardiographic data from the PRC at 1 Year post-irradiation.

Phenotype	units	1960	1962	1965	1967	1968	1969	1970	1971	1972	1973	1974	1975	1976	1977	1979	1982
A/E	{ratio}	0.5	0.6	0.9	0.6	0.8	0.7	0.5	0.5	0.7	0.7	0.7	0.8	0.5	0.8	0.6	0.6
Aa(I)	m/s	0.1	0.1	0.1	0.0	0.1	0.0	0.1	0.1	0.1	0.1	0.1	0.0	0.0	0.0	0.0	0.1
Aa(s)	m/s	0.1	0.1	0.1	0.1	0.1	0.0	0.1	0.1	0.0	0.1	0.0	0.0	0.0	0.0	0.0	0.1
Ao diam systole	mm	11.4	13.3	10.7	14.1	9.8	12.2	9.7	12.2	13.6	12.3	11.9	11.4	10.5	12.9	10.7	10.2
AOs/LAs	{ratio}	0.8	1.0	0.6	0.6	0.7	0.6	0.7	0.8	0.8	0.6	0.7	0.7	0.7	0.6	0.7	0.5
AV PGmax	mm[Hg]	9.5	5.3	8.1	9.6	7.0	7.3	9.3	4.2	5.5		5.7	11.7	6.9	3.8	5.5	4.6
AV PGmean	mm[Hg]	3.6	2.1	3.3	3.8	3.1	3.0	3.8	1.7	2.1		2.4	4.8	2.8	1.7	2.6	1.7
AV Vmax	m/s	1.5	1.1	1.4	1.5	1.3	1.3	1.5	1.0	1.2		1.2	1.7	1.3	1.0	1.2	1.1
AV Vmean	m/s	0.9	0.7	0.8	0.9	0.8	0.8	0.9	0.6	0.7		0.7	1.0	0.7	0.6	0.7	0.6
AV VTI	cm	15.3	14.0	18.7	18.5	14.3	16.1	18.7	13.6	14.8		14.1	19.7	17.2	12.1	16.4	14.0
CO	l/min	1.3	1.4	0.7	1.0	0.9	1.2	1.1	1.1	1.0	1.0	1.0	1.0	1.1	0.8	0.8	0.8
CO (A2C)	l/min	0.9	1.6	0.7	1.0	0.8	1.2	1.0	1.1	1.0	0.8	0.9	0.9	1.0	0.8	0.8	0.8
CO (A4C)	l/min	1.7	0.8	0.8	0.9	1.0	1.1	1.0	0.9	0.8	0.9	0.8	1.0	0.8	0.8	0.6	0.8
Dec Slope	m/s2	6.1	12.2	5.3	8.6	6.8	6.8	9.5	7.7	7.6	8.2	7.8	6.8	6.8	5.6	11.3	9.8
Dec Time	ms	146	92	109	111	143	133	116	123	83	103	113	131	134	133	94	117
difD	%	7.5	27.5	1.1	18.6	1.1	6.7	22.4	23.2	28.6	23.7	17.1	8.6	31.0	11.0	16.5	7.6
difS	%	8.5	27.3	20.4	24.9	5.0	6.2	26.9	27.0	38.0	12.2	15.1	19.4	28.0	21.3	24.7	15.3
E/A	{ratio}	1.9	1.7	1.1	1.5	1.3	1.4	2.1	2.0	1.5	1.4	1.4	1.2	1.9	1.3	1.6	1.6
E/Ea(I)	{ratio}	6.6	7.3	4.8	10.6	8.4	10.1	9.0	5.8	4.9	9.6	6.7	6.7	7.5	6.4	6.8	9.7
Ea(I)	m/s	0.1	0.2	0.1	0.1	0.1	0.1	0.1	0.2	0.1	0.1	0.1	0.1	0.1	0.1	0.2	0.1
Ea(s)	m/s	0.1	0.1	0.1	0.1	0.1	0.1	0.1	0.1	0.1	0.1	0.1	0.1	0.1	0.1	0.1	0.1
Ea/Aa(I)	{ratio}	2.1	2.6	1.9	2.1	1.7	1.9	2.3	2.1	2.2	1.5	2.2	2.9	2.7	2.4	3.2	1.5
Ea/Aa(s)	{ratio}	1.5	2.0	1.0	1.8	1.3	2.8	1.9	2.1	1.7	1.2	1.8	2.3	2.6	1.8	3.0	1.7
EDV	ml	17.5	18.0	10.3	11.6	10.5	12.5	17.4	13.8	13.4	12.2	11.6	11.9	15.1	12.7	12.4	11.2
EDV (A2C)	ml	13.5	19.3	9.4	11.6	9.4	12.3	15.9	13.2	13.3	11.4	10.9	10.7	13.6	12.7	11.6	11.4
EDV (A4C)	ml	21.3	12.3	11.6	9.8	11.6	11.9	15.4	11.8	10.2	10.5	10.5	12.1	11.9	11.5	11.3	10.3
EF	%	49.0	60.4	71.0	58.6	56.4	71.2	55.9	62.6	67.9	69.7	70.8	67.8	68.3	56.5	56.8	68.5
EF (A2C)	%	43.5	65.7	77.0	57.5	55.3	73.9	56.1	64.3	68.3	61.6	71.6	69.2	69.8	58.3	64.7	66.4
EF (A4C)	%	53.3	53.9	70.3	61.8	59.0	68.1	58.0	61.4	69.1	72.6	68.6	70.0	63.3	60.3	51.2	71.5
ESV	ml	8.9	7.1	3.0	4.8	4.6	3.6	7.7	5.2	4.3	3.7	3.4	3.8	4.8	5.5	5.4	3.5
ESV (A2C)	ml	7.6	6.6	2.2	4.9	4.2	3.2	7.0	4.7	4.2	4.4	3.1	3.3	4.1	5.3	4.1	3.8
ESV (A4C)	ml	10.0	5.7	3.4	3.7	4.7	3.8	6.5	4.5	3.2	2.9	3.3	3.6	4.4	4.6	5.5	2.9
GLS (2P)	%	-18.9	-27.2	-36.8	-23.5	-24.6	-27.7	-22.8	-24.9	-25.0	-32.0	-28.6	-26.8	-31.4	-19.8	-20.7	-23.2
HR	{H.B.}/min	149	125	100	147	150	133	113	125	113	121	117	121	110	110	109	103
LA diam systole	mm	14.5	13.0	19.4	21.9	14.5	19.1	14.8	16.0	16.6	22.3	17.4	16.1	15.0	20.3	15.3	19.2
LA Vol (A2C)	ml	3.6	2.3	1.8	3.6	3.1	3.1	3.9	3.0	2.7	3.0	1.9	1.9	1.6	4.7	1.8	5.6
LA Vol (A4C)	ml	5.1	4.9	7.5	6.2	3.4	5.6	3.4	4.9	5.2	5.6	3.9	4.0	4.2	7.0	5.1	7.0
LA Vol (BP)	ml	4.5	3.8	5.1	5.1	3.4	4.9	4.1	4.6	4.1	4.7	3.3	3.2	2.9	5.8	3.6	6.3
LAA (A2C)	cm2	3.0	2.1	1.8	2.7	2.7	2.4	2.9	2.4	2.4	2.7	1.9	1.9	1.7	3.5	1.8	4.2
LAA (A4C)	cm2	3.7	3.5	5.1	4.0	2.9	3.9	3.0	3.8	3.5	4.2	3.3	3.2	3.2	4.3	3.7	4.6
LAs/AOs	{ratio}	1.3	1.0	1.8	1.6	1.5	1.6	1.5	1.3	1.2	1.8	1.5	1.4	1.4	1.6	1.4	1.9
LVOT diam	mm	10.4	9.6	9.7	10.6	9.9	11.5	9.0	9.7	10.8	9.7	7.3	9.3	9.1	10.2	8.2	9.3
MV A pt	m/s	0.5	0.6	0.5	0.6	0.7	0.6	0.5	0.5	0.4	0.6	0.6	0.7	0.5	0.6	0.7	0.7
MV E pt	m/s	0.9	1.1	0.6	0.9	1.0	0.9	1.1	0.9	0.6	0.8	0.9	0.9	0.9	0.7	1.1	1.1
PV PGmax	mm[Hg]	6.4	5.3	2.1	3.5	4.8	3.1	3.0	2.8	3.1	5.5	4.6	5.3	6.4	2.8	3.8	4.2
PV Vmax	m/s	1.3	1.1	0.7	0.9	1.1	0.9	0.9	0.8	0.9	1.2	1.1	1.2	1.3	0.8	1.0	1.0
SV	ml	8.6	10.9	7.3	6.8	5.9	8.9	9.7	8.6	9.1	8.5	8.2	8.1	10.3	7.2	7.1	7.7
SV (A2C)	ml	5.9	12.7	7.3	6.7	5.2	9.1	8.9	8.5	9.1	7.0	7.8	7.4	9.5	7.4	7.5	7.6
SV (A4C)	ml	11.4	6.6	8.1	6.0	6.8	8.1	9.0	7.2	7.0	7.6	7.2	8.5	7.5	6.9	5.8	7.4

Table 2.2: Echocardiographic data abbreviations and full variable names

ID		
GP(Con1,Rad2)		
1 Year (Oct) BW	kg	Body Weight
1 Year (Oct) BSA	m^2	Body Surface Area
1 Year (Oct) Correction Factor		
A/E - 1 Year	{ratio}	Mitral Valve - A to E Ratio - Antegrade Flow - Doppler Mode
Aa(l) - 1 Year	m/s	Left Ventricle Doppler Tissue Imaging - LV Peak Diastolic Tissue Velocity During Atrial Systole - Lateral Mitral Annulus
Aa(s) - 1 Year	m/s	Left Ventricle Doppler Tissue Imaging - LV Peak Diastolic Tissue Velocity During Atrial Systole - Septal Mitral Annulus
Ao diam systole - 1 Year	mm	Aorta - Diameter - Systole - 2D mode
AOs/LAs - 1 Year	{ratio}	Left Atrium - Aortic Root to Left Atrium Ratio - 2D mode
AV PGmax - 1 Year	mm[Hg]	Aortic Valve - Peak Gradient - Antegrade Flow - Doppler Mode
AV PGmean - 1 Year	mm[Hg]	Aortic Valve - Mean Gradient - Antegrade Flow - Doppler Mode
AV Vmax - 1 Year	m/s	Aortic Valve - Peak Velocity - Antegrade Flow - Doppler Mode
AV Vmean - 1 Year	m/s	Aortic Valve - Mean Velocity - Antegrade Flow - Doppler Mode
AV VTI - 1 Year	cm	Aortic Valve - Velocity Time Integral - Antegrade Flow - Doppler Mode
CO - 1 Year	l/min	Left Ventricle - Cardiac Output - 2D mode - Method of Disks, Biplane
CO (A2C) - 1 Year	l/min	Left Ventricle - Cardiac Output - 2D mode - Method of Disks, Single Plane - Apical two chamber
CO (A4C) - 1 Year	l/min	Left Ventricle - Cardiac Output - 2D mode - Method of Disks, Single Plane - Apical four chamber
Dec Slope - 1 Year	m/s2	Mitral Valve - Deceleration Slope - Doppler Mode
Dec Time - 1 Year	ms	Mitral Valve - E-Wave Deceleration Time - Antegrade Flow - Doppler Mode
difD - 1 Year	%	Left Ventricle - Major axis length difference - End Diastole - 2D mode
difS - 1 Year	%	Left Ventricle - Major axis length difference - End Systole - 2D mode
E/A - 1 Year	{ratio}	Mitral Valve - E to A Ratio - Antegrade Flow - Doppler Mode
E/Ea(l) - 1 Year	{ratio}	Left Ventricle Doppler Tissue Imaging - Ratio of MV Peak Velocity to LV Peak Tissue Velocity E-Wave - Lateral Mitral Annulus
Ea(l) - 1 Year	m/s	Left Ventricle Doppler Tissue Imaging - Left Ventricular Peak Early Diastolic Tissue Velocity - Lateral Mitral Annulus
Ea(s) - 1 Year	m/s	Left Ventricle Doppler Tissue Imaging - Left Ventricular Peak Early Diastolic Tissue Velocity - Septal Mitral Annulus
Ea/Aa(l) - 1 Year	{ratio}	Left Ventricle Doppler Tissue Imaging - Left Ventricle E to A Tissue Velocity Ratio - Lateral Mitral Annulus
Ea/Aa(s) - 1 Year	{ratio}	Left Ventricle Doppler Tissue Imaging - Left Ventricle E to A Tissue Velocity Ratio - Septal Mitral Annulus
EDV - 1 Year	ml	Left Ventricle - End Diastolic Volume - 2D mode - Method of Disks, Biplane
EDV (A2C) - 1 Year	ml	Left Ventricle - End Diastolic Volume - 2D mode - Method of Disks, Single Plane - Apical two chamber
EDV (A4C) - 1 Year	ml	Left Ventricle - End Diastolic Volume - 2D mode - Method of Disks, Single Plane - Apical four chamber
EF - 1 Year	%	Left Ventricle - Ejection Fraction - 2D mode - Method of Disks, Biplane
EF (A2C) - 1 Year	%	Left Ventricle - Ejection Fraction - 2D mode - Method of Disks, Single Plane - Apical two chamber
EF (A4C) - 1 Year	%	Left Ventricle - Ejection Fraction - 2D mode - Method of Disks, Single Plane - Apical four chamber
ESV - 1 Year	ml	Left Ventricle - End Systolic Volume - 2D mode - Method of Disks, Biplane
ESV (A2C) - 1 Year	ml	Left Ventricle - End Systolic Volume - 2D mode - Method of Disks, Single Plane - Apical two chamber
ESV (A4C) - 1 Year	ml	Left Ventricle - End Systolic Volume - 2D mode - Method of Disks, Single Plane - Apical four chamber
GLS (2P) - 1 Year	%	Left Ventricle - Global Longitudinal Strain - 2D mode - Biplane
HR - 1 Year	{H.B.}/min	Left Ventricle - Heart Rate
LA diam systole - 1 Year	mm	Left Atrium - Diameter - Systole - 2D mode
LA Vol (A2C) - 1 Year	ml	Left Atrium - End Systolic Volume - 2D mode - Method of Disks, Single Plane - Apical two chamber
LA Vol (A4C) - 1 Year	ml	Left Atrium - End Systolic Volume - 2D mode - Method of Disks, Single Plane - Apical four chamber
LA Vol (BP) - 1 Year	ml	Left Atrium - End Systolic Volume - 2D mode - Method of Disks, Biplane
LAA (A2C) - 1 Year	cm2	Left Atrium - Area - Systole - 2D mode - Apical two chamber
LAA (A4C) - 1 Year	cm2	Left Atrium - Area - Systole - 2D mode - Apical four chamber
LAs/AOs - 1 Year	{ratio}	Left Atrium - Left Atrium to Aortic Root Ratio - 2D mode
LVOT diam - 1 Year	mm	Left Ventricle Outflow Tract - Cardiovascular Orifice Diameter
LVOT SV - 1 Year	ml	Left Ventricle Outflow Tract *Aortic Velocity Time Integral Stroke Volume
LVOT CO - 1 Year	l/min	Left Ventricle Outflow Tract *Aortic Velocity Time Integral Cardiac Output
MV A pt - 1 Year	m/s	Mitral Valve - A-Wave Peak Velocity - Antegrade Flow - Doppler Mode
MV E pt - 1 Year	m/s	Mitral Valve - E-Wave Peak Velocity - Antegrade Flow - Doppler Mode
PV PGmax - 1 Year	mm[Hg]	Pulmonary Valve - Peak Gradient - Antegrade Flow - Doppler Mode
PV Vmax - 1 Year	m/s	Pulmonary Valve - Peak Velocity - Antegrade Flow - Doppler Mode
SV - 1 Year	ml	Left Ventricle - Stroke Volume - 2D mode - Method of Disks, Biplane
SV (A2C) - 1 Year	ml	Left Ventricle - Stroke Volume - 2D mode - Method of Disks, Single Plane - Apical two chamber
SV (A4C) - 1 Year	ml	Left Ventricle - Stroke Volume - 2D mode - Method of Disks, Single Plane - Apical four chamber
EPSS - 1 Year	cm	End Point of Septal Separation- Mitral Valve
IVSd - 1 Year	cm	Interventricular Septal Thickness - Diastole
LVIDd - 1 Year	cm	Left Ventricle Internal Diameter - Diastole
LVPWd - 1 Year	cm	Left Ventricle Posterior Wall Thickness - Diastole
IVSs - 1 Year	cm	Interventricular Septal Thickness - Systole
LVIDs - 1 Year	cm	Left Ventricle Internal Diameter - Systole
LVPWs - 1 Year	cm	Left Ventricle Posterior Wall Thickness - Systole
EDV(Teich) - 1 Year	ml	End Diastolic Volume (Teich Method)
ESV(Teich) - 1 Year	ml	End Systole Volume (Teich Method)
EF(Teich) - 1 Year	%	Ejection Fraction (Teich Method)
%FS - 1 Year	%	Fractional Shortening
SV(Teich) - 1 Year	ml	Stroke Volume (Teich Method)

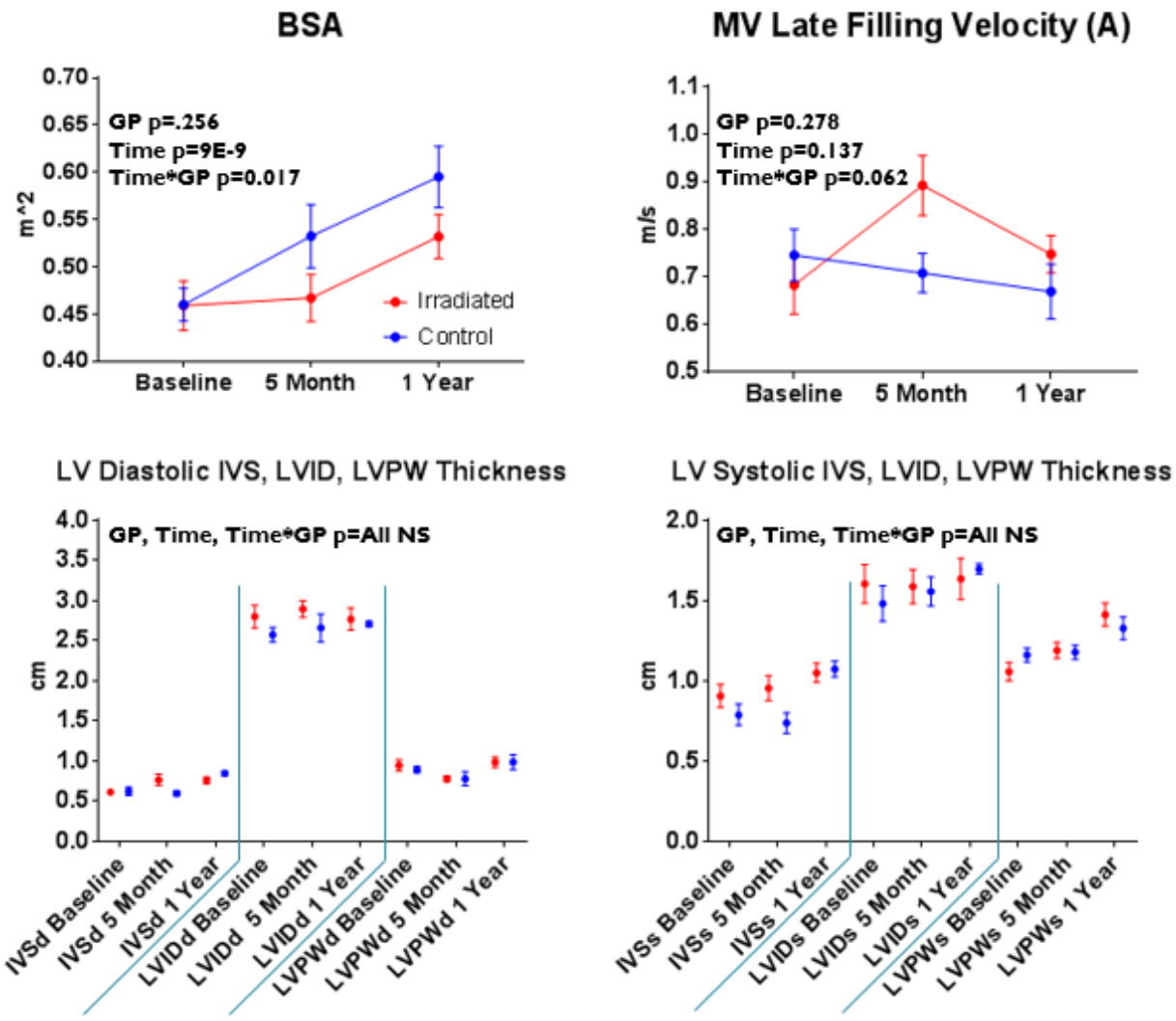

Figure 2.1: Body surface area and echocardiographic findings during the first year afer irradiation in the PRC. Abbreviations are defined in Table 2.2.

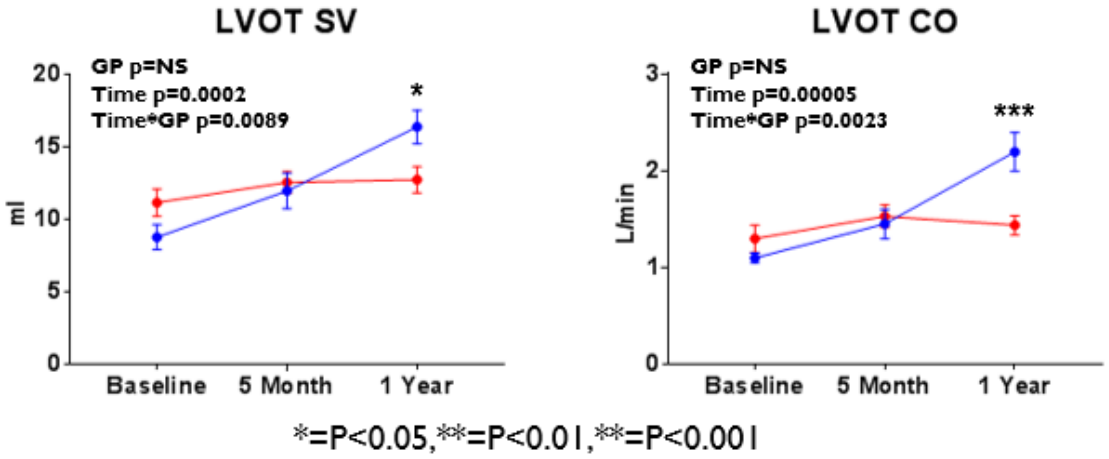

Figure 2.2: Echocardiographic findings during the first year afer irradiation in the PRC. Abbreviations are defined in Table 2.2.

Cardiac MRI: Measurements have been made on the baseline, 5 month, and 12 month images. Software is being modified to facilitate more automated data compilation and transfer into our database. Data analysis continues. Key MRI measures include left ventricular (LV) mass, posterior and interventricular wall thickness, right ventricular thickness, aortic wall thickness, and the presence of myocardial fibrosis. Functional parameters include systolic and diastolic function, ejection fraction, aortic stiffness/pulse wave velocity (PWV), and electrocardiography (ECG). MR grid tag mapping is being used to assess strain and LV volume, contrast enhanced perfusion MR will be used to assess microvascular function. T1 mapping techniques are being to evaluate myocardial extracellular volume fraction (ECVF), which corresponds to diffuse subclinical myocardial fibrosis (using customized software: MIMP). Measurements are being made in collaboration with Drs. Dalane Kitzman, Craig Hamilton, and staff, who have significant expertise in human and nonhuman primate cardiac analyses. We continue to develop and optimize software for both the MR image analysis and the data transfer to the database.

Echocardiographic Outcomes in the RSC: Echocardiographic data collected in the entire RSC over two consecutive years (2016-2017) have been analyzed. The monkeys in the RSC have a bimodal age distribution and sort out fairly well into young and old cohorts. We selected a subset of subjects from the young (range:5-8 years) to facilitate better age matching with young controls along with all of the old (range:12-20 years) (Figure 2.3) group (Table 2.3). All analyses of cardiac parameters were covaried for BSA. Relative to the respective age matched controls, there was no evidence of systolic dysfunction in either the young or the old RSC survivors. The “Old” RSC survivors have evidence of increased filling pressures (E/e'), and decreased tissue Doppler annular velocities indicating increased myocardial stiffness and diastolic dysfunction relative to ‘old’ controls. They also have decreased stroke volume and cardiac output, a new observation. In addition, their LV had smaller internal diameters during both systole and diastole, supporting our previous findings reported by DeBo et al. 2016). Likewise, the “Young” RSC survivors have increased filling pressures and also decreased tissue Doppler early annular velocities, indicating increased myocardial stiffness and diastolic dysfunction relative to their age matched cohort. The degree of these differences was not as severe as in the “Old” cohort. Interestingly young survivors also had an increased LV PW

thickness, and a tendency for increased IVS thickness, suggesting some degree of LV hypertrophy.

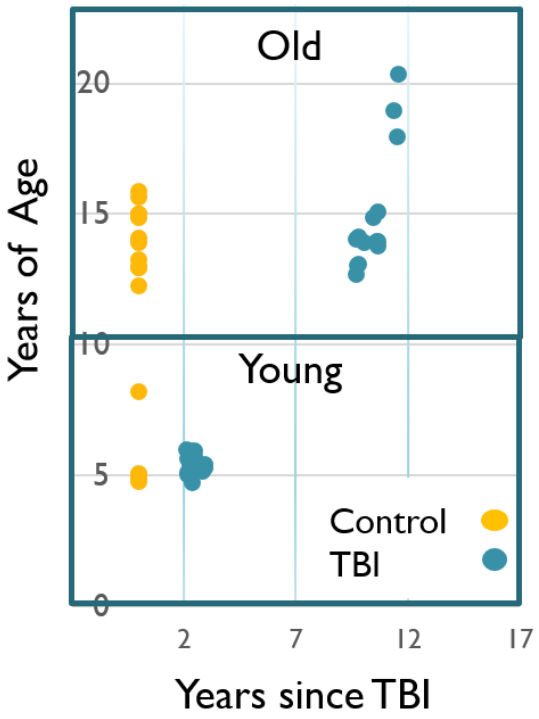

Figure 2.3: Plot of age and years since irradiation, showing clustering used for cardiac analysis.

Table 2.3	Echocardiographic Data in Young and Old Cohorts in the RSC									
	Young (5-8 Years)					Old (12-20 years)				
Abbreviation	Young Survivors	n	Young Controls	n	p	Old Survivors	n	Old Controls	n	p
Age (Years)	5.47 ± 0.08	20	5.25 ± 0.33	10	0.4	14.96 ± 0.63	14	14.15 ± 0.28	15	0.25
Years Since TBI	2.51 ± 0.07	20	---	10	---	10.48 ± 0.18	14	---	15	---
Dose (Gy)	7.01 ± 0.14	20	---	10	---	7.40 ± 0.16	14	---	15	---
Body Weight (kg)	9.22 ± 0.56	20	8.77 ± 0.35	10	0.86	11.31 ± 1.11	14	14.62 ± 1.25	15	0.06
BSA (m^2)	0.42 ± 0.29	20	0.41 ± 0.01	10	0.97	0.48 ± 0.03	14	0.55 ± 0.03	15	0.16
a'	0.054 (0.003)	20	0.059 (0.013)	9	0.55	0.074 (0.005)	14	0.084 (0.013)	15	0.51
AO/LA	0.668 (0.027)	20	0.626 (0.027)	9	0.35	0.637 (0.032)	14	0.578 (0.024)	15	0.11
AV Vmax	1.075 (0.059)	20	0.998 (0.061)	9	0.38	1.163 (0.065)	14	1.183 (0.103)	15	0.86
AV Vmean	0.681 (0.039)	20	0.647 (0.043)	9	0.52	0.739 (0.047)	14	0.784 (0.076)	15	0.60
AV VTI	14.827 (0.762)	20	13.618 (0.434)	9	0.32	14.61 (0.748)	14	15.224 (1.166)	15	0.56
CO BP	0.765 (0.068)	20	0.706 (0.086)	9	0.52	0.828 (0.068)	13	1.006 (0.075)	14	0.07
CO A2C	0.716 (0.057)	20	0.663 (0.08)	9	0.52	0.808 (0.067)	13	0.937 (0.069)	14	0.17
CO A4C	0.679 (0.064)	20	0.688 (0.096)	9	0.92	0.717 (0.049)	14	0.981 (0.058)	14	0.001
Dec Slope	8.61 (0.462)	20	9.921 (1.26)	10	0.15	8.41 (0.488)	13	6.797 (0.486)	15	0.03
Dec Time	124.052 (4.964)	20	114.93 (8.446)	10	0.33	118.918 (6.151)	13	114.462 (4.878)	15	0.58
E/A	1.515 (0.075)	20	1.774 (0.167)	10	0.10	1.14 (0.086)	13	1.056 (0.064)	15	0.43
E/e'	10.681 (0.496)	20	9.036 (0.611)	9	0.050	12.532 (0.981)	13	6.916 (0.587)	15	0.00003
e'	0.099 (0.004)	20	0.121 (0.006)	9	0.010	0.083 (0.004)	14	0.118 (0.012)	15	0.01
e'/a'	1.928 (0.129)	20	2.636 (0.431)	9	0.046	1.207 (0.11)	14	1.621 (0.173)	15	0.05
EDV BP	9.784 (0.639)	20	9.689 (0.694)	9	0.92	10.412 (0.873)	13	12.574 (0.839)	14	0.07
EDV A2C	9.232 (0.569)	20	9.332 (0.726)	9	0.91	10.107 (0.842)	13	11.681 (0.736)	14	0.16
EDV A4C	8.681 (0.609)	20	9.159 (0.711)	9	0.60	8.973 (0.718)	14	12.206 (1.006)	14	0.01
EF	63.778 (1.474)	20	59.359 (1.822)	9	0.10	64.22 (2.043)	13	63.225 (2.371)	14	0.76
ESV BP	3.443 (0.184)	20	3.97 (0.366)	9	0.13	3.846 (0.499)	13	4.76 (0.571)	14	0.23
ESV A2C	3.287 (0.201)	20	3.956 (0.372)	9	0.08	3.707 (0.502)	13	4.377 (0.442)	14	0.32
ESV A4C	3.055 (0.161)	20	3.624 (0.367)	9	0.06	3.345 (0.498)	14	4.542 (0.765)	14	0.20
HR	121.1 (3.824)	20	123.733 (9.903)	10	0.69	128.2 (5.582)	14	128.4 (5.214)	14	0.98
LA Vol BP	2.958 (0.187)	20	2.748 (0.132)	9	0.45	3.254 (0.376)	14	3.282 (0.237)	14	0.95
LVOT	7.632 (0.232)	20	7.976 (0.305)	10	0.38	8.169 (0.169)	14	9.284 (0.343)	15	0.01
LVOT AV VTI SV	6.928 (0.531)	20	6.707 (0.471)	9	0.79	7.764 (0.600)	14	9.889 (1.065)	14	0.09
LVOT AV VTI CO	0.838 (0.068)	20	0.843 (0.115)	9	0.96	1.000 (0.091)	14	1.279 (0.165)	13	0.13
A	0.708 (0.042)	20	0.652 (0.089)	10	0.41	0.905 (0.077)	13	0.758 (0.078)	15	0.20
E	1.029 (0.036)	20	1.055 (0.056)	10	0.63	0.978 (0.047)	13	0.748 (0.049)	15	0.002
SV BP	6.341 (0.548)	20	5.719 (0.394)	9	0.46	6.565 (0.430)	13	7.813 (0.462)	14	0.05
SV A2C	5.945 (0.474)	20	5.376 (0.402)	9	0.45	6.400 (0.435)	13	7.304 (0.444)	14	0.15
SV A4C	5.627 (0.508)	20	5.535 (0.408)	9	0.91	5.628 (0.319)	14	7.664 (0.404)	14	0.001
IVSd	0.715 (0.036)	20	0.632 (0.047)	10	0.08	0.716 (0.063)	14	0.672 (0.053)	15	0.59
LVIDd	2.14 (0.054)	20	2.153 (0.069)	10	0.88	2.171 (0.084)	14	2.488 (0.089)	15	0.01
LVPWd	0.692 (0.028)	20	0.568 (0.039)	10	0.001	0.716 (0.045)	14	0.822 (0.056)	15	0.06
IVSs	0.964 (0.037)	20	0.853 (0.05)	10	0.05	0.996 (0.068)	14	0.946 (0.068)	15	0.57
LVIDs	1.155 (0.042)	20	1.23 (0.08)	10	0.37	1.058 (0.057)	14	1.323 (0.109)	15	0.05
LVPWs	1.028 (0.051)	20	0.823 (0.059)	10	0.002	1.066 (0.051)	14	1.193 (0.061)	15	0.07
FS	45.663 (2.062)	20	43.271 (2.479)	10	0.48	51.424 (1.691)	14	47.324 (2.957)	15	0.25

Coronary Artery Atherosclerosis in the RSC: Hearts obtained from RSC and control rhesus monkeys which have gone to necropsy were evaluated for atherosclerosis extent using standard methods and approaches developed at Wake Forest. Briefly, three blocks from each of the main epicardial coronary arteries (left circumflex, left anterior descending and right epicardial arteries (shown in Figure 1) were sectioned and then stained with Verhoeff-van Gieson stain in order to facilitate identification of the internal and external elastic lamella (stained black), cell nuclei (stained black), and collagen (stained red) and the measurement of

atherosclerosis (intimal area). Intimal area and other parameters (maximal intimal thickness, maximal medial thickness, internal elastic lamella length) were measured using algorithms and protocols developed in the Register lab for Visiopharm. Images of the unfiltered raw data from each of the coronary blocks are shown in Figure 2.4. Data are shown in Figure 2.5. Statistical analysis of these data are underway, and will require correction for amount of time while consuming the moderately atherogenic diet, age, and other key parameters. Note: controls are animals that have been euthanized due to illness and are not true age and time matched healthy controls.

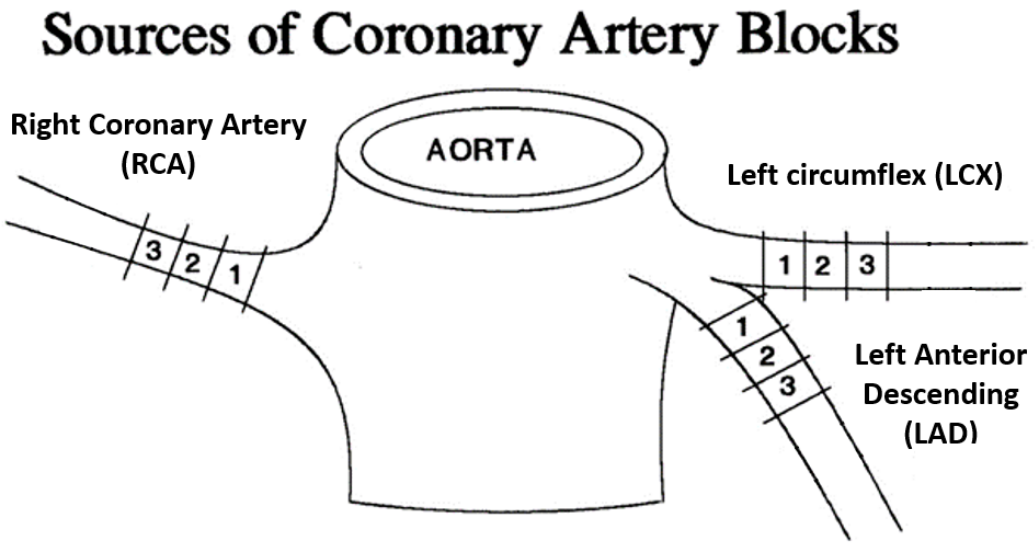

Adapted from Register, Appt, Clarkson Methods Mol Biol. 2016;1366:517-532.

Figure 2.4: Illustration of the sources of the coronary arteries evaluated in the RSC.

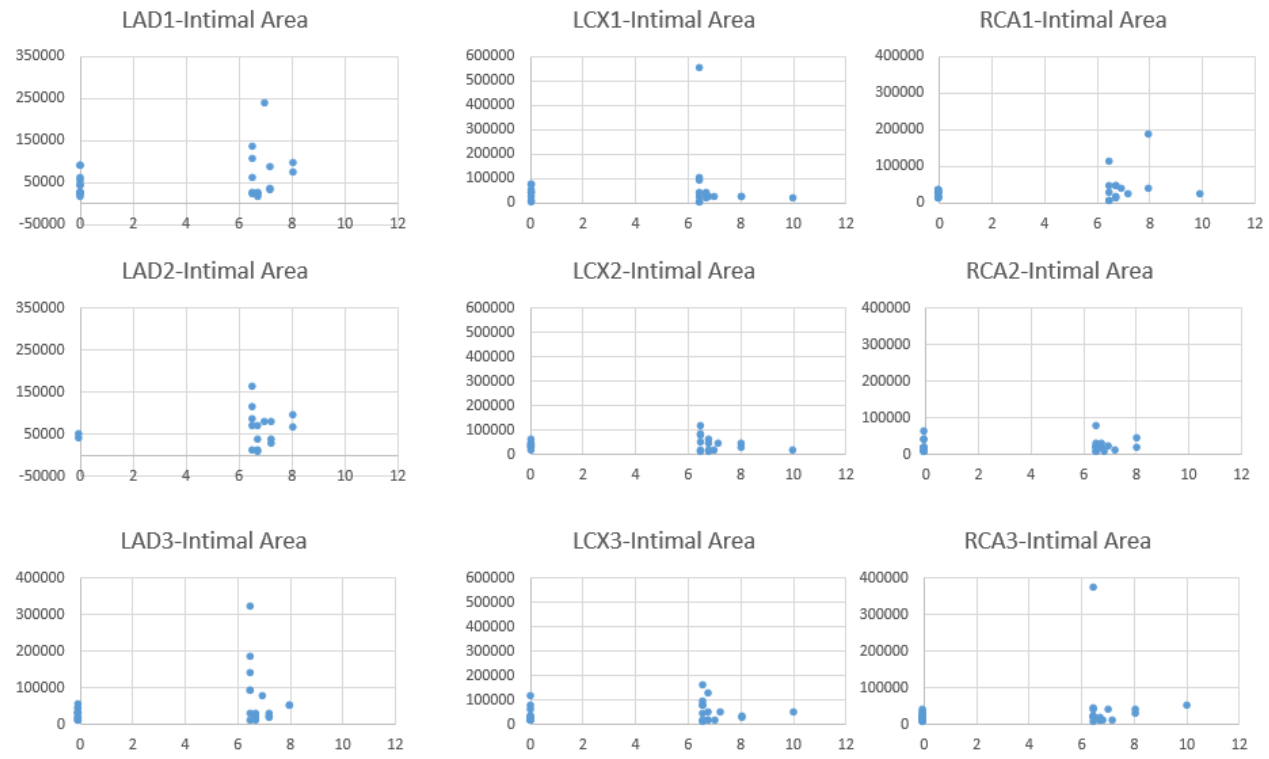

Figure 2.5: Raw data of atherosclerosis (intimal area in um^2) from the 9 blocks of coronary arteries illustrated in Figure 2.4, plotted against irradiation dose in Gy on the x axis.

Monocyte Polarization in the PRC as a Potential Mediator of Cardiac and Systemic Radiation Induced Fibrosis: Radiation induced fibrosis (RIF) is a delayed effect of acute ionizing radiation exposure (DEARE) affecting not only the heart, but other tissues including the lungs, liver and skin, and resulting in reduced tissue function and increased morbidity. Monocytes may be classified into classical (CD14++, CD16-), intermediate (CD14++, CD16+), and non-classical (CD14+^{low}, CD16++) subtypes in humans and non-human primates (NHPs), and it is likely one or more subpopulations of monocytes may play an integral role in the pathogenesis of RIF. We are exploring the hypothesis that moderate to high levels of total body irradiation (TBI) can alter monocyte polarization and produce phenotypes which could promote multi-organ fibrosis. To date we have evaluated the PRC subjects (16 young adult male rhesus macaques, 10 with TBI with 4 Gy high-energy X-rays (IRR) vs 6 non-irradiated controls (CTL, n=6). Total monocyte counts were obtained from CBCs that were collected before irradiation, then weekly after irradiation for two months and monthly thereafter. Total monocytes were acutely depleted in IRR animals ($p<0.05$), but recovered by day 30 post-irradiation and did not differ from CTL levels thereafter (Figure 2.6).

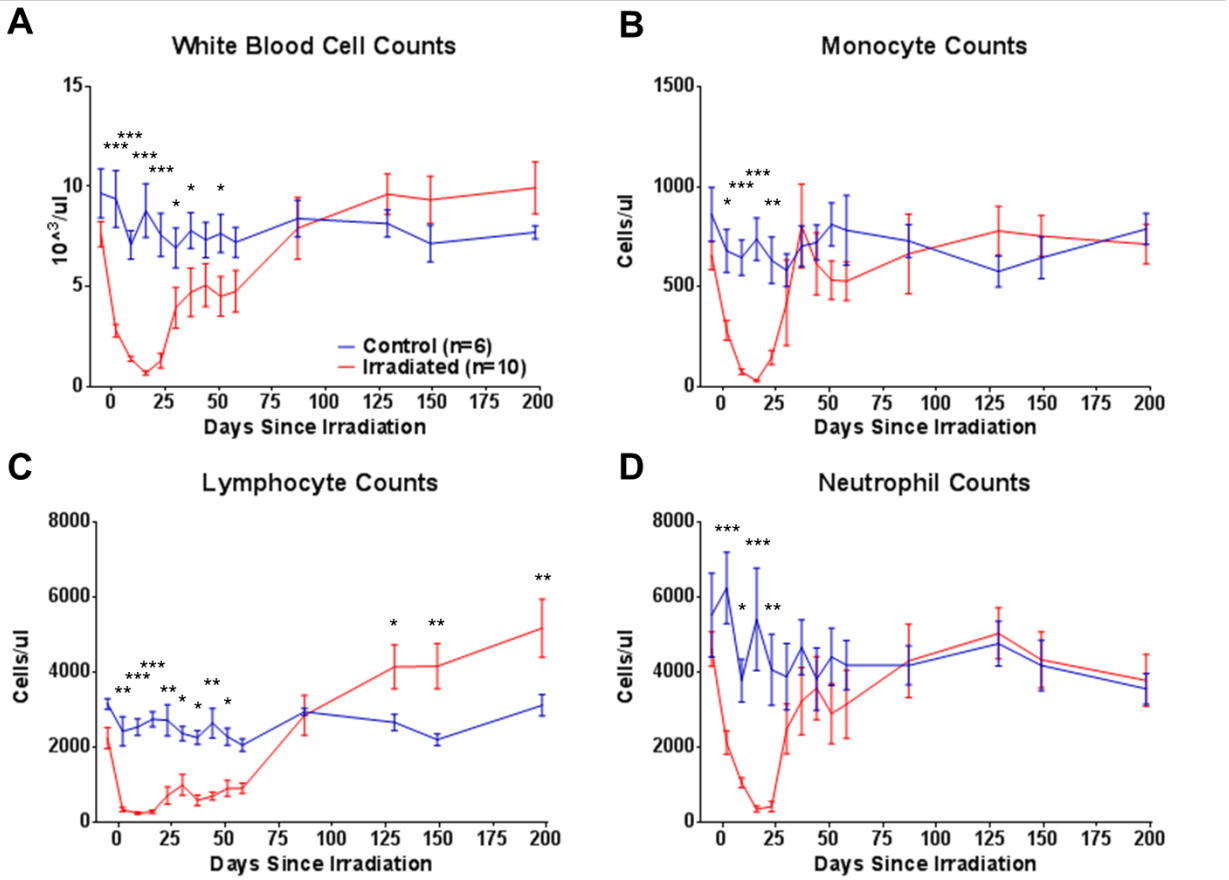

Figure 2.6: Peripheral Immune Cell Recovery after Total Body Irradiation. Total white blood cells (A), monocyte (B), lymphocyte (C), and neutrophil counts (D) were all acutely depleted by TBI. Monocytes and neutrophils recovered by 30 days post-irradiation while total white blood cells and lymphocytes remained significantly decreased until days 51 and 58 post-irradiation respectively. After recovery, total white blood cells, monocytes, and neutrophils in IRR animals did not differ from CTL but lymphocytes increased above CTL animals at day 129 post irradiation and remained elevated thereafter. *p<0.05, **p<0.01, ***p<0.001

Monocytes were isolated from peripheral blood mononuclear cells (PBMCs) by a positive selection strategy using anti-CD14+ magnetic beads. The monocyte fraction was then sorted into classical, intermediate, and non-classical monocyte subsets using fluorescence-activated cell sorting (FACS) prior to and 6 months after TBI (isolation scheme Figure 2.7 and gating strategy Figure 2.8).

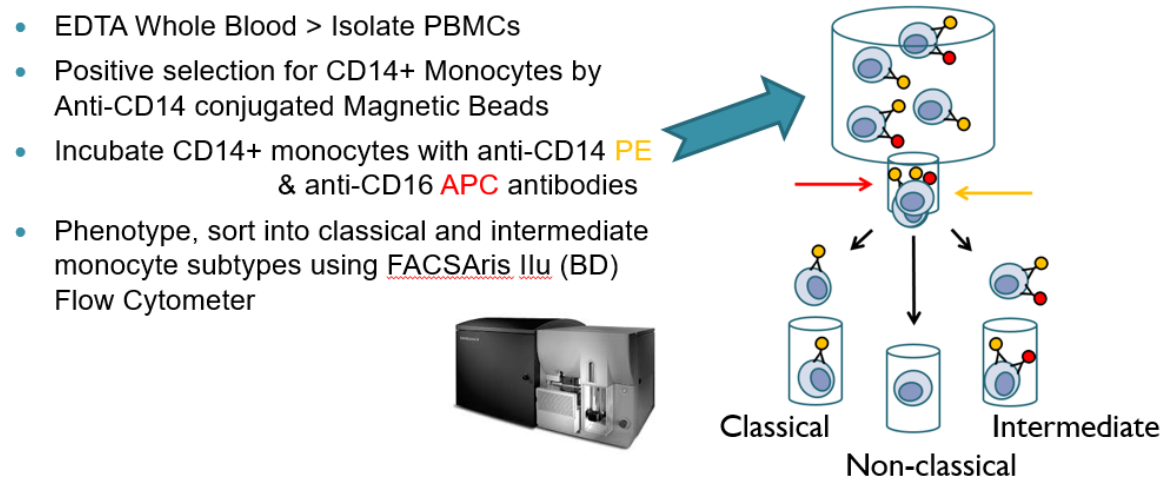

Figure 2.7: Strategy for monocyte subset isolation using magnetic bead sorting.

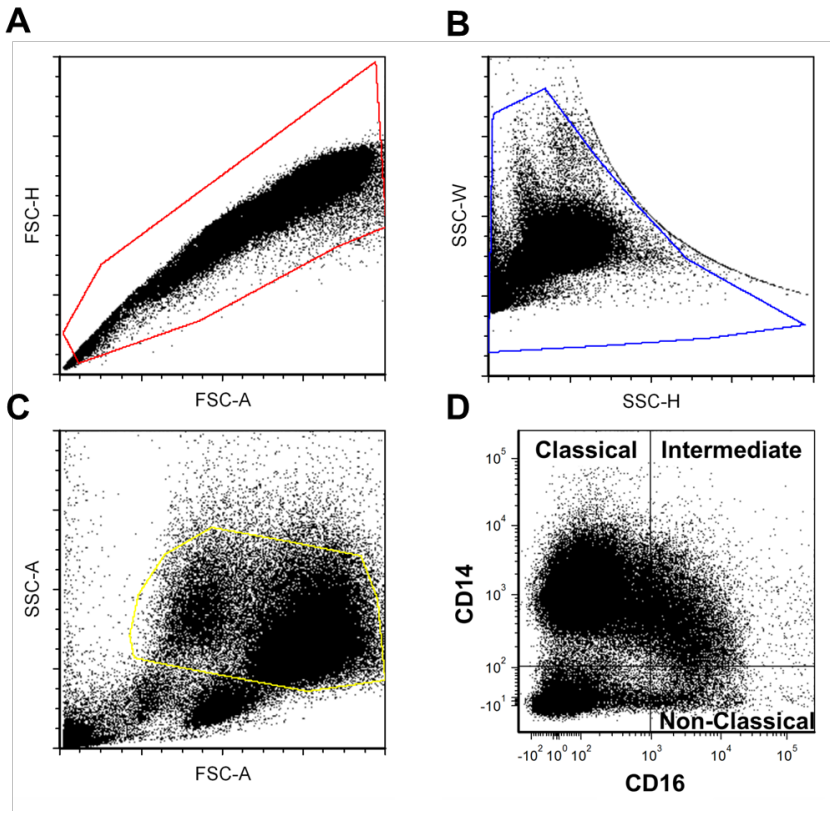

Figure 2.8: Gating Strategy to Obtain Monocyte Subsets. Magnetic bead selected CD14+ monocytes were gated based on forward and side scatter parameters before final gating into classical (CD14++, CD16-), intermediate (CD14++, CD16+) and non-classical (CD14+low, CD16++) phenotypes. Panel A: Forward scatter plot; Panel B: Side scatter plot; Panel C: Forward scatter- Side scatter; Panel D: Final representation of monocyte subsets by CD14 & CD16 labeling. Profiles from a representative sample from an irradiated animal at 6 months post-irradiation are shown.

At 6 months post irradiation, monocyte polarization shifted towards lower classical (92% ↓ 86%) and higher intermediate (7% ↑ 12%) and non-classical monocyte subsets (0.6% ↑ 2%) (all $p<0.05$) in IRR animals compared to baseline (Figure 2.9). No change in monocyte subsets was observed in CTL animals.

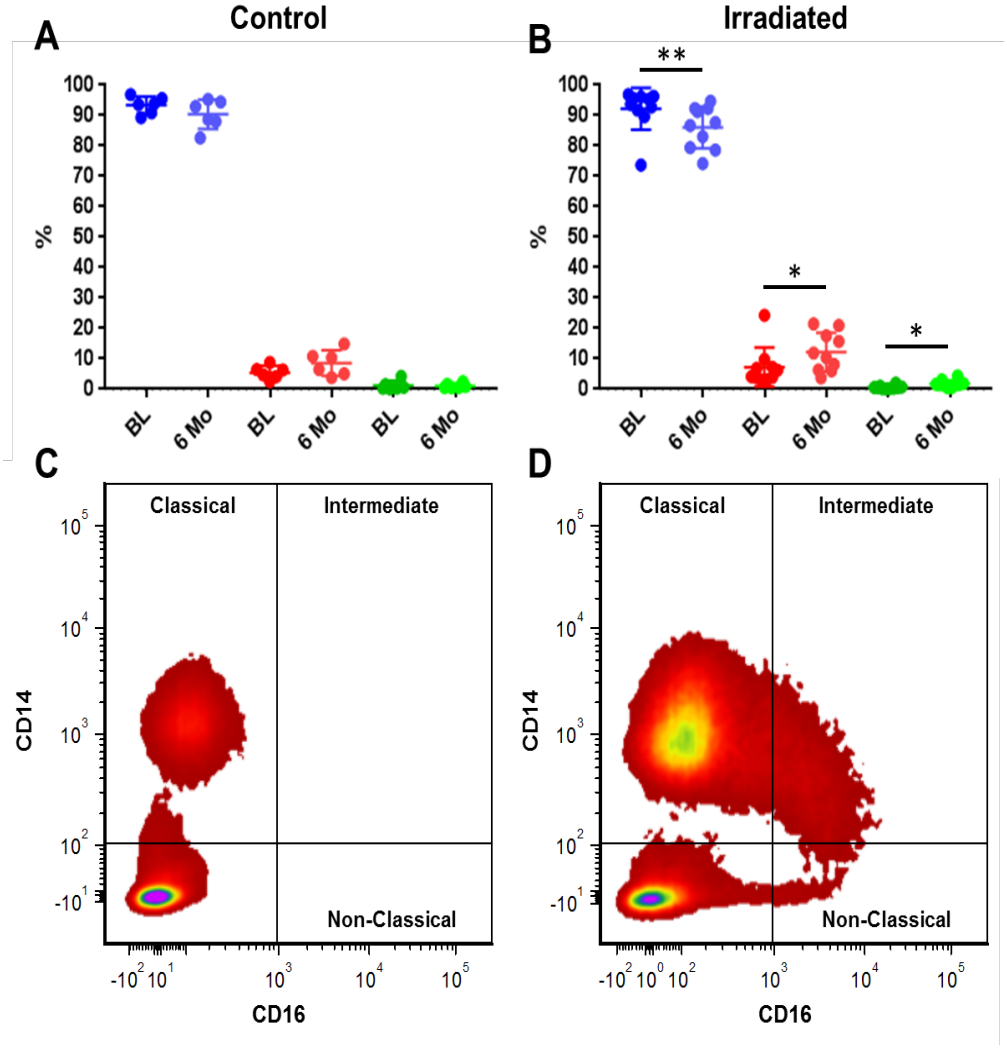

Figure 2.9: Alterations in Distribution of Monocyte Subtypes after Total Body Irradiation. Monocyte polarization was unaltered in control animals at 6 months post sham-irradiation (A). In contrast in irradiated animals has significant shifts shifted towards lower classical and higher intermediate and non-classical monocyte subsets compared to baseline (B). Flow cytometry density plots from a representative control (C) and irradiated (D) animal are shown at 6 months post-irradiation. (*$p<0.05$, **$p<0.01$)

Monocyte Subtypes Exhibit Distinct Transcriptional Profiles Which Differentially Respond to TBI

Transcriptional profiles in classical and intermediate monocyte subsets were assessed using RNAseq. Prior to irradiation, classical monocytes significantly differed from intermediate monocytes, with greater expression of pathways involved in

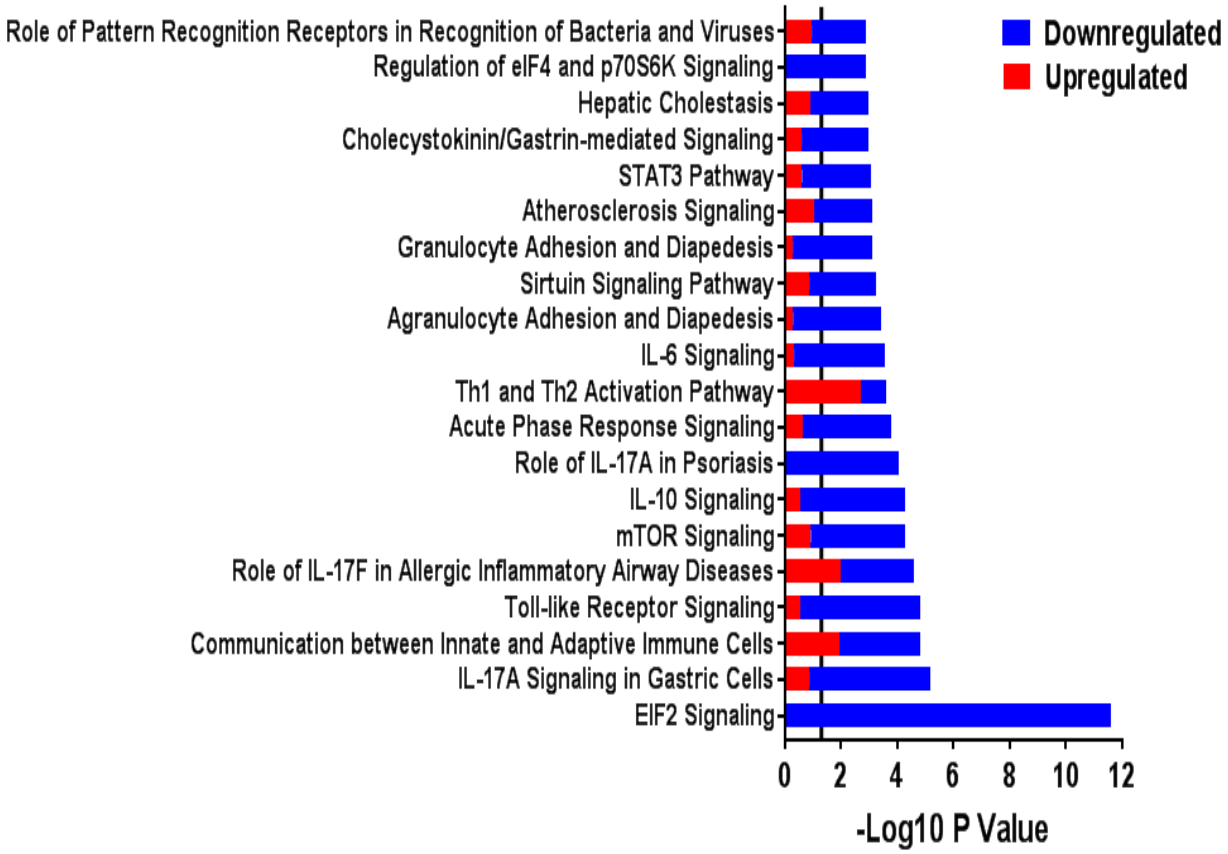

Figure 2.10: Canonical Pathways Differentiating Intermediate from Classical Monocyte Subtypes at Baseline (All Subjects, Pre-Irradiation). Within each pathway, red bars indicate the proportion of upregulated DEGs in the Intermediate Monocyte, blue bars indicate proportions of downregulated DEGs. The vertical line indicates the threshold for significance based on a -Log10 P Value of 1.3 (equal to $p<0.05$).

Classical monocyte gene expression did not change significantly over time or cross-sectionally between IRR or CTL groups. In contrast, significant numbers of differentially expressed genes (DEGs) were detected in intermediate monocyte comparisons between IRR vs. all animals at baseline (BL) (304 DEGs), and in IRR vs. CTL animals 6 months after irradiation (67 DEGs). Intermediate monocytes also differed between baseline and 6 months in CTL animals (147 DEGs). Pathway analysis was used to identify genes within significant canonical pathways, yielding 60 DEGs that were specific to IRR intermediate monocytes (data not shown). These DEGs and significant canonical pathways were associated with pro-fibrotic and anti-inflammatory signaling pathways that have been noted to induce M2 macrophage polarization upon extravasation (Figure 2.11). These findings support the hypothesis that TBI may alter monocyte programming and polarization towards a profibrotic phenotype, providing a novel target opportunity for therapies to inhibit or prevent RIF.

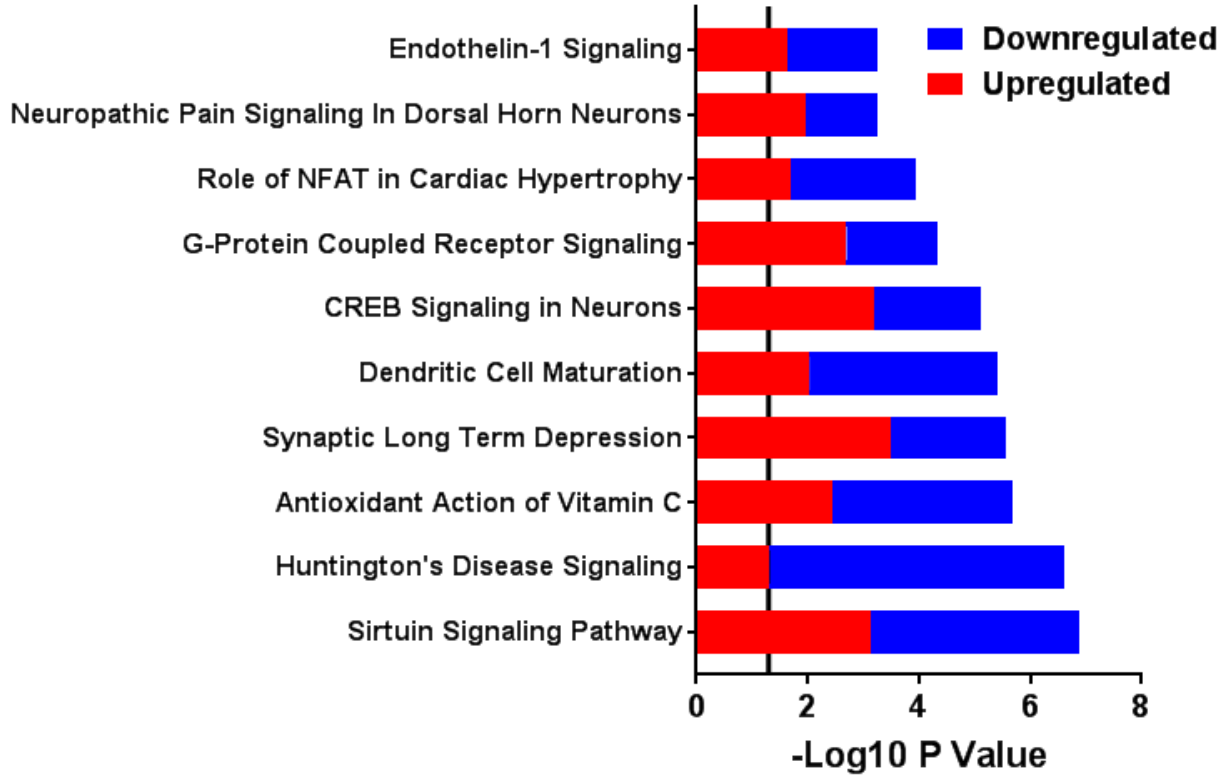

Figure 2.11: Canonical Pathways in Differentiating Irradiated vs. Control Intermediate Monocytes in both Cross-Sectional and Longitudinal DEG. Red bars indicate upregulated and blue bars indicate downregulated proportions of DEGs in Irradiated subjects within the respective pathway. The vertical line indicates the threshold for significance based on a -Log10 P Value of 1.3 (equal to $p<0.05$).

4) Other Achievements:

Grants: We leveraged the availability of the PRC to conduct further explorations of radiation effects through an institutional pilot grant, which led to submission and funding of a large pilot grant to the Center for Medical Countermeasures Program entitled *"Monocyte Polarization in Acute & Delayed Responses to Total Body Irradiation in Nonhuman Primates"*. Year 01 of the work has been accomplished and a manuscript is about to be submitted.

Abstracts: An abstract was submitted and accepted for the 2018 Radiation Research Meeting, describing the effects of radiation on circulating cell populations from the RSC in collaboration with Project 3. Abstracts, presentations, and manuscripts are listed in section 6.

Awards:
Ryne J. DeBo 2017 Radiation Research Editors' Award Lecture for the publication: DeBo RJ, Lees CJ, Dugan GO, Caudell DL, Michalson KT, Hanbury DB, Kavanagh K, Cline JM, Register TC. "Late Effects of Total Body Gamma Irradiation on Cardiac Structure and Function in Male Rhesus Macaques." 2017 Radiation Research Society Scholars in Training Workshop, Cancun, Mexico, October 2017

Project 3: Immune Recovery (Chen/Sempowski - Duke)

1) Major Activities (Year 3)

- **a)** Biobanked aliquots of PBMC from the Prospective NHP cohort (X-15-03) were thawed and processed for molecular analysis in Projects 3 and 4.
- **b)** Fresh bleeds from the Long-term survivor NHP cohort (X-10-12) were received and processed at Duke in October, November and December 2017 (68 NHP samples total). Bleeds from the long-term survivor cohort (X-10-12) were also received in January, February and March (42 NHP samples total, including 23 new additions to the cohort and 1 terminal bleed). PBMC were isolated from each blood sample and used for immunophenotying with previously described flow cytometry panels.
- **c)** We completed all flow cytometry gating on all PBMC samples received in Year 2 and 3 and used these data to prepare draft to stimulate statistical model development and manuscript preparation.
- **d)** Purified CD4 and CD8 T cells from PBMC collected from the Prospective NHP cohort (X-15-03) and the long-term survivor cohort (X-10-12) for sjTREC analysis.
- **e)** In collaboration with Project 1 (Kavanagh), the Project 3 group performed flow cytometry to phenotype the thymic and peripheral T cell populations in irradiated mice left untreated or treated with an anti-fibrotic (via TGFβ1R inhibition) +/- an angiogenic (tadalafil) in a 2x2 design.
- **f)** We continued to study the roles of thymopoiesis and peripheral expansion in overall T cell recovery in a classic mouse radiation injury model. We have monitored these animals for up to 480 days after irradiation to determine whether TBI induces permanent quantitative immune defects. Total T, B, and T cell subsets were monitored in peripheral blood overtime.
- **g)** We acquired the animals to study the roles of thymopoiesis and peripheral expansion in overall T cell recovery in a second mouse radiation injury model.
- **h)** We developed a bioluminescent imaging technique that allows tracking of T cell recovery in whole body over time. More complete picture of T cell recovery will be generated.
- **i)** We studied the effect of IGF-1 on phenotypic immune recovery pos-irradiation.

2) Specific Objectives (Year 3)

SA1 Major Task 1: NHP Studies
Milestone 1.1. Phenotypic analyses in long-term cohort
Milestone 1.2. Molecular analysis in long-term cohort
Milestone 1.3. Phenotypic analyses in prospective cohort
Milestone 1.4. Molecular analysis in prospective cohort
Milestone 1.5. Determine primary immune response to vaccination (Prospective Cohort)

SA1 Major Task 2: Murine Studies
Milestones 2.2. Determine the roles of thymopoiesis and peripheral expansion in overall T cell recovery in the classic radiation injury model.
Milestones 2.3. Determine the roles of thymopoiesis and peripheral expansion in overall T cell recovery in a second radiation injury model.

SA2 Major Task 4: Murine Studies

Milestones 4.1. Determine the effect of IGF-1 on phenotypic T cell reconstitution

3) Results/Key Outcomes
SA1 Major Task 1: NHP Studies (Sempowski, Duke)

Milestone 1.1. Phenotypic analyses in long-term cohort (X-10-12)

The X-10-12 Long-term Survivor cohort of 108 NHP (control and irradiated) cross-sectionally analyzed at distinct dates over the five year study to monitor immune recovery and correlate with radiation dose and age.

Progress this year:

- The first set of 108 samples were shipped and processed in November 2016. The shipping and processing of the second set of samples started in late August 2017 and was staggered across the fall to ensure the process remains manageable as the cohort increases in size. Specifically this year bleeds from the long-term survivor NHP cohort were received in October, November and December (68 NHP samples total).
- Additional bleeds from the long-term survivor cohort (X-10-12) were received in January, February and March (42 NHP samples total, including 23 new additions to the cohort and 1 terminal bleed). All original animals phenotyped in Year 2 have now been profiled twice and all newly added animals have been phenotyped once.
- All phenotype data from the now complete two Long-term cohort phenotypic analyses were merged and analyzed by the team for changes over time with respect to age, radiation dose, etc. (See Figures 3.1 – 3.4 below)

***Approach*:** The sample collection and shipment schedule is coordinated by the WF Primate Core team. On each shipment day, fresh NHP blood (two 10 mL GTT sodium heparin tubes) from the long-term survivor NHP cohort is packaged and shipped via first overnight Federal Express shipment (room temp) to the Sempowski lab at Duke. Blood receipt is confirmed with WF and processed by standard ficoll separation to isolate peripheral blood mononuclear cells (PBMC) and plasma. Aliquots of PBMC are retained for a fresh immunophenotype and viability assessment. The remainder of the PBMC are cryopreserved using standard DMSO freeze medium and stored in liquid nitrogen for batch processing for sjTREC, sharing with Project 4 and possible TCR sequencing. Aliquots of Plasma and Serum are also crypopreserved for potential add on studies, such as multiplex cytokine profiling in collaboration with Project 2. All samples and aliquots are inventoried in the Sempowski group FreezerPro lab inventory control system. All freezers are on 24/7 emergency power back up and 24/7 remote temperature monitoring (Minus 80 Inc.) with alarm notifications via phone, text and email. An empty backup -80°C freezer is kept at the ready in case a freezer fails. The Sempowski lab is housed in the Duke Regional Biocontaiment laboratory, which has an external bulk liquid nitrogen (LN2) storage tank containing sufficient LN_2 to supply all storage tanks for one month without refill.

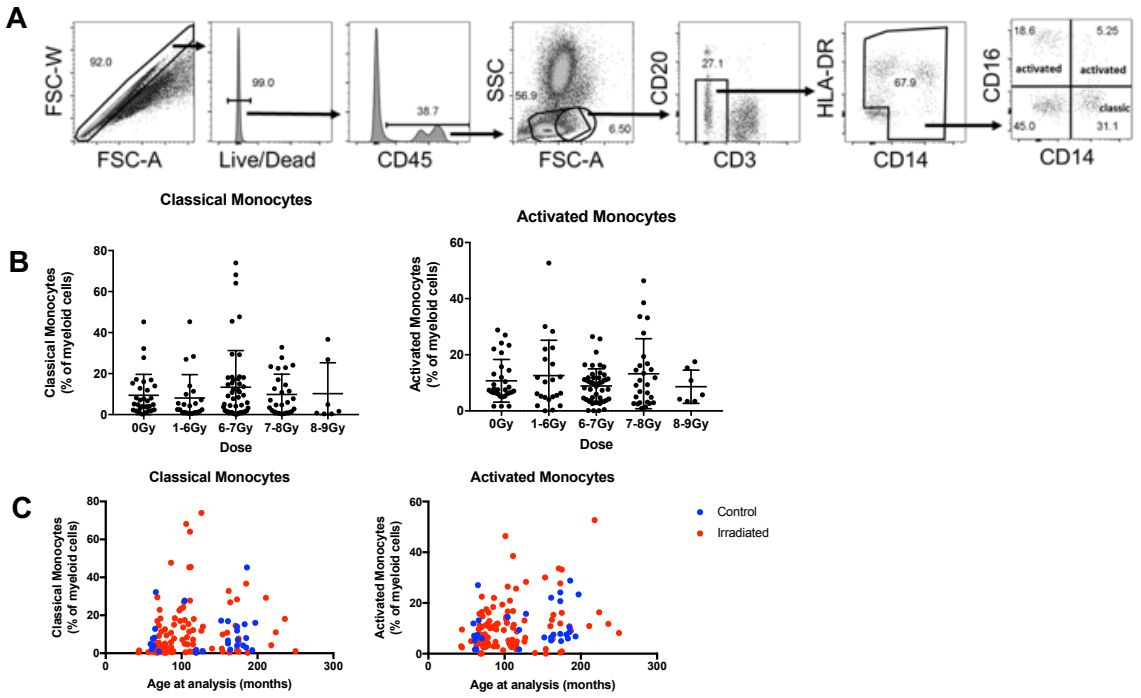

Figure 3.1. Immunophenotyping of monocyte populations in PBMC from survivor cohort in Year 2. (A) gating strategy. (B) monocyte percentages relative to dose. (C) Monocyte percentages relative to age at analysis.

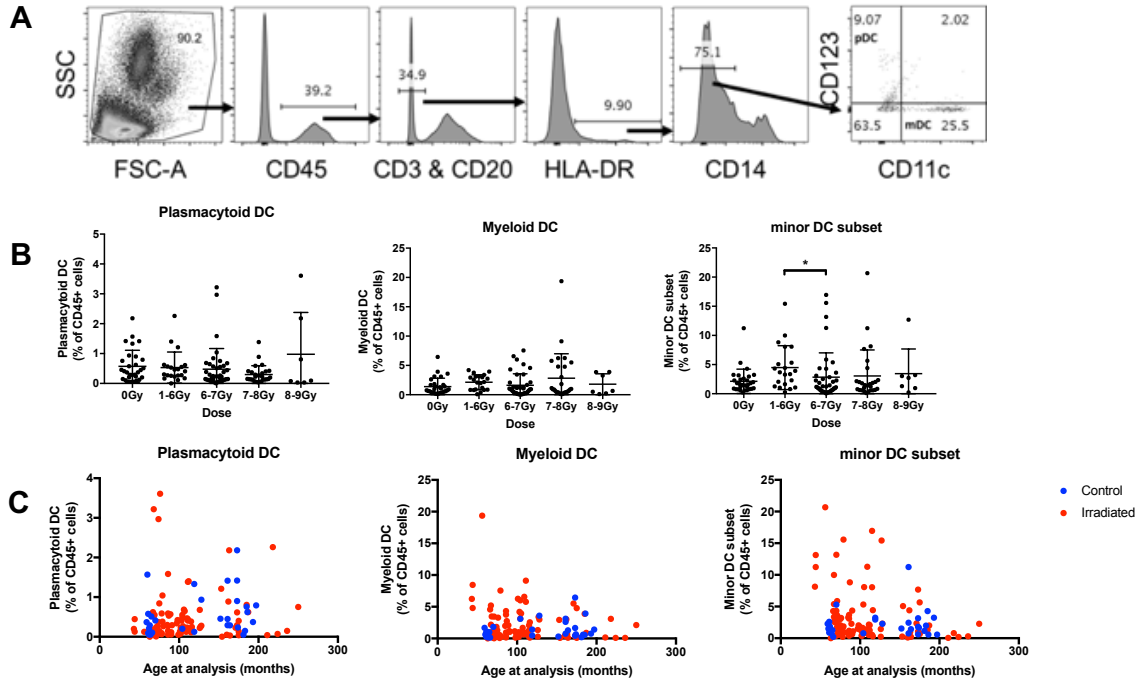

Figure 3.2. Immunophenotyping of dendritic cell (DC) populations in PBMC from survivor cohort in Year 2. (A) gating strategy. (B) DC percentages relative to dose. (C) DC percentages relative to age at analysis.

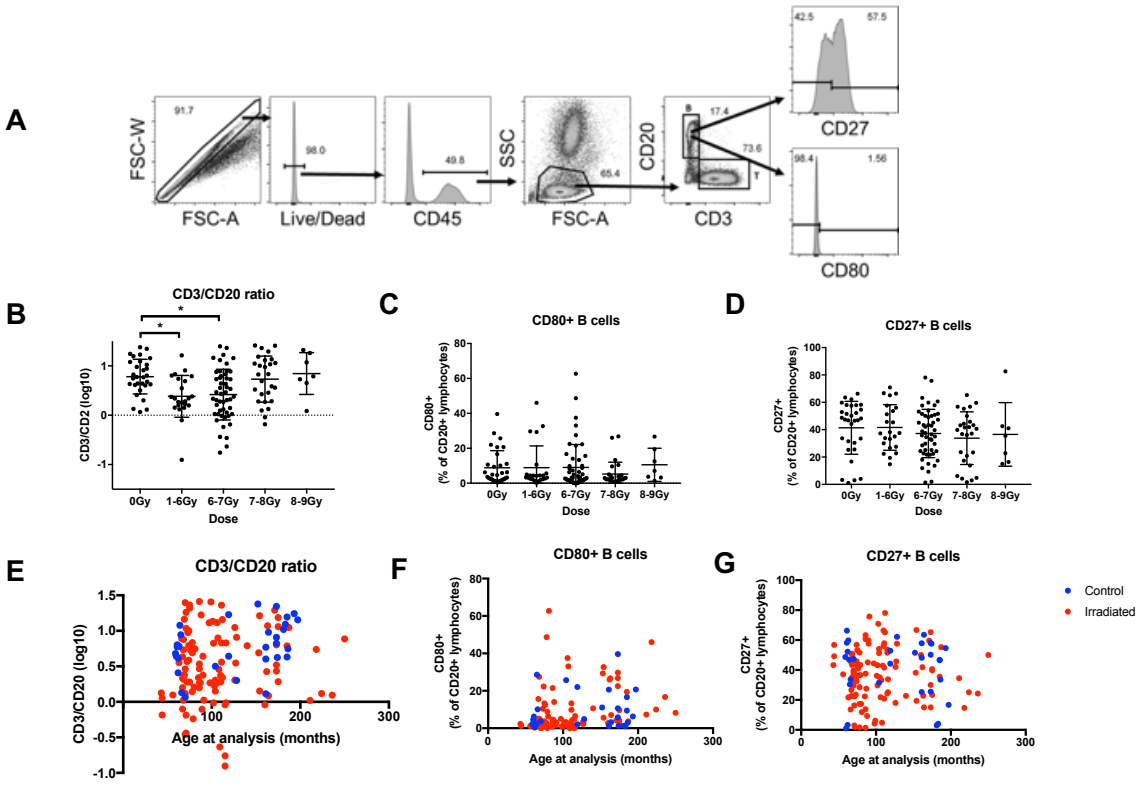

Figure 3.3. Immunophenotyping of B cell populations in PBMC from survivor cohort in Year 2. (A) gating strategy. T cell/B cell ratio (log(CD3/CD20)) in proportion to (B) dose and (E) age. B cell CD80 expression proportion to (C) dose and (F) age. B cell CD27 expression proportion to (D) dose and (G) age.

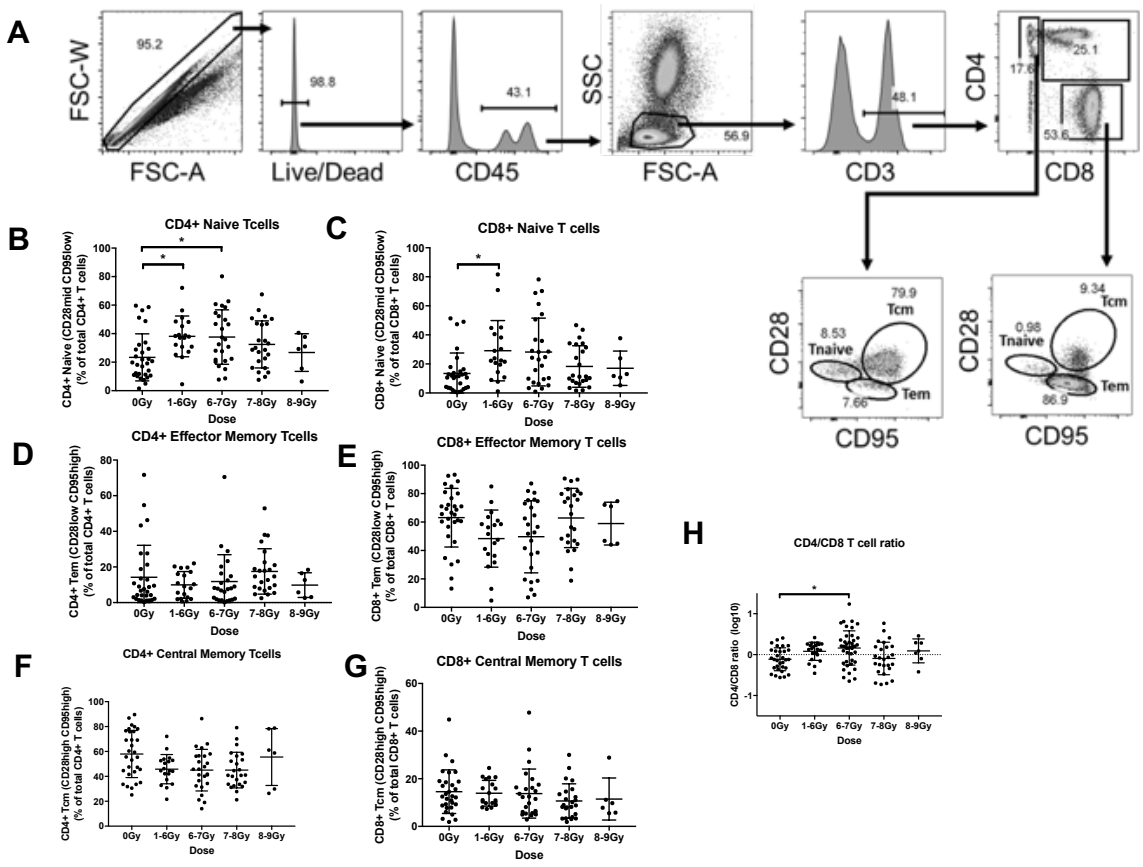

Figure 3.4. Immunophenotyping of T cell populations in PBMC from survivor cohort in Year 2. (A): gating strategy. Proportion of (B) CD4 and (C) CD8 naïve, (D) CD4 and (E) CD8 effector memory T cells and (F) CD4 and (G) CD8 effector memory T cells relative to dose. (H) CD4:CD8 T cell ratio in proportion to dose.

<u>Milestone 1.2. Molecular analyses in long-term cohort (X-10-12)</u>

sjTREC (a molecular qPCR assay for monitoring thymopoiesis) are reported as number of sjTREC Molecules/100,000 isolated T cells (CD4 or CD8). These non-replicating extrachromasomal circles of excised genomic DNA are the result of TCR gene rearrangement and are diluted out in a given T cell population. Each new/naive T cell emigrating the thymus gland starts with two circles and they are then transferred without being replicated to daughter T cells as the population of naïve T cells expands and matures. A high frequency of sjTREC in a population indicates robust thymopoiesis and thus export of naïve T cells into the the periphery. A low frequency of sjTREC in a populations suggests poor thymic function (due to age, stress, damage) and a resultant peripheral t cell pool of older memory phenotype T cells.

In Year 2, PBMC were collected and stored from all 108 animals present in the long-term survivor cohort at the time. In Year 3, we used magnetic-bead positive selection to isolate CD4 and CD8 T cells from these PBMC and quantified sjTREC in each population (Figure 3.5). These preliminary sjTREC results were evaluated by Kruskal-Wallis one-way ANOVA. The results suggest that CD8 sjTRECs levels increase following radiation exposure but decrease with time post-irradiation. These sjTREC data are being used to create a longitudinal mixed-effects model to determine the relative contributions of age, dose, time since radiation exposure and sex.

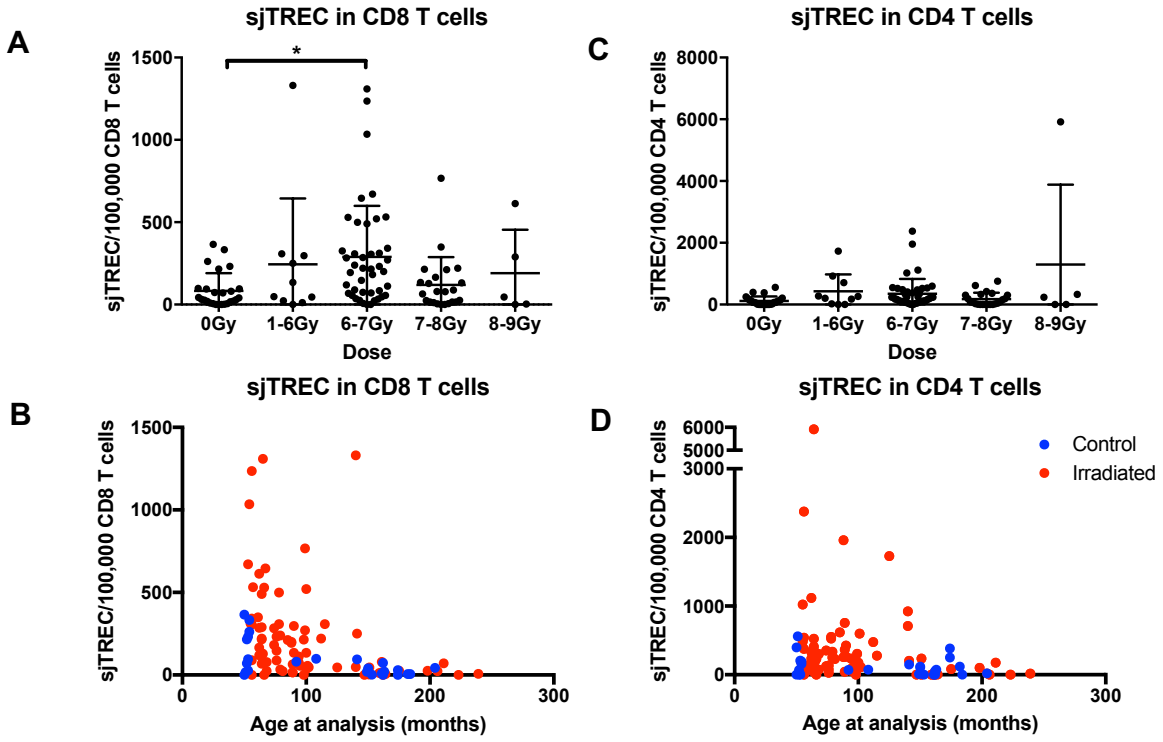

Figure 3.5. Number of molecules of sjTREC in CD8+ (A, B) and CD4+ (C, D) T cells isolated from the long-term survivor cohort in Year 2 (CD8: n=107; CD4: n=106). Mean ± SD). Data expressed relative to (A, C) dose and (B, D) age at analysis.

At intervals throughout Year 3, PBMC and plasma from all 137 animals in the long-term survivor cohort were isolated and stored. CD4 and CD8 T cell populations from a subset of these PBMC samples were isolated using magnetic-bead positive selection and sjTREC were quantified (CD4 n= 60, CD8=50; Figure 3.6). Cell isolation and sjTREC quantification from the remaining Year 3 PBMC samples is ongoing.

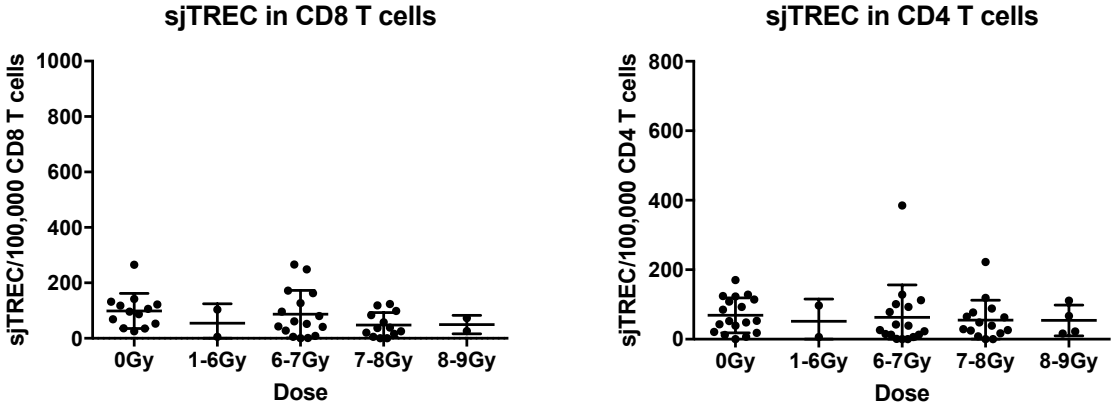

Figure 3.6. Preliminary sjTREC analysis in CD8+ and CD4+ T cells isolated from a subset of the long-term survivor cohort collected during Year 3 (CD8: n=46; CD4: n=56. Mean ± SD).

***Summary to Date - Long-term cohort (X-10-12)*:** Draft publication-quality figures from the Year 2 and 3 immunophenotyping (Figures 3.1-3.4) illustrate the dose-related effects of TBI on the naïve T cell populations, with animals receiving 6-7Gy TBI showing an increased percentage of naïve T cells (Figure 3.4 B, C). This correlates with the finding that there are higher sjTREC per 100,000 T cells in these animals (Figures 3.5 and 3.6). Other immune cell populations do not show major differences between irradiated and non-irradiated animals at this timepoint. However, as shown in Figures 3.5B, 3.1C, 3.2C and reported elsewhere (Asquith et al, *Pathobiol Aging Age Relat Dis.* 2012;2; *Eur J Immunol,* 2000, 30(4):1145), many changes in NHP immunophenotype correlate strongly with age and hence time since irradiation. The impact of age and potential statistical interactions with irradiation, sex and other factors will be tested through analysis of the accumulating repeated measure dataset.

In Progress - TCR Repertoire: To address the need to determine T Cell Receptor (TCR) repertoire in our PBMC samples, we have enlisted the help of two investigators at Duke (Drs. Bradley and Wiehe). Dr. Bradley runs the Duke Human Vaccine Institute Sequencing Facility and has internally developed a TCR sequencing approach to analyze NHP TCR repertoire. We are using his facility on a fee-for-service basis to run this assay described below). Dr. Wiehe is an accomplished computational immunologist and will provide the analytics to the TCR analysis with help from Dr. Shterev. Pilot samples to determine RNA / cell number input for this assay have been sequenced and the files are currently being analyzed
Approach: RNA from bulk PBMC or isolated T cell populations will be extracted and TCR sequencing libraries will be prepared using the Rhesus TCR profiling amplification kit (Takara). Primers specific for the rhesus TCR constant regions are used to amplify cDNA adding a custom adapter to the 5' end of the sequence. Libraries will be quantified and sequenced on the Illumina MiSeq platform to generate full-length TCRa and TCRb reads. TCR sequences will be annotated using the computational program MiXCR, an annotation software that is designed to efficiently process high throughput TCR sequencing datasets [Bolotin/Chudamov Nat Meth 2015]. Custom Rhesus-specific TCR annotation libraries will be built using data from the IMGT database [Lefranc NAR 2009] and supplemented with TCR sequence data from a recent genomic sequencing of the TCR locus of 10 Indian rhesus macaques that greatly expands the characterization of rhesus antigen receptor allelic diversity [Ramesh/Kepler Front. Imm 2017]. TCR sequences will be grouped into clonotypes and quantitated using a combination of MiXCR and custom-built computer programs.

Milestone 1.3. Phenotypic analyses in prospective cohort (X-15-03)
In August 2018 we isolated and stored PBMC and plasma from all 16 surviving animals in the prospective cohort. This was one year after the previous collection date for this cohort and approximately 21 months from the original date of irradiation. PBMC from all 16 animals were immunophenotyped via flow cytometry using previously described panels for T cells, B cells, dendritic cells, NK, NK-T and monocytes. Analysis of these data is ongoing.

Milestone 1.4. Molecular (sjTREC) analyses in prospective cohort (X-15-03)
Frozen aliquots of PBMC from the prospective NHP cohort at baseline, 4 months and 9 months post irradiation (49 samples total) were thawed and the number of viable cells in each aliquot counted. 0.5 to 1 million PBMC from each aliquot were provided to Project 4 (Dave) for RNASeq analysis. CD4 and CD8 T cells were then isolated from the remaining PBMC via magnetic-bead positive selection and the cell pellets analyzed for sjTREC (Figure 3.7).
As with previous timepoints, defrosting of the PBMC from the 21-month timepoint will be coordinated with Project 4 so that a single PBMC aliquot can be used for both sjTREC quantification and RNASeq.

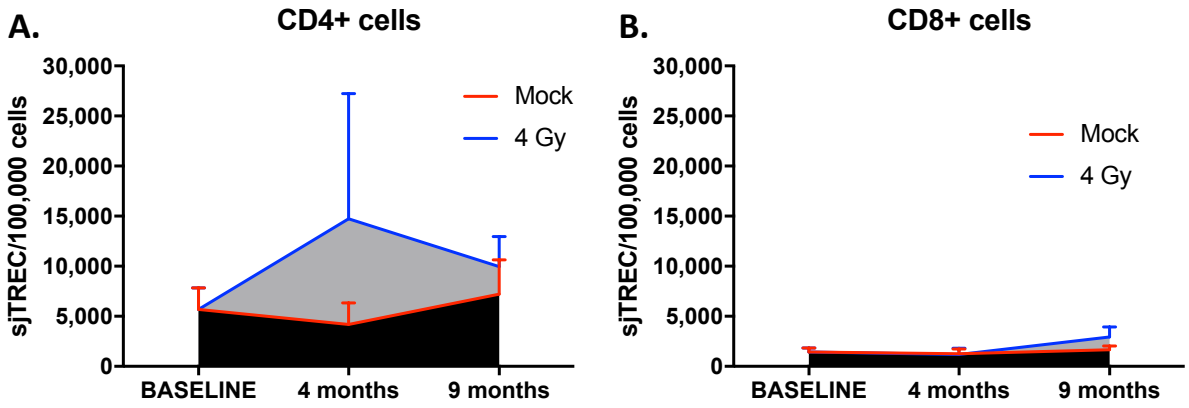

Figure 3.7. sjTREC levels in CD8+ and CD4+ T cells isolated from the prospective cohort (n=20 at baseline; n=16 at 4 and 9 months; mean ± SD).

***Summary to Date - Prospective cohort (X-15-03)*:** Mock and 4Gy irradiated animals start with equivalent sjTREC levels in both the CD4 and the CD8 compartments. At 4 months post irradiation the 4Gy group appears ot have a burst of thymic output of new CD4 T cells which then normalized to a level similar to the mock treated animals by 9 months. This is consistent with a "damage and recovery" surge in thymopoiesis typically observed following damage. That is the thymus over compensates and send out a burst of Naïve T cells to rebuild the peripheral pools that may have been damaged by the stress event, in this case acute radiation. The baseline and sjTREC levels are much lower in the CD8 compartment and this may be due to CD8 cellular responses 9proliferative expansion of naïve T cells clonal pools) in these cohorts that are resulting in a dilution and thus reduction in the frequency of the sjTREC in the CD8 compartment. We do not appear to see a a burst at 4 months of CD8 export from the thymus.

Additional Collaboration Effort

In collaboration with Project 1 (Kavanagh), the Project 3 group (Sempowski et al.) used flow cytometry to phenotype the thymic and peripheral T cell populations in 35 sub-lethally irradiated mice left untreated or treated with an anti-fibrotic (via TGFβ1R inhibition) +/- an angiogenic (tadalafil) in a 2x2 design. Thymic tissue, thymocytes and splenocytes were also cryopreserved for later sjTREC and or RT-PCR analysis. Preliminary data from this experiment are discussed in the report from Project 1.

SA1 Major Task 2: Murine Studies (Chen, Duke)

Milestones 2.2. Determine the roles of thymopoiesis and peripheral expansion in overall T cell recovery in the classic radiation injury model.

As described in the Year 2 annual report, we started an experiment to determine the roles of thymopoiesis and peripheral expansion in overall T cell recovery in a classic radiation injury model. The data from the first 180 days after irradiation were presented in the Year 2 annual report. Due to the unexpected observations that T and B cell numbers were able to recover back to normal level up to 180 days post-irradiation, we continued to follow these animals to see whether these results hold with longer follow-up in Year 3. The updated data from this experiment are presented below:

As previously reported, 8-12 week-old C57BL/6 mice were irradiated with three different doses of radiation (2, 5, 7 Gy). Two additional control groups were added in this experiment. The first control is age-matched non-irradiated mice. The second control group was irradiated with 7 Gy and transplanted with 1x10e5 Lin- bone marrow cells from normal C57BL/6 mice. The data through day +180 were described in detail in the previous report. In this report, we will only describe the data after day +180.

Total T cells (CD3+) and B cells (B220+) were measured in peripheral blood over time post-irradiation. Figure 3.8 shows that the numbers of both T and B cells in all irradiated groups were no longer lower than those in the non-irradiated control group at day +270. In fact, T cells were even higher in 2 Gy, 5 Gy, and 7 Gy when compared with those in non-irradiated control mice. At day +480, the numbers of T cells in all groups were lower than those measured at day +270. There were no differences in T cell numbers among experimental groups. The decline in B cells was not as much as that in T cells at day +480 in the non-irradiated control group. However, the numbers of B cells dropped more in all irradiated groups.

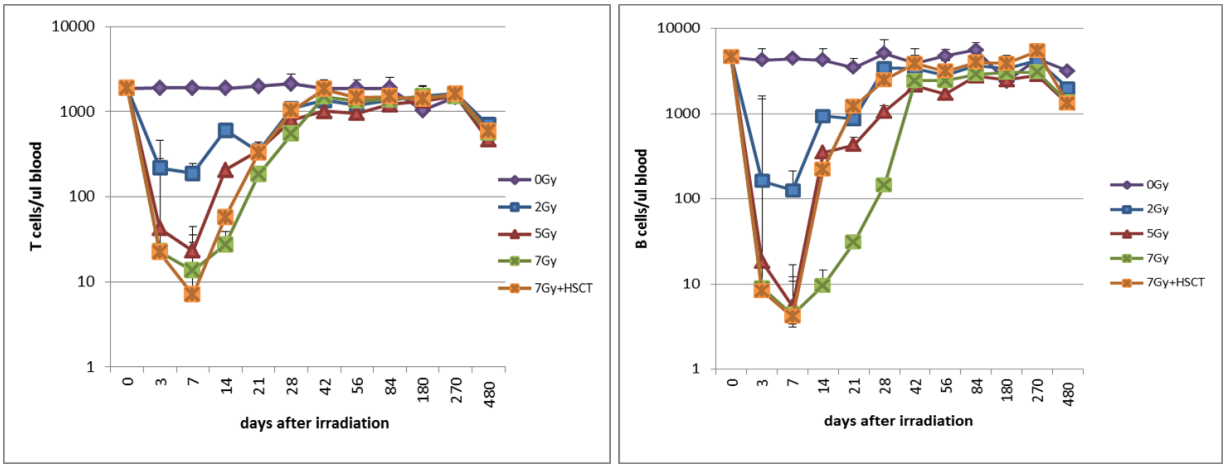

Figure 3.8. Mouse studies - T and B cell recovery in peripheral blood after irradiation.

As shown in Figures 3.9 and 3.10, the recovery of total CD4 and CD8 T cells followed a very similar pattern as that of total T cells (Figure 3.8). Similar results were obtained for both CD4+ and CD8+ naive (TN), central memory (TCM), and effector memory (TEM) T cells despite some minor differences at day +270.At day +480, the recovery of total CD4 and CD8 T cells followed a very similar pattern as that of total T cells (Figure 3.2). Similar results were obtained for both CD4+ and CD8+ naive (TN). In contrast, the numbers of both CD4+ and CD8+ central memory (TCM), and effector memory (TEM) T cells increased at day +480 compared with those at day +270.

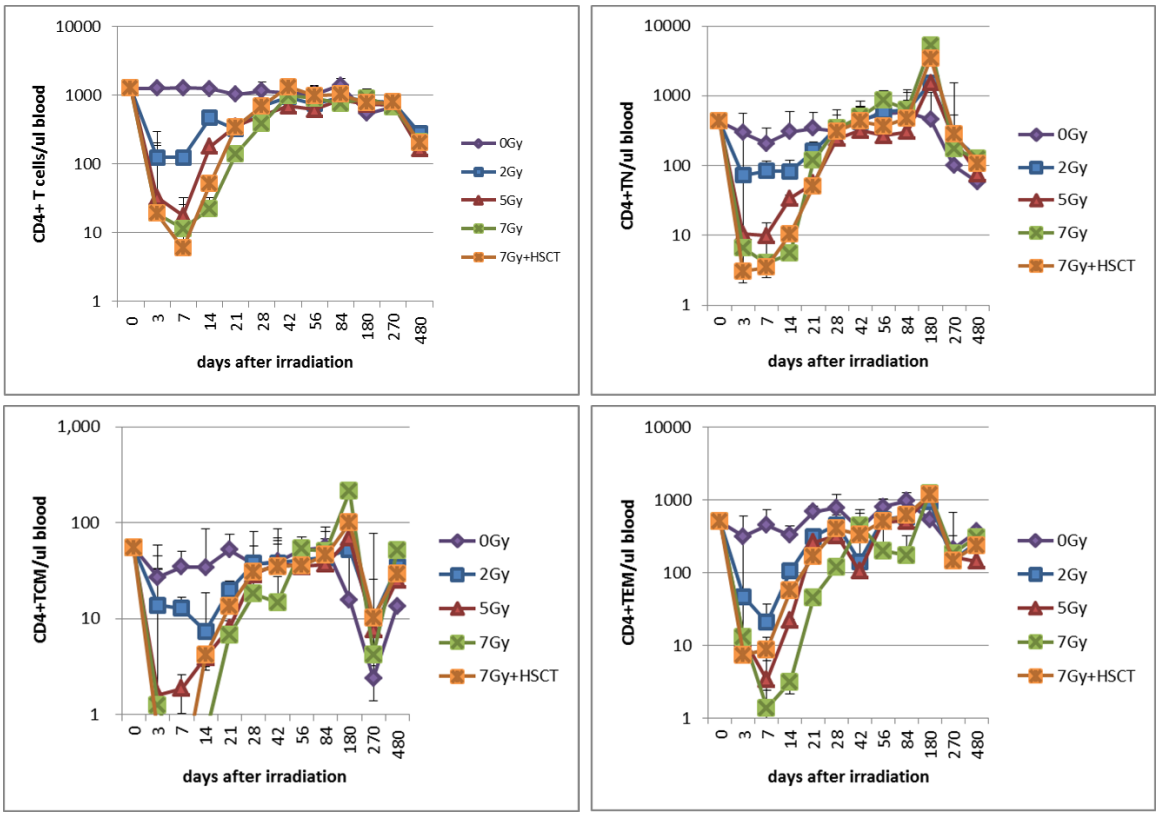

Figure 3.10. CD8 T cell recovery in peripheral blood after irradiation

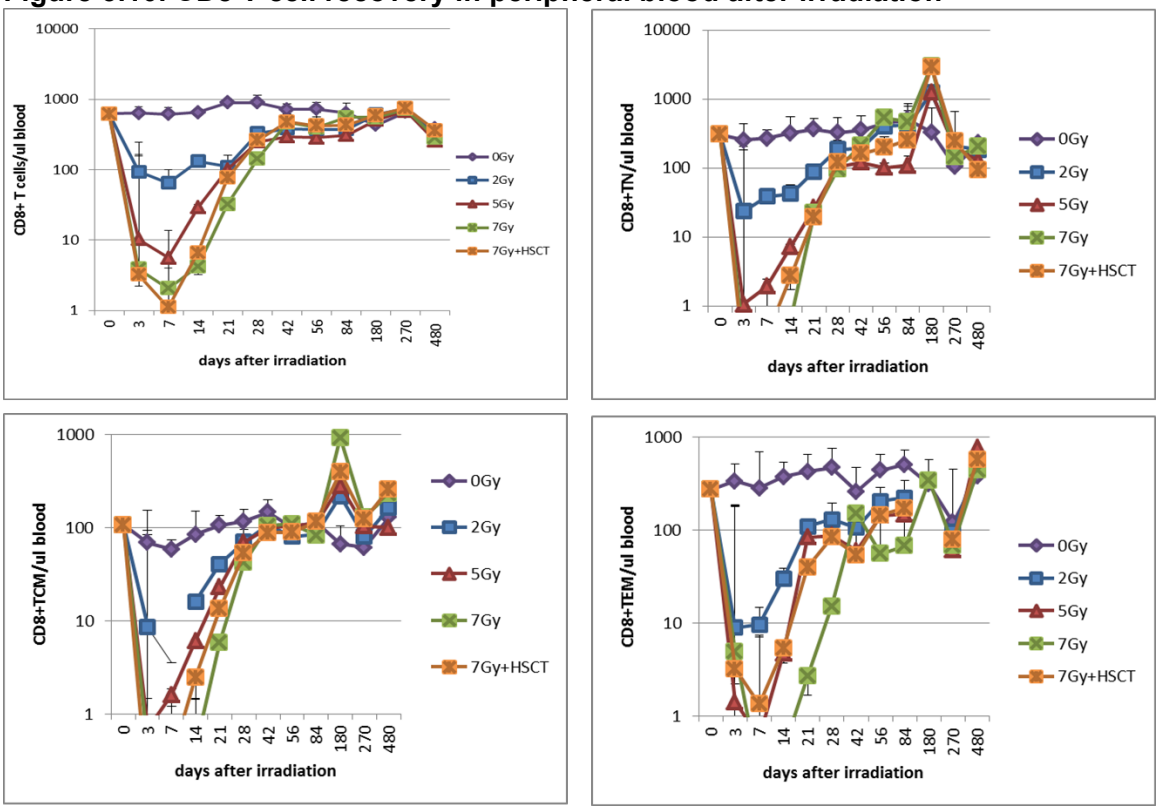

Figure 3.9. Mouse studies - CD4 T cell recovery in peripheral blood after irradiation

We also monitored the recovery of CD4+CD25+ regulatory T cells. As shown in Figure 3.11, Treg cells remained at very low level at day +270 and +480 in all groups.

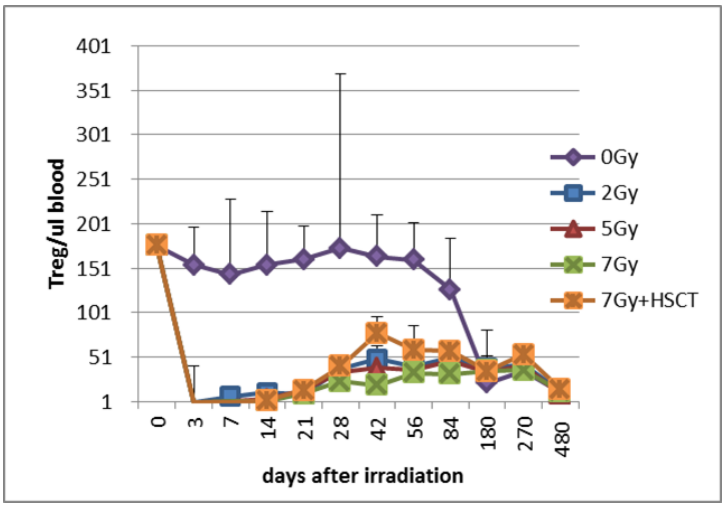

Figure 3.11. Mouse studies - Regulatory T cell recovery in peripheral blood after irradiation

Milestones 2.3. Determine the roles of thymopoiesis and peripheral expansion in overall T cell recovery in a second radiation injury model.

New Model: We have developed a novel animal model to study the role of peripheral expansion in the overall T cell recovery post-irradiation, (Figure 3.12). In this model, luciferase-transgenic T cells were first irradiated with several different doses of radiation (2, 5, 7 Gy). $1x10^7$ irradiated or control T cells were then transferred into lethally irradiated (10.5 Gy) beige C57BL/6 mice along with $1x10^5$ linage-negative bone marrow cells (to rescue lethally irradiated mice). T cell reconstitution was then followed in these mice over time by bioluminescent imaging (BLI).

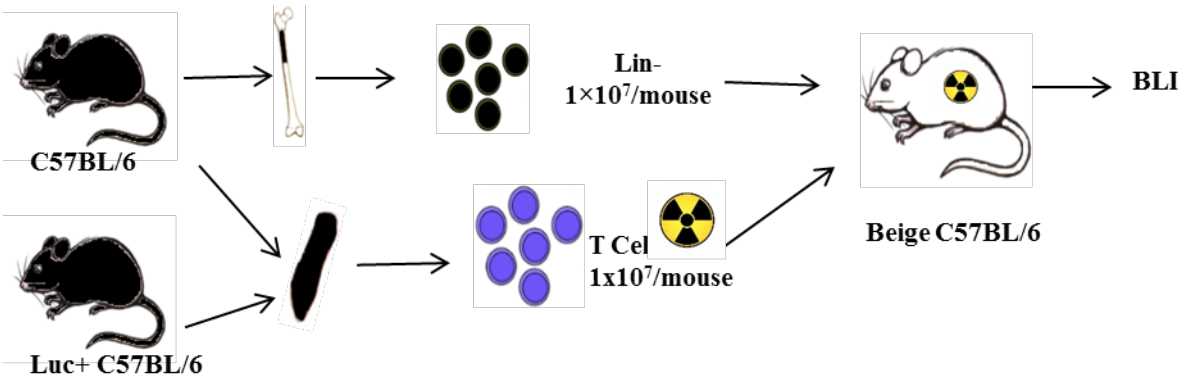

Figure 3.12. A schematic showing a novel model to study peripheral expansion of radio-resistant T cells using bioluminescent imaging

As shown in Figure 3.13 and 3.14, non-irradiated control T cells could be detected as early as day 7 after transfer; these T cells peripherated dramatically by day 14 and continued to expand through day 28. T cells irradiated by 2 Gy could not be detected until day 14 and strong signals were detected through day 28. At 5 Gy, T cells could also be detected at day 14 after transfer; however, the signals were much weaker than those in the control or 2 Gy groups; T cell signal could still be detected at day 21 but started to decline t day 28. At 7 Gy, no T cells could be detected by BLI at any time points.

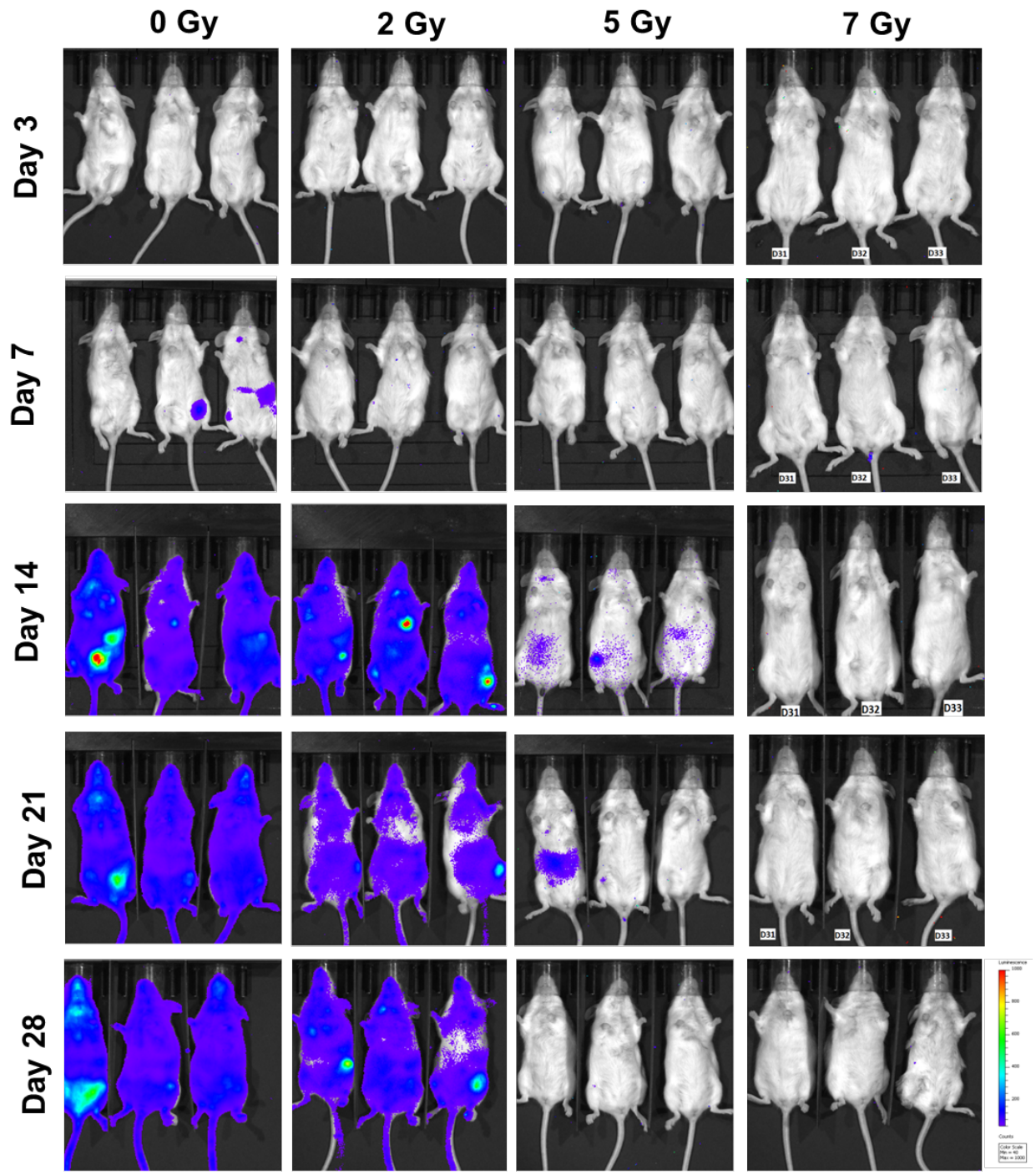

Figure 3.13. Bioluminescent imaging of peripheral expansion of radio-resistant T cell reconstitution. Representative images.

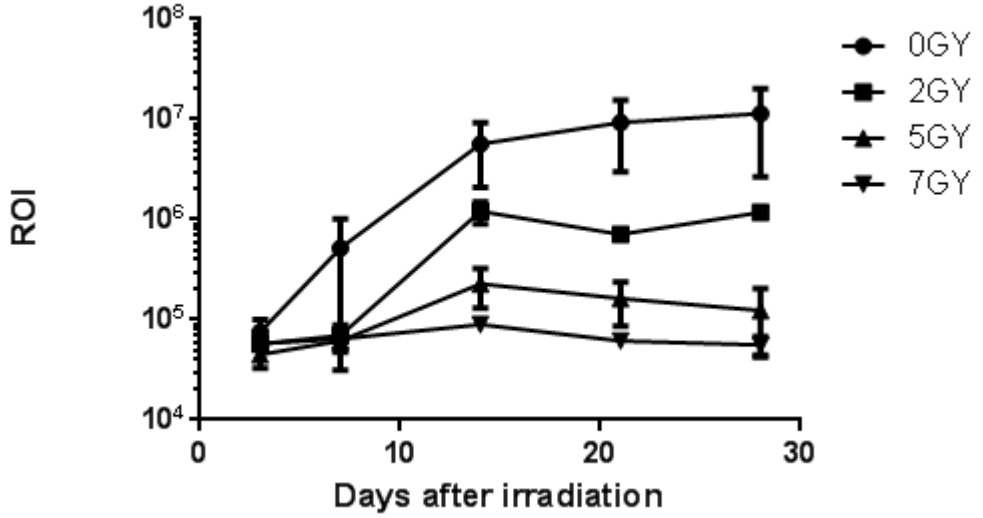

Figure 3.14. Peripheral expansion of radio-resistant T cells correlates negatively with radiation dose.

SA2 Major Task 4: IGF-1 Mouse Studies

Milestone 4.1. Determine the effect of IGF-1 on phenotypic T cell reconstitution

Based on our previous observations demonstrating that IGF-1 facilitates the recovery of hematopoietic stem cells (Zhou et al, Int J Radiat Oncol Biol Phys. 2013) and stem cell numbers positively correlate with immune recovery (Chen et al Blood. 2004), we hypothesized that IGF-1 can enhance T cell recovery post radiation exposure. In the first experiment, BALB/c mice were irradiated with 5 Gy and treated with IGF-1 intravenously at a dose of 100 µg/dose/day once a day for 5 days starting within one hour post radiation exposure.

As shown in Figure 3.15, we were unable to detect any effects of IGF-1 on the recovery of total white blood cells and multiple lymphocyte subsets including B cells, CD4 and CD8 T cells, NK cells, NKT cells. Even though these data suggested that IGF-1 might not be able to facilitate immune reconstitution post irradiation, another possibility could be the immune recovery was too fast for IGF-1 to show any effects at this dose of radiation. In fact, 500 cGy was reported to be a LD50/30 dose. However, none of the animals died within 90 days after irradiation in our studies.

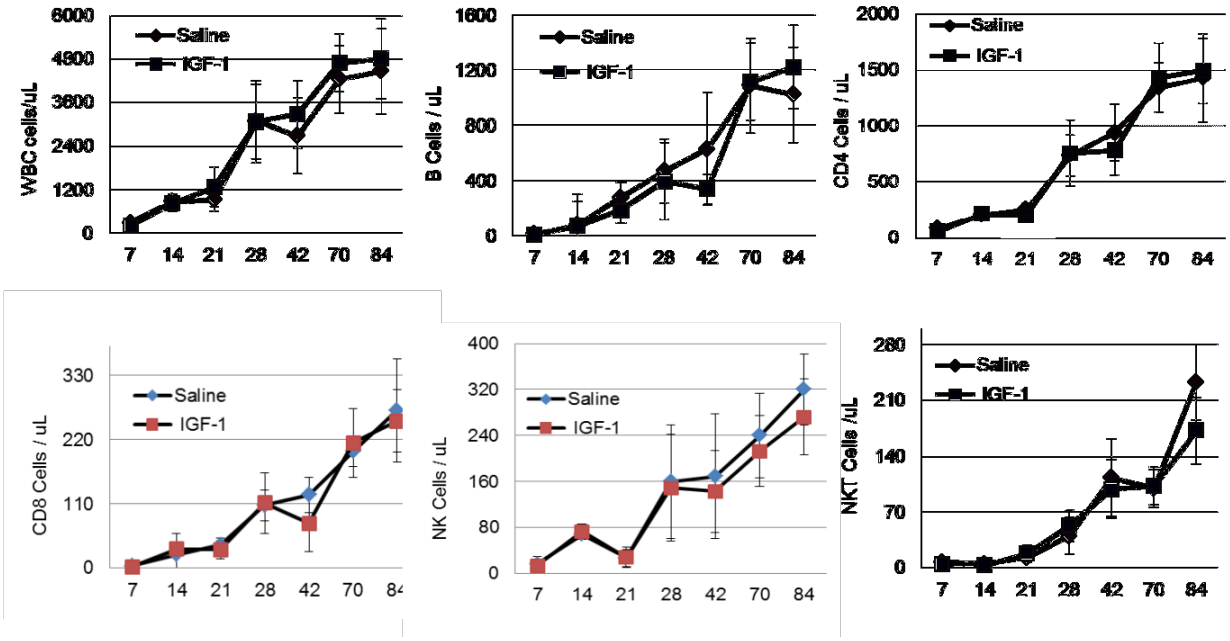

Figure 3.15. Effects of IGF-1 on phenotypic immune reconstitution post irradiation

4) Other Achievements:

Nothing to report.

Project 4 - Genomic Sequencing and Stem Cell Lines (Dr. Dave)

Major Activities

a) Collection and processing of blood samples in the prospective cohort during the subacute post-radiation phase for planned genomic analyses.
b) Completion of exome sequencing proposed in Aim 1. This include method development for reliable mutation and expression identification from NHPs for which no standard methods currently exist.
c) Continued discussions with Duke and Wake Forest investigators on cross-project technical collaboration on cell collections, processing, and analysis.
d) Generation and analysis of RNAseq data from NHPs: We continue to improve the analytical approaches for gapped alignments in NHPs that is important to measure expression from the RNA sequencing reads while skipping the introns in the NHP reference genomes.
e) Development of deconvolution approaches to resolve different cell types in RNAseq performed on peripheral blood mononuclear cells obtained from NHPs.
f) Development of in vivo stem cell regeneration model that provides a functional approach to validation of genetic alterations. We performed ex vivo studies of iPS differentiation and are now developing in vivo approaches to overcome the limitations of the ex vivo approaches.
g) Monthly DOD Conference calls

MAJOR OBJECTIVES

There were two main goals of project 4. First, to define the genetic mutations and gene expression signatures induced by radiation. Second, define the molecular basis of immune deficiency and hematologic malignancies induced by radiation.

SIGNIFICANT RESULTS

Define genetic mutations induced by radiation (Aim #1)
In the past year, we continued to develop and have now finalized our methodologies for DNA whole exome sequencing n order to define the genetic mutations in rhesus macaques, we had to fully develop the methodologies for next generation sequencing and bioinformatics analysis. In the past year, we completed the development of methodologies for whole exome sequencing from rhesus macaque DNA and developed the methodology for transcriptome sequencing from rhesus macaque RNA.

Results/Key Outcomes

We have now performed DNA/RNA extraction on a total of 48 cases from 16 individuals before and at two time points after treatment with radiation. Of these, 13 individuals (N=39 cases) yielded sufficient amounts of starting DNA and RNA for sequencing.
All sequencing libraries were carefully quantified using Agilent Bioanalyzer. Representative sequencing library size-distribution plots for whole exome sequencing (Figure 4.1A) and RNA sequencing (Figure 4.1B) are shown. We also preliminarily sequenced on library on the Illumina Miseq and confirmed even distribution of A/C/G/T bases with very few called as unknown (N).
These results indicate that our library construction process has worked well.

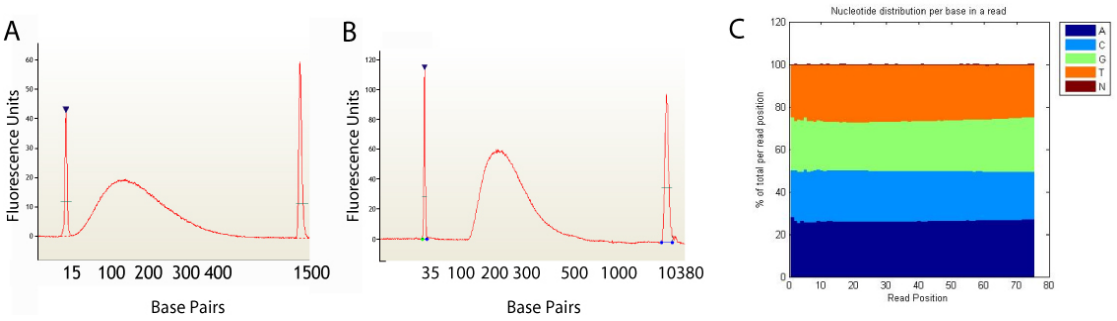

Figure 4.1: Quantification of bar codes for different RNAseq library reads.

RNA-seq Preprocessing

RNA sequence reads were trimmed (Bolger et al., 2014) to remove any remaining Illumina adapter sequences and aligned to the hg19 transcriptome using STAR, a spliced read aligner which allows for sequencing reads to span multiple exons. On average, we were able to align 90% of the sequencing reads for each sample to the reference rhesus macaque genome. Transcript quantification at the gene and transcript level was performed (Li et al., 2011) and expression values were then FPKM normalized, to account for differences in library depth across samples.

Principal Components Analysis (PCA) was used to identify major patterns of gene expression across samples. Data were log2 normalized prior and sequencing reads filtered to a minimum of 10 million prior to PCA to minimize the effects of outlier genes/samples. These results are shown in Figure 4.2 with samples with fewer than 10 million filtered sequencing reads not shown for uniformity of analysis. The yellow dots represent expression patterns from individuals prior to radiation and purple dots are samples from the late (8 weeks) time point. The green dots represent samples the early time point (4 weeks) post-radiation. Thus, the pre-radiation and late (8 weeks) post-radiation time points are more closely related to each other than the time point 4 weeks post-radiation. As shown in PCA plot, the dominant axis of separation (PC1, 26.5% VE) present in the data separates mid-timepoint samples (4 weeks post radiation) from baseline and late-timepoint samples (8 weeks post radiation). A secondary axis of separation (PC2, 17.2% VE) does not appear to separate across groups in a meaningful way.

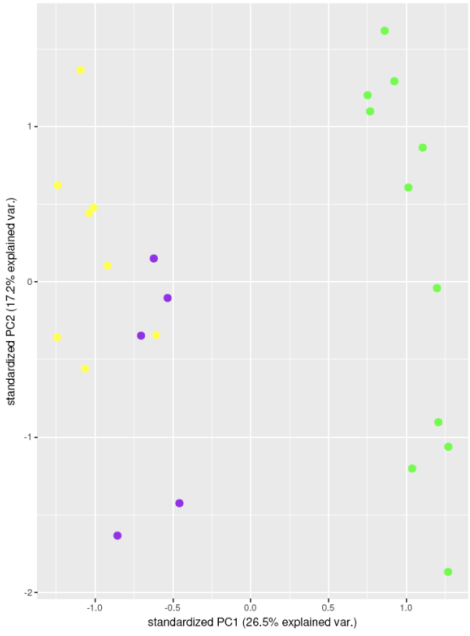

Figure 4.2: Principal components analysis of RNAseq data before and after radiation exposure in rhesus macaques.

This raised two major possibilities as to the origins of the large changes in gene expression at the middle time point. First, it was possible that radiation affected many cell types in a predictable, radiation-dependent fashion, changing different cellular and signaling pathways. Second, it was possible that radiation predominantly affected one or more cell types that resulted in changes in observed gene expression arising from an admixture of cell types.

To evaluate the effects of radiation on different cell types, we examined (Newman et al., 2015) the proportions of leukocyte subpopulations in each sample from the normalized expression data. We used validated gene expression profiles to define signatures associated with each

lymphocyte type and used 100 permutations to estimate the significance of results. ANOVA tests were then used to determine whether the percentage of each cell type differed across treatment groups.

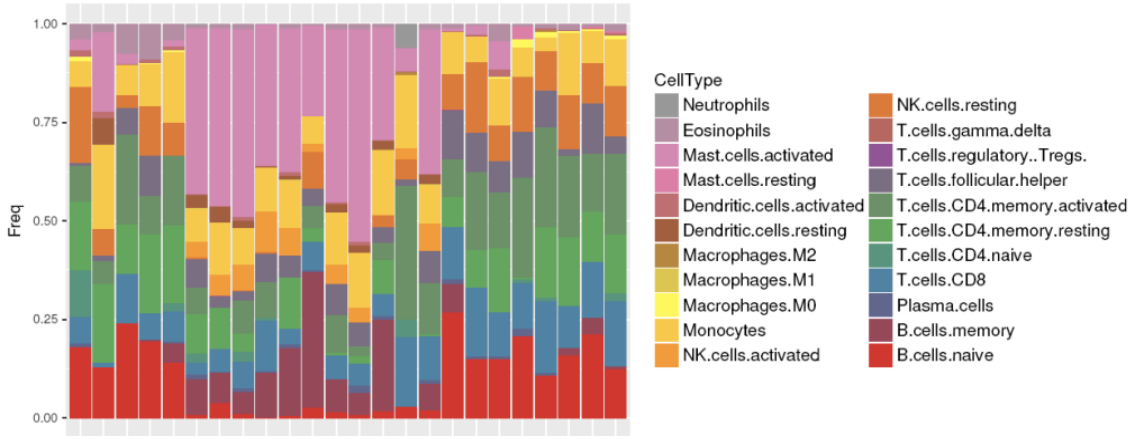

Figure 4.3: Deconvolution analysis of immune populations after exposure to radiation.

Early analysis indicates a large increase ($p < 0.05$) in the proportion of activated mast cells in mid-timepoint samples relative to baseline and late-timepoint samples. We also found that baseline and late-timepoint samples had significantly higher levels of naïve B-cells whereas mid-timepoint samples had significantly higher levels of memory B-cells. There were far fewer significant differences in the proportion of immune cell types between baseline and late-timepoint samples, suggesting the broad effects of radiation on the immune system may be largely reversible in these samples.

Additional, ongoing analysis will help define the immune cell types that are affected by radiation and the degree to which particular cell types can recover after exposure to radiation.

Exome sequencing analysis
A critical question in post-radiation exposure and recovery is whether there are clonal effects that guide recovery, i.e. whether radiation leads to the development or selection of clones of hematopoietic stem cells that disproportionately contribute to hematopoiesis. We examined this question by performing whole exome sequencing on the same individuals subjected to RNAseq. We have DNA sequencing from each of the three time points for each individual.

The methods for high resolution comparisons across the rhesus macaque genome are still being developed. Our early results suggest that there are no clonal effects post radiation, i.e. there is no dominant clone being selected by radiation. We are continuing to analyze these data across individuals to examine whether such approaches will increase our power for detecting subclones.

Develop a stem-cell based model to generate immune B cells in vitro (AIM #2)
Given the potential multigenic nature of genetic variation and the emerging role for B cell receptor signaling and other immune functions, we proposed to differentiate stem cells from irradiated macaques (or human stem cells with the genetic modifications present in irradiated macaques) into B cells to better understand their function and the long-term effects of radiation on immune function.
We have previously developed the schema shown in Figure 4 below to differentiate B cells from stem cells.

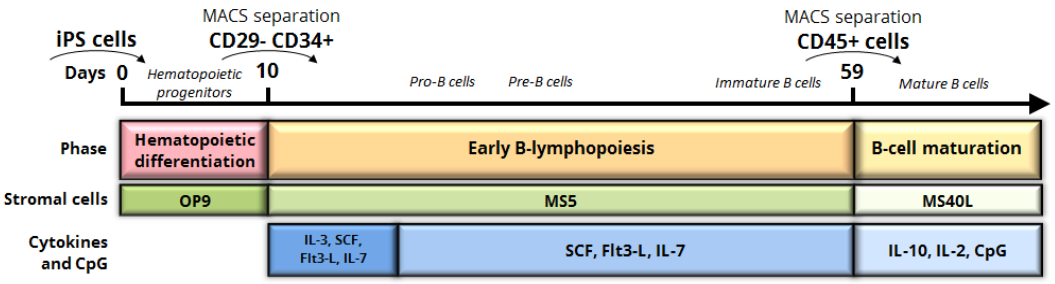

Figure 4.4: Schema for generating B lymphoid cells.

The yields of B cells from three consecutive experiments at at 90 days are shown below, and were on-average, less than 1%. Two additional experiments with new reagents yielded no measurable B cells.

Recognizing these critical limitations, we initiated experiments using a humanized mouse model that transplants human stem cells to regenerate intact and functional human immune cells into an immune compromised mouse to generate the preliminary data shown in Figure 4.5.

Generation of humanized mouse model:
We used the NOD,B6.SCIDIl2rγ$^{-/-}$kit$^{W41/W41}$ (NBSGW) mice as the base model to generate a humanized mouse. NBSGW mice are ideal for this type of project as they contain a polymorphism in the *Sirpa* gene providing for phagocytic tolerance of human cells, PRKDC^{scid} mutation and Il2rγ$^{-/-}$ mutations which lead to absence of T, B, and NK cells thus preventing xenoreactivity, and a c-kit mutation resulting in impairment of hematopoiesis of the mouse cells, providing a competitive advantage to transplanted cells.We have comprehensively tested this system in experiments transplanting CD34+ hematopoietic stem cells from anonymized human donors.

Figure 4.5 shows our success with generation complete human lineages in mice by implanting as few as 125,000 human stem cells. As shown, we were able to identify substantial numbers of human derived circulating B cells (CD19+), T cells (CD3+) and myeloid cells (CD33+) in blood, spleen, bone marrow and thymus of the mice. Importantly, these humanized mice have an essentially unlimited supply of B and T cells for future experiments.
Interestingly, stem cell dosage did not have a large impact on the recovery of mature human immune cells by the time mice were 10 weeks old. Thus, we can reliably generate humanized mouse models by injecting human stem cells. Human embryonic stem cell lines can be used as an alternative starting point for stem cells.
This model will be used as a starting point for comparing the immune phenotypes in cells arising from different genetic alterations observed from the DEARE data generated in Aim #1.
We have formal approval to this new mouse model to be included as part of Aim 2.

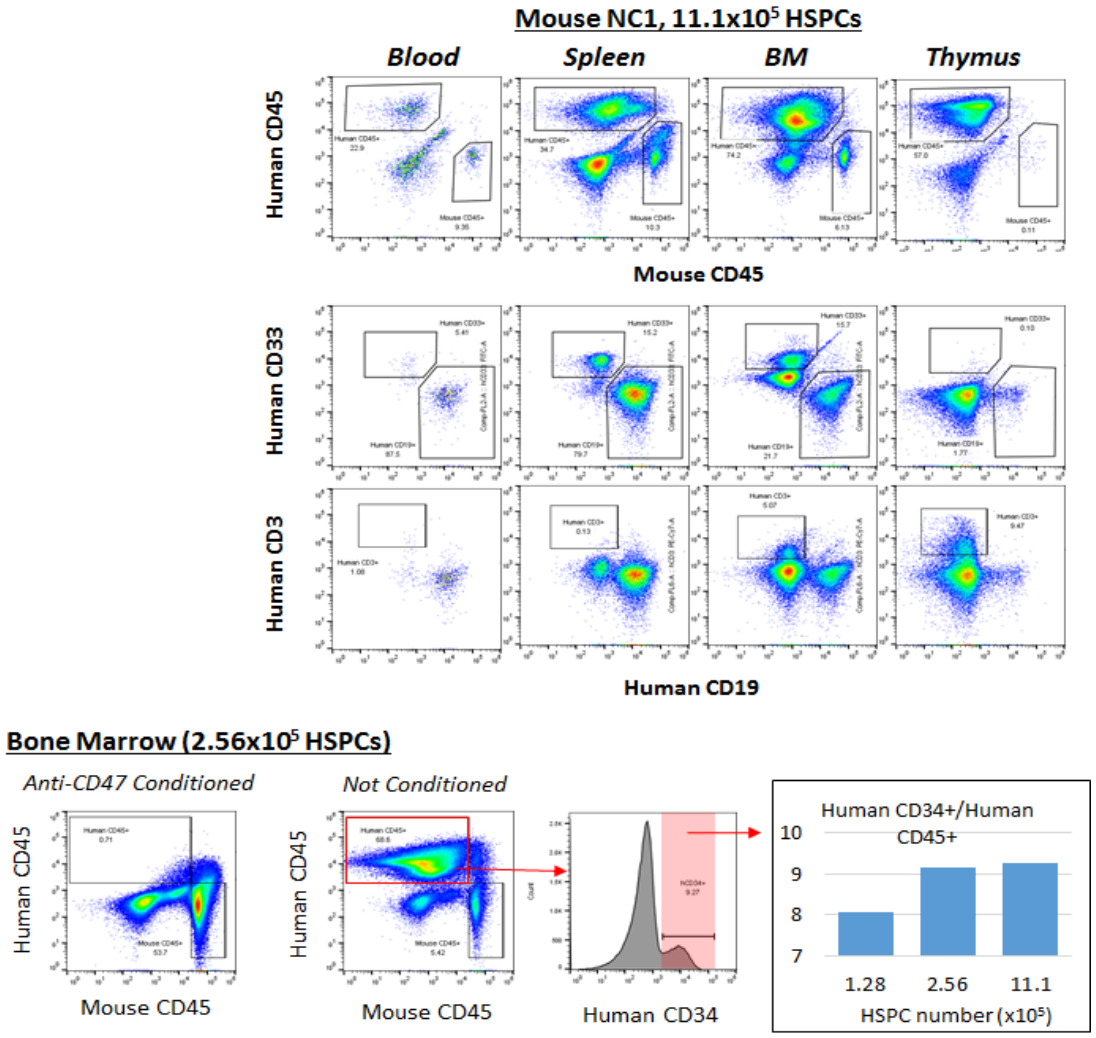

Figure 4.5: Presence of B cells (CD19+), T cells (CD3+), and myeloid cells (CD33+) in blood, spleen, bone marrow, and thymus at 10 weeks post transplantation.

Apart from the change in model that utilizes an in vivo rather than in vitro approach, Aim 2 is unchanged. We will evaluate B and T cell activation, Ig secretion, and cell proliferation and compare in the context of genetic alterations data from Aim 1. B and T cells will be isolated by flow sorting and the rate of proliferation over 2 weeks will be measured by a BrdU assay. Cell viability will be measured by activated caspase 3 and 7-AAD staining.

We will then use shRNAs and/or CRISPR constructs targeting the gene of interest to knock down its expression in stem cells prior to generating the humanized mouse model from those cells. We will then perform identical experiments as above to characterize B and T cell function in that context. These experiments will establish the viability of the humanized mouse model as a nearly unlimited source of cells for experimentation and for modeling the effects of other genes identified in Aim #1.

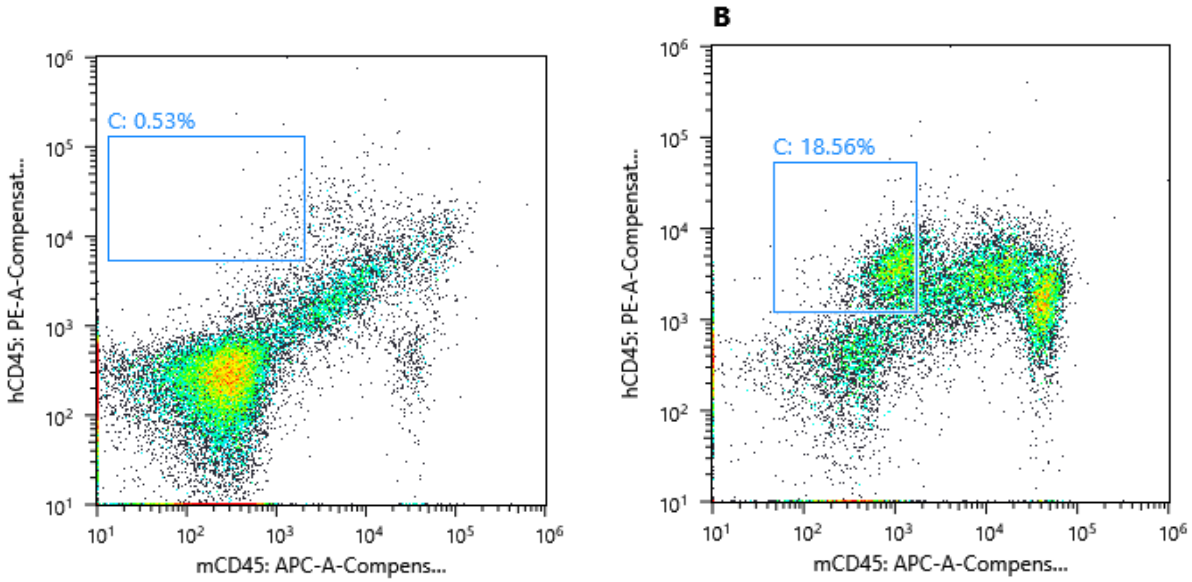

Figure 4.6: Presence of human cells (hCD45) vs. mouse cells (mCD45) in spleen and liver respectively.

Interestingly, we have also found differences in engraftment rates in different hematopoietic tissues, with significantly higher engraftment (18.56% compared to 0.53%) in liver compared to spleen. These experiments inform our approaches going forward, where we will plan to sample multiple tissues for engraftment and ensure that the cell types being sampled are of human origin.

Expected Outcomes: At the end of this revised Aim, we will have generated and characterized hematopoietic lineages from genetic alterations observed in DEARE macaques and demonstrated the feasibility of our approach for modeling complex genetic interactions.

4) Other Achievements

Nothing to report.

What opportunities for training and professional development has the project provided?

Overall (PI Cline)

1. All investigators participated in an in-depth discussion of this program's goals and objectives on July 18, 2018 hosted by the PI's team at Wake Forest School of Medicine.
2. Investigators (Drs Cline and Register) and Fellows (Drs. Andrews, Michalson and Thakur) attended the 2018 Radiation Research Society meeting, which provided education and professional development.

Project 1 Diabetes (PI Kavanagh).

We have two students working on this project. Dr. Bacarella is a laboratory animal medicine resident (veterinarian) and Allistaire Ruggerio is a graduate student who together are evaluating the structural and functional changes related to adipose tissue in irradiated animals.

Project 2 RIHD (PI Register)

1. Image Analysis Software, Cardiac Ultrasound, Cardiac MRI, and RNAseq analysis
2. Tissues: VisioPharm, programmable, development of semi-automated programs to assess myocardial, arterial, and other histologic and immunohistochemical phenotypes including fibrosis and atherosclerosis. Some of this work has resulted in training experience for undergraduate students (Ben Williams, University of South Carolina Sophomore), Matthew O'Brien, Wake Forest University Junior-Senior, Abby Anderson, Wake Forest University Junior).
3. Cardiac Ultrasound: CV ultrasound applications and measurements has been optimized through interactions with Cardiology faculty and vendors, establishing new SOPs for prospective cohort.
4. Cardiac MRI: Register and Michalson have ongoing interactive discussion sessions with Clinical Cardiology staff and faculty
5. Gene expression analyses: Ongoing practical experience in the utilization of Bioconductor and R to conduct RNAseq and other genomics analyses and in the the use of Ingenuity Pathways software.

Project 3 (Immune Recovery) PI Sempowski and Chen

Dr. Xinhua Che is a visiting scholar with Dr. Chen at Duke. He has performed work in *in vitro* flow cytometric studies and was mentored by Dr. Chen.

Project 4 (Genomics) PI Dave

Nothing to Report

How were the results disseminated to communities of interest?

Overall Program (Cline)

All investigators presented data at the CDMRP Focused Program Milestones meeting on Nov 16-17, 2017 in Washington, DC.

Study design, public health and strategic relevance, and opportunities for collaboration were presented by Dr. Cline at several venues:

- The NIH/NIAID Centers for Medical Countermeasures Against Radiation (Annual meeting 12/5-6/17, and reports during monthly teleconferences with the CMCR Steering Committee)
- Invited Speaker, Cornell University, April 10, 2018, Ithaca NY.
- The Conference on Normal Tissue Radiation Effects and Countermeasures triennial meeting, May 14, 2018, Little Rock, AR
- Wake Forest Cores Symposium, Keynote Speaker, June 7, 2018
- The annual Radiation Countermeasures Center of Research Excellence (RadCCORE) meeting at Duke University, Durham, NC, July 13, 2018
- Department of Pathology, Grand Rounds, Sept 5, 2018
- Comparative Medicine Research Strategy Meetings, Wake Forest School of Medicine
- Department of Radiation Oncology, Wake Forest School of Medicine
- Wake Forest Animal Resources Program Continuing Education Seminar

Project 1 - Diabetes (Kavanagh)

- Comparative Medicine Research Strategy Meetings
- Presentation at the CDMRP Milestones Meeting
- Dr. Kavanagh attended a DOD-focused research retreat (18th of July 2018) to share research progress and discuss collaborative opportunities.
- The radiation monkey model was also described in an invited oral presentation at American Association of Aging annual scientific meeting in Philadelphia, PA (27th June 2018) where many discussions with outside collaborators were initiated.

Project 2 - Radiation-Induced Heart Disease (Register)

- Comparative Medicine Research Strategy Meetings
- Presentations at the annual Radiation Research meeting, at the annual RADCCORE meeting at Duke University, in Departmental and other seminars at Wake Forest, along with special presentations and discussion with visiting Cardiologists from other institutions.
- Presentation at the CDMRP Milestones Meeting.

Project 3 - (Immune Recovery) (Sempowski/Chen)

- Presentations at the annual Radiation Research meeting, at the annual RADCCORE meeting at Duke University, and the CDMRP Milestones Meeting.

Project 4 - Genomics (Dave)

- Presentation at the CDMRP Milestones Meeting.

What do you plan to do during the next reporting period to accomplish the goals?
If this is the final report, state "Nothing to Report."

Describe briefly what you plan to do during the next reporting period to accomplish the goals and objectives.

Overall (PI Cline):

No Change from Statement of Work.

For all projects we anticipate continued local and national presentations of results at relevant scientific meetings, and publications of results in the peer-reviewed literature.

Project 1 (Diabetes, PI Kavanagh):

No Change from Statement of Work.

Project 2 (RIHD, PI Register):

No Change from Statement of Work.

During the next year, we will be:

1) Completing the 24-month post-radiation Cardiac MRI and echocardiographic imaging in the PRC
2) Immunohistochemical analysis of individual cell types and macrophage polarization in myocardium from deceased RSC and Control rhesus monkeys
3) We are characterizing the Collecting fasted blood samples from the PRC and the RSC
4) Continuing statistical analyses of the effects of radiation exposure on echocardiographic outcomes in the RSC
5) Continuing image analysis of cardiac MR images in the PRC
6) Statistical analysis of data collected to date from the cardiac MRI
7) Continuing plans for analysis of ECM and other biomarkers
8) Planning for MR assessments of the RSC
9) Ongoing molecular and cellular phenotyping of the monocytes in the PRC and the RSC (ancillary study funded through Center for Medical Countermeasures Program)
10) Submission of manuscript describing the effects of radiation on monocyte phenotypes

Project 3 (Immune Recovery, PI Sempowski/Chen):

1) Continue working with Wake Forest to receive regular blood draws from the long-term and prospective cohorts to perform phenotypic and molecular analysis of T cell recovery post irradiation (Tasks 1.1-1.4).
2) Perform the experiment to determine the roles of thymopoiesis and peripheral expansion in overall T cell recovery in a second radiation injury model (Task 2.3).
3) Start to perform the experiment to determine the effect of HGH on phenotypic T cell reconstitution (Task 3.1)

4) Continue to perform the experiment to determine the effect of IGF-1 on phenotypic T cell reconstitution (Task 4.1)

Project 4 (Genomics, PI Dave): Abstracts/meetings and manuscripts as studies mature.

In the coming year, we will scale up the sequencing. We will sequence 30 whole exomes and 30 transcriptomes to preliminarily define the genomic signatures associated with DEARE. For AIM #2, we will repeat our experiments to generate B cells from stem cells. We will increase the exposure to CD40L, which is known to stimulate B cell production and differentiation. We will carefully monitor these experiments for increased efficiency of lymphoid differentiation.

4. **IMPACT:** Describe distinctive contributions, major accomplishments, innovations, successes, or any change in practice or behavior that has come about as a result of the project relative to:

What was the impact on the development of the principal discipline(s) of the project?

Overall (PI Cline):

The findings produced by this program have increased awareness of the multi-systemic nature of late radiation effects, in the domains of radiation biology, radiation mitigation, and medical management of affected individuals post-exposure.

Project 1 (Diabetes, PI Kavanagh):

The work described in this report indicates that radiation exposure produces systemic dysregulation of metabolic functions, leading to altered protein signaling pathways, impaired tissue blood flow and deranged metabolic activity, including overt diabetes mellitus.

Project 2 (Radiation Induced Heart Disease, PI Register):

The project has produced new data on the effects of radiation on myocardial fibrosis and cardiac function, producing evidence of restrictive cardiomyopathy, and on monocyte polarization, implicating monocyte driven pathways in promoting pro-fibrotic pathways.

Project 3 (Immune Recovery, PI Sempowski/Chen):

Our findings indicate that total body irradiation produces both acute and long-term impairment of immune function.

Project 4 (Genomics, PI Dave): Abstracts/meetings and manuscripts as studies mature.

Nothing to report. Future elucidation of the underlying genomic, transcriptomic and functional consequences is anticipated as Project 4 (Genomics/Dave) progresses into the analytic phase in year 3.

What was the impact on other disciplines?

The impact of our findings is broad, and spans multiple groups and agencies working to understand and mitigate delayed effects of acute radiation exposure, including the DOD, BARDA, NIH, FDA, and NASA. We anticipate that our data will influence response strategies, biomarker development, and re-adjustment of regulatory assumptions regarding the modeling, prediction and treatment of the long-term consequences described herein.

What was the impact on technology transfer?

Nothing to Report

What was the impact on society beyond science and technology?

Nothing to Report

5. CHANGES/PROBLEMS: The Project Director/Principal Investigator (PD/PI) is reminded that the recipient organization is required to obtain prior written approval from the awarding agency Grants Officer whenever there are significant changes in the project or its direction. If not previously reported in writing, provide the following additional information or state, "Nothing to Report," if applicable:

Changes in approach and reasons for change

Overall (Cline, PI):

Nothing to report.

Project 1 (Diabetes, PI Kavanagh):

Nothing to report.

Project 2 (RIHD, PI Register):

Nothing to Report.

Project 3 (Immune Recovery, PI Sempowski/Chen):

Due to the unexpected observations that T and B cell numbers are able to recover back to normal level post-irradiation, we have postponed the experiment using a second radiation injury model. This delay has affected this milestone. We are still waiting to determine whether this is also true in NHPs. If it is true, we will focus our efforts on phenotypic recovery in the first two months post-irradiation, TCR repertoire, and functional changes. If the results in NHPs are different, we will focus our efforts on studies using NHP model.

Unfortunately, we could not demonstrate that IGF-1 was able to promote immune reconstitution post-irradiation. Even though we have previously demonstrated that HGH is able to facilitate T cell recovery post-irradiation in both mouse and NHP models when administered immediately after irradiation, there is also a possibility that we may not be able to observe the same effect when administered weeks after irradiation as proposed in the original proposal because T cells can recover back to normal without any treatment. If this occurs, we may propose to test other candidates such as IL-7 and IL-15 as proposed in the Alternative approach section in the original proposal.

We will obtain prior written approval if significant changes in objectives and scope will need to be made.

Project 4 (Genomic, PI Dave):

The expected yield of B cells from differentiation experiments was roughly 10%. However, the actual yields that we observed at 90 days was on-average, less than 1%. Repeating these experiments did with new reagents did not improve the yields of B cells. Therefore, we have change the approach to differentiate the stems cells in vivo using a Nod-Scid-gamma (NSG) mouse model. This new approach was scientifically approved in 2017 and received ACURO approval 8/1/18.

Actual or anticipated problems or delays and actions or plans to resolve them

Overall:

Nothing to report.

Project 1 (Diabetes, PI Kavanagh):

Nothing to report.

Project 2 (Radiation Induced Heart Disease, PI Register)

Nothing to Report.

Project 3 (Immune Recovery, PI Sempowski/Chen)

Nothing to Report.

Project 4 - Genomic Sequencing and Stem Cell Lines (PI Dave)

Nothing to Report.

Changes that had a significant impact on expenditures

Overall/Primate Core

Nothing to report.

Project 1 (Diabetes, PI Kavanagh)

Nothing to report.

Project 2 (Radiation-Induced Heart Disease, PI Register)

Nothing to report.

Project 3 (Immune Recovery, PI Sempowski/Chen)

The mouse experiment using a second radiation injury model was postponed. The funds allocated for this experiment have thus not been spent yet.

Project 4 (Genomics, PI Dave)

Nothing to report.

Significant changes in use or care of human subjects, vertebrate animals, biohazards, and/or select agents

Significant changes in use or care of human subjects

Not applicable - No human subjects

Significant changes in use or care of vertebrate animals

Overview

1. For the Nonhuman Primate Prospective Cohort Protocol PR141508.01, the Wake Forest Protocol number A15-083 was renewed & replaced by Protocol A18-062, without a major change in scope, as part of institutional policy (all Wake Forest protocols are replaced and renumbered at 3 year intervals)..

2. For PR141508.2 (Project 2 mice): This protocol was replaced with Wake Forest IACUC protocol number #A18-024 (all Wake Forest protocols are replaced and renumbered at 3 year intervals). The ACURO Assigned Number is unchanged as PR141508.02. The protocol remains identical to that of #A15-068 but the animal number is reduced on account of the work that has already been completed.

3. A new protocol PR141508.05 (Duke IACUC protocol number A010-17-01) was instituted in support of mouse studies in Project 4.

4. A variety of minor protocol amendments were made throughout the year, reflecting personnel changes and minor procedural changes.

Specific details are given below.

Core Primate Studies (Cline)

Protocol 1 of 5 total: [ACURO Assigned Number]: PR141508.04

Title: Radiation Countermeasures Long Term Response of Rhesus Macaques

Target required for statistical significance: 120

Target approved for statistical significance: 132

Submitted to and Approved by:

Wake Forest IACUC (9/17/13; WF IACUC no. A13-117; Renewed/reapproved 6/23/16 as A16-094 as part of routine full renewal every 3 years as per IACUC policy)

Amendments since our prior annual report are shown below.

Protocol # A16-094 - Radiation Survivor Core

Amendment No.	Reason for amendment	Wake Forest IACUC approval date	ACURO approval date
12	Personnel change request	11/27/17	11/30/17
13	Addition of procedures and experimental drugs to the protocol to evaluate effects of metabolic disease.	2/9/18	2/23/18
14	Adding Jovanna Perez - Handling, blood collection, experimental measurements, sedation, anesthesia, monitoring, environmental enrichment, supportive care, euthanasia, Necropsy; Removing Ryne DeBo and Katherine Fanning	2/8/2018	2/14/2018
15	Amendment withdrawn	NA	NA
16	Added the option of performing CT scans on a mobile unit (our primary CT was down).	4/2/18	4/3/18
17	Added Carson Sakamoto	4/11/18	4/20/18
18	Addition of lidocaine and bupivicaine for local anesthesia for muscle and fat biopsies Addition of Pneumovax vaccination to test antibody responses	4/16/2018	4/20/2018
19	Personnel replacement; removed Chrystal Bragg, added Masha Block	5/22/18	5/29/18
20	Added summer students (Rachel Amato, Aleaya Bowie, Jayda Bussey-Spratling, Ethan Bloomer, Jessica Kendziorski. Removed Kelly Mahoney	6/18/18	6/19/18
21	Mistaken duplicate of amendment 20	Withdrawn	Withdrawn
22	Personnel; addition of McKinley Williams-McDowell	6/21/18	6/25/18
23	Personnel; addition of William Carrera	8/7/18	8/7/18
24	Addition of Skin Biopsies ; changing name of procedure to 'tissue biopsy'	8/22/18	8/28/18
25	Personnel; addition of Jacob Cleary. Removing summer students Rachel Amato, Aleaya Bowie, Jayda Bussey-Spratling, Ethan Bloomer, Jessica Kendziorski	8/17/18	8/27/18
26	Personnel; addition of Jovanna Perez, Margaret Greven and Jessica Weinstein	9/10/18	9/13/18
27	Updating animal housing buildings on Clarkson campus	10/1/18	10/5/18

Status

This long-term cohort is under study as planned.

Protocol 2 of 5 total [ACURO Assigned Number]: PR141508.01

Title: Prospective Radiation Cohort: Cardiac and Metabolic Studies

Target required for statistical significance: 20

Target approved for statistical significance: 28

Submitted To And Approved By:

Wake Forest IACUC (Protocol #A15-083, approved 7/6/15)

ACURO approval (9/3/15, ACURO no. PR141508.01)

Replaced by Protocol #A18-062 as part of routine full renewal every 3 years as per IACUC policy

Amendments since last annual progress report.

A15-083

Amendment No.	Reason for amendment	Wake Forest IACUC approval date	ACURO approval date
25	Adding Laura Cousins- animal handling, blood collection, euthanasia; Removing- Ryne Debo, Cathirine Si, Adam Jesinowski, Clarissa Hernandez, Rebecca Marcus, Jordyn Whitfield, Katie Fanning	1/19/2018	1/23/2018
26	Added option of CT scans using a mobile unit since primary unit was down	4/4/18	4/13/18
27	Added Chrissy Sherill	4/23/18	4/30/18
28	Removed Chrystal Bragg, added Masha Block	5/22/28	5/29/18
29	Added summer students Rachel Amato, Aleaya Bowie, Jayda Bussey-Spratling, Ethan Bloomer, Jessica Kendziorski. Removing Kelly Mahoney	6/18/18	6/19/18

A18-062

Amendment No.	Reason for amendment	Wake Forest IACUC approval date	ACURO approval date
1	Personnel; addition of McKinley Williams-McDowell:	7/10/18	10/3/18
2	Addition of local analgesia to monkey biopsy sites to reduce pain and potential for the individual to irritate incision sites, and inclusion of the option to do an insulin tolerance test, in addition to glucose tolerance testing, so as to more directly stimulate tissues of interest	8/10/18	10/3/18
3	Personnel; addition of Nicole Bacarella:	8/15/18	10/3/18
4	adding Skin Biopsies ; changing name to 'tissue biopsie'	8/22/18	10/3/18
5	Personnel; addition of Jacob Cleary.	8/17/18	10/3/18
6	Personnel; addition of Jovanna Perez	9/14/18	10/3/18
7	Modification of the number of animals transferred from the old protocol A15-083 to the replacement protocol A18-062 from 28 to 16 to reflect number of animals transferred (excluding blood donors no longer needed for this study)	9/20/18	10/3/18
8	Addition of a literature search for alternatives to surgical removal for foreign metallic material	9/27/18	10/3/18

Status

Studies continue as planned; animals are now 2 years out from irradiation.

Protocol 3 of 5 total: ACURO Assigned Number PR141508.02

Title: **Prospective Evaluation of Diabetogenesis Post-irradiation in Mice (Metabolic Effects of Radiation Exposure)**

Target required for statistical significance: 200

Target approved for statistical significance: 200

Submitted To And Approved By:

Wake Forest IACUC (A15-068, Approved 5/20/15

ACURO (PR141508.02, Approved 10/19/15)

Amendments since prior annual report:

This protocol was replaced with Wake Forest IACUC protocol number #A18-024 (all Wake Forest protocols are replaced and renumbered at 3 year intervals). The ACURO Assigned Number is unchanged as PR141508.02. The protocol remains identical to that of #A15-068 but the animal number is reduced on account of the work that has already been completed.

Amendment No.	Reason for amendment	Wake Forest IACUC approval date	ACURO approval date
12	Personnel change; addition of student	10/9/17	10/13/17
13	Addition of walking speed and rotarod testing to the behavioral measures	10/11/17	10/16/17

Status:

Approved studies are in progress.

Protocol 4 of 5 total:

Protocol [ACURO Assigned Number]: PR141508.03

Title: IMMUNOLOGICAL INJURY AND RECOVERY AFTER RADIATION INJURY

Target required for statistical significance: 4184 mice

Target approved for statistical significance: 4184 mice

Submitted to and approved by:

Duke IACUC (A142-15-05, Approved on 5/28/15)

ACURO (PR141508.03, Approved on 3/3/16)

Amendments:

Amendment No.	Reason for amendment	Duke IACUC approval date	ACURO approval date
1	Personnel change	9/12/17	10/13/17

Status: Approved, work in progress.

Protocol 5 of 5 total:

Protocol [ACURO Assigned Number]: PR141508.05

Title: HUMANIZED MOUSE MODEL OF LYMPHOMA BY ENGRAFTMENT OF CRISPR-CAS9-EDITED HUMAN HEMATOPOIETIC CELLS

Target required for statistical significance: 4184 mice

Target approved for statistical significance: 4184 mice

Submitted to and approved by:

Duke IACUC (A010-17-01, Approved on 1/27/18)

ACURO (PR141508.05, Approved on 8/1/18)

Amendments: None

Status: Approved, work in progress.

Significant changes in use of biohazards and/or select agents

Nothing to report

6. PRODUCTS: List any products resulting from the project during the reporting period. If there is nothing to report under a particular item, state "Nothing to Report."

- **Publications, conference papers, and presentations**

Report only the major publication(s) resulting from the work under this award.

Journal publications.

Overall (Cline): Nothing to Report.

Project 1 (Diabetes, PI Kavanagh):

Nothing to Report.

Papers described above are in preparation and will be published in the upcoming year.

Project 2 (Radiation-Induced Heart Disease, PI Register):

David L. Caudell, Kristofer T. Michalson, Rachel N. Andrews, William W. Snow, J. Daniel Bourland, Ryne J. DeBo, J. Mark Cline, Gregory D. Sempowski, Thomas C. Register. Transcriptional Profiling of Nonhuman Primate Lymphoid Organ Responses to Total Body Irradiation. (*Under revision for Radiation Research)*

DeBo RJ, Michalson KT, Lees CJ, Dugan GO, Hanbury DB, Caudell DL, Andrews RN, Vujaskovic Z, Batinic-Haberle I, Bourland JD, Cline JM, Register TC. SOD mimetic (MnTnHex-2-PyP5+) alters cardiovascular gene expression profiles in the absence of phenotypic improvement in NHP's following 10Gy irradiation to the thorax. *(In preparation)*

Kristofer T. Michalson, Andrew N. Macintyre, Gregory D. Sempowski, Gregory O. Dugan, J. Mark Cline, Thomas C. Register. Monocyte Polarization is Shifted Post-Irradiation in Male Rhesus Macaques. (*In preparation*)

Kristofer T. Michalson, Gregory O. Dugan, J. Mark Cline, Thomas C. Register. Cardiac Structural and Functional Characteristics in Long Term Rhesus Macaque Survivors of Ionizing Radiation Exposure. (*In preparation*)

Project 3 (Immune Recovery, PI Sempowski/Chen):

Xinhua Chen, Ying Huang, Yiqun Jiao, Xiaoli Nie, and Benny J. Chen. Division of Cellular Therapy/BMT, Duke University Medical Center, Durham, NC T cell reconstitution following ionizing irradiation
Abstract was presented in The 63rd Radiation Research Society Annual Meeting 2017
Federal support acknowledged

Project 4 (Genomics, PI Dave):

Reddy A, Zhang J, Davis NS, Moffitt AB, Love CL, Waldrop A, Leppa S, Pasanen A, Meriranta L, Karjalainen-Lindsberg ML, Nørgaard P, Pedersen M, Gang AO, Høgdall E, Heavican TB, Lone W, Iqbal J, Qin Q, Li G, Kim SY, Healy J, Richards KL, Fedoriw Y, Bernal-Mizrachi L, Koff

JL, Staton AD, Flowers CR, Paltiel O, Goldschmidt N, Calaminici M, Clear A, Gribben J, Nguyen E, Czader MB, Ondrejka SL, Collie A, Hsi ED, Tse E, Au-Yeung RKH, Kwong YL, Srivastava G, Choi WWL, Evens AM, Pilichowska M, Sengar M, Reddy N, Li S, Chadburn A, Gordon LI, Jaffe ES, Levy S, Rempel R, Tzeng T, Happ LE, Dave T, Rajagopalan D, Datta J, Dunson DB, Dave SS. Genetic and Functional Drivers of Diffuse Large B Cell Lymphoma. Cell. 2017 Oct 5;171(2):481-494.e15. doi: 10.1016/j.cell.2017.09.027. PubMed PMID: 28985567; PubMed Central PMCID: PMC5659841.
This paper utilized methods developed for this project, and was reported last year.
Federal Support was acknowledged.

Books or other non-periodical, one-time publications.

Overall (PI Cline)

Nothing to report.

Project 1 (Diabetes, PI Kavanagh)

Nothing to report.

Project 2 (Radiation Induced Heart Disease, PI Register):

Abstracts

Kristofer T. Michalson "Evaluation of monocyte polarization in long term non-human primate survivors of acute ionizing radiation exposure" Cardiovascular Sciences Center Dean's Research Symposium Poster Session, Wake Forest University School of Medicine, February, 21st, 2018

Kristofer T. Michalson "Effects of Total Body Irradiation on Echocardiographic Phenotypes in Male Rhesus Macaques".
Radiation Research Society Annual Meeting, October, 2017.
Federal support acknowledged

Kristofer T. Michalson "Evaluation of monocyte polarization in long term non-human primate survivors of acute ionizing radiation exposure"
Radiation Research Society Annual Meeting, October, 2017.
Federal support acknowledged

Ryne J. DeBo 2017 Radiation Research Editors' Award Lecture for the publication: *DeBo RJ, Lees CJ, Dugan GO, Caudell DL, Michalson KT, Hanbury DB, Kavanagh K, Cline JM, Register TC. "Late Effects of Total Body Gamma Irradiation on Cardiac Structure and Function in Male Rhesus Macaques."*
Radiation Research Society Scholars in Training Workshop, October 2017
Federal support acknowledged

Project 3 (Immune Recovery, PI Sempowski/Chen):

Xinhua Chen, Ying Huang, Yiqun Jiao, Xiaoli Nie, and Benny J. Chen.
T cell reconstitution following ionizing irradiation
Radiation Research Society Annual Meeting, October, 2017.
Federal support acknowledged

Project 4 (Genomics, PI Dave):

Nothing to report.

Other publications, conference papers, and presentations.

Overall: (PI Cline):

Rotating monthly presentations of project progress via WebEx to Progam Team.

Overview Presentation, Annual Retreat, Wake Forest School of Medicine, August 9th 2017. Federal Support was acknowledged.

Primate Radiation Survivor Core
J Mark Cline; John Olson; Greg Dugan; Rachel Andrews; Kylie Kavanagh; Daniel Bourland; David Hanbury; Ann Peiffer; Thomas Register; Ryne DeBo; David Caudell; Greg Sempowski and Nelson Chao
Centers for Medical Countermeasures against Radiation Annual Meeting, Rockville, MD, December 6-7, 2017
Federal Support was acknowledged.

Project 1 (Diabetes, PI Kavanagh):

Rotating monthly presentations of project progress via WebEx to Program Team.

Project 1 Presentation, Program Annual Retreat, Wake Forest School of Medicine, August 9th 2017. Federal Support was acknowledged.

Sherrill C and **Kavanagh K**. Comparison of Housing Conditions to Ameliorate Aggression in Male Mice. 69th American Association of Laboratory Animal Sciences National Meeting, Baltimore MD, 2018. Federal Support was acknowledged.

Dr. Kavanagh presented at an internal Wake Forest Cancer Center Symposia on the irradiated mouse model (16th March 2018) to stimulate discussion about aging and cancer synergy. Federal Support was acknowledged.

Project 2 (Radiation-Induced Heart Disease, PI Register):

Rotating monthly presentations of project progress via WebEx to Progam Team.

Project 3 Presentation, Program Annual Retreat, Wake Forest School of Medicine, August 9th 2017.
Federal Support was acknowledged.

Ryne J. DeBo 2017 Radiation Research Editors' Award Lecture for the publication: *DeBo RJ, Lees CJ, Dugan GO, Caudell DL, Michalson KT, Hanbury DB, Kavanagh K, Cline JM, Register TC. "Late Effects of Total Body Gamma Irradiation on Cardiac Structure and Function in Male Rhesus Macaques."* 2017 Radiation Research Society Scholars in Training Workshop, Cancun, Mexico, October 2017
Federal Support was acknowledged.

Project 3 (Immune Recovery, PI Sempowski/Chen):

Rotating monthly presentations of project progress via WebEx to Progam Team.

Project 3 Presentation, Program Annual Retreat, Wake Forest School of Medicine, August 9th 2017.
Federal Support was acknowledged.

Project 4 (Genomics, PI Dave):

Rotating monthly presentations of project progress via WebEx to Progam Team.

Project 4 Presentation, Program Annual Retreat, Wake Forest School of Medicine, August 9th 2017.
Federal Support was acknowledged.

- **Website(s) or other Internet site(s)**

Nothing to report

- **Technologies or techniques**

Nothing to report

- **Inventions, patent applications, and/or licenses**

Nothing to report

- **Other Products**

Overall (PI Cline):

Nothing to report.

Project 1 (Diabetes, PI Kavanagh):

Nothing to report.

Project 2 (Radiation Induced Heart Disease, PI Register):

Grant applications submitted and funded

Pathology Internal Pilot Grant Application (funded) $25,000 Thomas C. Register, PhD. “In Situ Molecular Profiling of Myocardial Responses to Ionizing Radiation in Rhesus Macaques” July 2017-June 2018

RADCCORE Pilot Grant Application (funded)
5U19AI067773-13 (Register-PI) $100,000 (Year 1) 08/01/17-07/31/18
“Monocyte Polarization in Acute and Delayed Responses to Total Body Irradiation in Nonhuman Primates” This project is designed to determine the effect of total body irradiation on circulating monocyte polarization and transcriptional programming in the acute and chronic phases post irradiation, and to explore relationships of these monocyte phenotypes with radiation induced conditions in male rhesus macaques.

Grant applications submitted and pending

Peer Reviewed Medical Research Program for a Discovery Award ($200,000, pending)
“Effects of Ionizing Radiation (IR) on Myocardial DNA Methylation Profiles in Relation to Cardiomyopathy in a Nonhuman Primate Model”. (Register-PI 2018)

Project 3 (Immune Recovery, PI Sempowski/Chen):

Nothing to report.

Project 4 (Genomics, PI Dave):

Nothing to report.

7. PARTICIPANTS & OTHER COLLABORATING ORGANIZATIONS

What individuals have worked on the project?

Core Primate Studies (Cline)

Name:	J. Mark Cline *No change*
Name:	Daniel Bourland *No change*
Name:	David Caudell *No change*
Name:	Janet Tooze *No change*
Name:	Jean Gardin *No change*
Name:	Matt Dwyer *No change*
Name:	Russell O'Donnell *No change*
Name:	Chrystal Bragg *Left lab for another position; replaced by McKinley Williams-McDowell*
Name:	McKinley Williams-McDowell *Replacement hire for Chrystal Bragg*
Name:	Renae Hall *No change*
Name:	Patricia Warren *No change*

Project 1 – Diabetes (Kavanagh)

Name:	Kylie Kavanagh *No change*
Name:	Ashley Davis *No change*

Name: Christina Sherrill
No change

Name: Cristina Furdui
No change

Name: Xiaofei Chen
No change

Project 2 – Radiation/Heart Disease (Register)

Name: Thomas Register
No change

Name: Sujethra Vasu
No change

Name: Craig Hamilton
No change

Name: Kris Michalson, DVM
No change

Name: James Bottoms
No change

Name: Maryanne Post
No change

Name: Ryan DeBo, PhD
Project Role: Research Fellow
Researcher Identifier: N/A
Nearest person month worked: Effort removed 12/27/17
Contribution to Project: Dr. DeBo took a position at another Institution

Name: Matthew O'Brien
Project Role: Undergraduate Student Project
Nearest person month worked: 1
Contribution to Project: Mr. O'Brien participated in the digitization (scanning) and image analysis of histologically stained sections of coronary arteries from the RSC.

Name: Ben Williams
Project Role: Undergraduate Student Project
Nearest person month worked: 1
Contribution to Project: Mr. Williams participated in the digitization (scanning) and image analysis of histologically stained sections of heart and coronary arteries from the RSC.

Project 3 – Immune Recovery (Chen & Sempowski)

Name:	Benny Chen No change
Name:	Gregory Sempowski No change
Name:	Lesslee Arwood No change
Name: Project Role: Researcher Identifier (e.g. ORCID ID): Nearest person month worked: Contribution to Project:	Xinhua Chen Visiting Scholar N/A 6 Dr. Chen has performed flow cytometry experiments and data analyses
Name:	Laura Hale No change
Name:	Yiqun Jiao No change
Name:	Andrew Macintyre, PhD No Change
Name: Project Role: Researcher Identifier (e.g. ORCID ID): Nearest person month worked: Contribution to Project	Xiaoli Nie Visiting Scholar N/A 1 Dr. Nie has performed flow cytometry experiments and data analyses
Name: Project Role: Researcher Identifier (e.g. ORCID ID): Nearest person month worked: Contribution to Project:	Brittany Sanders, MS Research Analyst N/A 1 NEW HIRE. Ms Sanders performs tissue processing And flow cytometry experiments.

Project 4 - Genomic Sequencing and Stem Cell Lines (Duke Consortium – Dave)

Name:	Sandeep Dave No change
Name:	Anupama Reddy No change

Name: Cassandra Love
No change

Name: Guojie Li
No change

Has there been a change in the active other support of the PD/PI(s) or senior/key personnel since the last reporting period?

J. Mark Cline (PI)

Changes in *Current* Support as reported in the original application:

Nothing to report

Daniel Bourland (Co-Investigator)

Changes in *Current* Support as reported since the last reporting period (annual report):

Project Title: Evaluation of a Red Duroc Porcine Model to Address Cutaneous Radiation Injury in Black (Type III/VI) Skin
Change: New award

Project Title: Biodosimetry for Irradiated Blood
Change: New award

David Caudell (Co-Investigator)

Changes in *Current* Support as reported since the last reporting period (annual report):

Project Title: Determining the Effects of Duavee on Pain and Lesion Volume In a Non-human primate Model of Naturally Occurring Endometriosis
Change: Project Complete

Christina Furdui (Co-Investigator)

Changes in *Current* Support as reported since the last reporting period (annual report):

Project: New Oxidation-Sensing Probes to Evaluate Mitochondrial Dysfunction in Lung Injury
Change: New Award

Project: Redox Biology and Medicine Training Program
Change: New Award

Project: Human Peroxiredoxin 3: A Novel Target for the Treatment of Mesothelioma
Change: New Award

Project: Bioenergetic and Epigenetic Reprogramming by Obesity in Sepsis
Change: New Award

Kylie Kavanagh (Co-Investigator)

Changes in *Current* Support as reported since the last reporting period (annual report):

Project Title: Age-Related Changes in Intestinal Function and Sarcopenia in Monkeys
Change: Project Complete

Project Title: Copper is a Host Effector in Protection Against Urinary Tract Infection
Change: New award

Project Title: Assessment of ARCUS Nuclease Driven Gene Editing Following Lipid Nanoparticle
Change: New award

Project Title: Assessment of the Pharmacological Effects of TAK-XXX in Obese Female Cynomolgus Monkeys
Change: New award

Thomas Register (Project 3 PI)

Changes in *Current* Support as reported in the original application:

Project Title: Monocyte Polarization in Acute and Delayed Responses to Totla Body Irradiation
Change: Project Complete

Project Title: Effects of Western & Mediterranean Diets on Metabolic & Neuropathologic Risk Factors for Alzheimer's Disease in Non-human Primates
Change: New award

Janet Tooze (Co-Investigator)

Changes in *Current* Support as reported since the last reporting period (annual report):

No changes to report

Greg Sempowski (Project 3 Co-PI - Duke)

Changes in *Current* Support as reported since the last reporting period (annual report):

No changes to report

Benny Chen (Project 3 Co-PI - Duke)

Changes in *Current* Support as reported since the last reporting period (annual report):

No changes to report

Sandeep Dave (Project 4 PI - Duke)

Changes in *Current* Support as reported since the last reporting period (annual report):

No changes to report

What other organizations were involved as partners?

Nothing to report

8. SPECIAL REPORTING REQUIREMENTS

COLLABORATIVE AWARDS: For collaborative awards, independent reports are required from BOTH the Initiating PI and the Collaborating/Partnering PI. A duplicative report is acceptable; however, tasks shall be clearly marked with the responsible PI and research site. A report shall be submitted to **https://ers.amedd.army.mil** for each unique award.

Not Applicable

QUAD CHARTS: If applicable, the Quad Chart (available on https://www.usamraa.army.mil) should be updated and submitted with attachments.

See page 105

9. APPENDICES:

Attach all appendices that contain information that supplements, clarifies or supports the text. Examples include original copies of journal articles, reprints of manuscripts and abstracts, a curriculum vitae, patent applications, study questionnaires, and surveys, etc.

Attachments:

1 Recent Program-Related Abstracts

2 Quad Chart

Radiation Research Society Annual Meeting, October, 2017

(PS3-51) Evaluation of monocyte polarization in long term non-human survivors of acute ionizing radiation exposure

Kristofer T. Michalson, DVM1; Andrew N. MacIntyre, PhD2; Ryne J. DeBo, PhD1;
Gregory D. Sempowski, PhD2; J Mark. Cline, DVM, PhD, DACVP1; and Thomas C. Register1
Wake Forest School of Medicine, Winston Salem, NC1 and Duke University, Durham, NC2

Radiation induced fibrosis (RIF) is an incompletely understood, multi-organ, chronic adverse effect of ionizing radiation. Monocyte-macrophages may play a key role in the pathogenesis of RIF. Monocytes can become programmed into classical, intermediate, or non-classical phenotypes. Classical monocytes are linked to pro-inflammatory responses, while intermediate monocytes have been linked to profibrotic signaling and systemic pathologic fibrotic disorders. The role of classical and intermediate monocytes in RIF is currently unclear. We evaluated the effects of prior total body irradiation (TBI) on monocyte polarization in male rhesus macaques. Subjects were 25 non-irradiated controls (9.63 ± 0.90 years old) and 67 irradiated macaques (8.69 ± 0.50 years old) exposed to a single dose of TBI (6.81 ± 0.12 Gy) at 4.25 ± 0.25 years old and were 1.72 to 11.3 years post-irradiation (mean interval 4.44 ± 0.41 years). Classical (CD14++, CD16-) and intermediate (CD14++, CD16+) monocyte percentages were quantified from gated total monocytes using flow cytometry. Total monocytes were not influenced by time since irradiation or dose. Additionally, proportions of classical and intermediate monocyte subsets did not differ by dose. However, the monocyte fractions obtained from monkeys 1-2 years post-irradiation had higher classical and intermediate monocyte percentages (15.08 ± 3.41%, 2.01 ± 0.36%) relative to controls (3.58 ± 1.10%, 1.02 ± 0.27%), and to monocytes 2-3 years (6.80 ± 2.31%, 1.23 ± 0.38%) and 3-5 years (5.63 ± 1.97%, 0.84 ± 0.17%) post-irradiation (ANOVA, $p < 0.05$). These data suggest that post-radiation recovery phenotypes of circulating monocytes may be initially shifted towards classical and intermediate pathways, later tapering towards more normal proportions. Prospective studies evaluating monocytemacrophage polarization and co-localization with organ fibrosis are needed to confirm and extend these data. Ultimately, monocytes may shape the inflammatory and fibrotic response in RIF and monocyte programming presents a novel target opportunity for preventative therapies.
Supported by NIH/NIAID U19 AI67798, NIH T32 OD010957, and DOD W81XWH-15-1-0574

Radiation Research Society Annual Meeting, October, 2017

(PS8-31) Effects of total body irradiation on echocardiographic phenotypes in male rhesus macaques

Kristopher Michalson, DVM; Greg Dugan, DVM; Ryne J. DeBo, MS, PhD; Dalane Kitzman, MD; J MarkCline, DVM, PhD; Thomas C. Register, PhD Wake Forest School of Medicine, Winston-Salem, NC

Radiation induced heart disease is a serious delayed effect of acute radiation exposure (DEARE). The effects of total body irradiation on the heart are being evaluated longitudinally in a cohort of male rhesus macaques. Subjects are young adult (ages 6-8 years) male rhesus monkeys randomized to receive no radiation (Control, n=6) or 4 Gy total body irradiation (TBI, n=10) with longitudinal assessments of cardiac structure and function using echocardiography and Cardiac Magnetic Resonance Imaging (CMRI). Echocardiographic data from baseline and 20 week follow-up examinations are presented here. There were no significant differences between groups in any of the baseline echocardiographic measures of CV structure or function. At 20 weeks post TBI, no significant changes over time or differences between groups were observed in chamber diameters, fractional shortening, ejection fraction, cardiac output, aorta/left atrium ratio. Mitral annular tissue velocity parameters (e', a', or E/e', or e'/a') did not appear to change over time or differ by group. Early left ventricular diastolic filling velocity (E) was unchanged over time and there was no difference between groups. However, irradiated monkeys showed a significant increase in the late filling velocity (A) across the mitral valve ($p<0.05$ vs baseline) which differed from controls at 20 weeks ($p<0.01$), and the E/A ratio showed a non-significant trend ($p=0.12$) towards reduction, potentially indicative of impairment of LV relaxation. Color flow doppler echo indicated mitral regurgitation in one of the irradiated monkeys which was evident at 20 weeks post TBI but not at baseline. These preliminary results, ongoing evaluations of CMRI data, and planned evaluations of key biomarkers should provide useful insights into early stage intermediate phases in the development of RIHD phenotypes.

Radiation Research Society Annual Meeting, October, 2017

(PS3-24) T cell reconstitution following ionizing irradiation

Xinhua Chen; Ying Huang; Yiqun Jiao; Xiaoli Nie; Benny J. Chen Duke University Medical Center, Durham, NC

The immune system is one of the most sensitive organs to ionizing radiation. Among all the immune cells, the lack of T cells is one of the most problematic given that they are rapidly depleted by the irradiation, and there is no replacement therapy. In this study, we examined how T cells were reconstituted following different doses of total body irradiation. 8- 12 weeks old C57BL/6 mice were irradiated with 2 Gy, 5 Gy, and 7 Gy (sublethal). Age-matched non-irradiated mice were included as a control. Absolute numbers of total T cells (CD3+) and T cell subsets were followed in peripheral blood at different time points after irradiation by flow cytometry. T cells dropped rapidly in all irradiated groups at day 3 after irradiation. Recovery of T cells was noted at day +14. T cell recovery was radiation dosedependent at least up to day +28. Even though they were still lower than those in the non-irradiated age-matched controls, T cell numbers were similar among different radiation dose groups after day +42. By day +84, the numbers of T cells in all irradiated groups were not significantly different from those in the non-irradiated control group despite the means were around 20% less. The recovery of total CD4 and CD8 T cells followed a very similar pattern as that of total T cells. Similar results were obtained for both CD4+ and CD8+ naive, central memory, and effector memory T cells. Similar observations were also made in spleen. Since T cells are produced in thymus, we next studied the effect of radiation on thymopoiesis after irradiation. Similar to peripheral T cells, total thymocytes dropped rapidly in irradiated mice in a radiation dose-dependent manner at day +3. Thymocytes in the 2Gy group recovered rapidly, with total thymocyte number recovered to the pre-irradiation level by day +14. It took 84 days for thymocytes to recover to the pre-irradiation levels in the mice irradiated at 5 Gy. In the 7 Gy group, total thymocytes had not recovered to normal when examined at day +84. Double positive thymocytes (CD4+CD8+) dropped significantly in all irradiated mice at day +3, but recovered back to normal as early as 14 days after irradiation in all groups. These data demonstrate that peripheral T cells are able to recover back to normal level after irradiation. However, thympopoiesis may be impaired long-term following sublethal irradiation.

Radiation Research Society Annual Meeting, October, 2017

(PS3-51) Evaluation of monocyte polarization in long term non-human survivors of acute ionizing radiation exposure

Kristofer T. Michalson, DVM1; Andrew N. MacIntyre, PhD2; Ryne J. DeBo, PhD1; Gregory D. Sempowski, PhD2; J Mark. Cline, DVM, PhD, DACVP1; and Thomas C. Register1 Wake Forest School of Medicine, Winston Salem, NC1 and Duke University, Durham, NC2

Radiation induced fibrosis (RIF) is an incompletely understood, multi-organ, chronic adverse effect of ionizing radiation. Monocyte-macrophages may play a key role in the pathogenesis of RIF. Monocytes can become programmed into classical, intermediate, or non-classical phenotypes. Classical monocytes are linked to pro-inflammatory responses, while intermediate monocytes have been linked to profibrotic signaling and systemic pathologic fibrotic disorders. The role of classical and intermediate monocytes in RIF is currently unclear. We evaluated the effects of prior total body irradiation (TBI) on monocyte polarization in male rhesus macaques. Subjects were 25 non-irradiated controls (9.63 ± 0.90 years old) and 67 irradiated macaques (8.69 ± 0.50 years old) exposed to a single dose of TBI (6.81 ± 0.12 Gy) at 4.25 ± 0.25 years old and were 1.72 to 11.3 years post-irradiation (mean interval 4.44 ± 0.41 years). Classical (CD14++, CD16-) and intermediate (CD14++, CD16+) monocyte percentages were quantified from gated total monocytes using flow cytometry. Total monocytes were not influenced by time since irradiation or dose. Additionally, proportions of classical and intermediate monocyte subsets did not differ by dose. However, the monocyte fractions obtained from monkeys 1-2 years post-irradiation had higher classical and intermediate monocyte percentages (15.08 ± 3.41%, 2.01 ± 0.36%) relative to controls (3.58 ± 1.10%, 1.02 ± 0.27%), and to monocytes 2-3 years (6.80 ± 2.31%, 1.23 ± 0.38%) and 3-5 years (5.63 ± 1.97%, 0.84 ± 0.17%) post-irradiation (ANOVA, $p < 0.05$). These data suggest that post-radiation recoveryphenotypes of circulating monocytes may be initially shifted towards classical and intermediate pathways, later tapering towards more normal proportions. Prospective studies evaluating monocyte macrophage polarization and co-localization with organ fibrosis are needed to confirm and extend these data. Ultimately, monocytes may shape the inflammatory and fibrotic response in RIF and monocyte programming presents a novel target opportunity for preventative therapies. Supported by NIH/NIAID U19 AI67798, NIH T32 OD010957, and DOD W81XWH-15-1-0574

CONTREC 2018

Delayed Effects of Acute Radiation Exposure on Normal Tissues: Insights from Nonhuman Primate Studies

J. Mark Cline D.V.M., Ph.D., DACVP[1], Greg Dugan D.V.M.[1], Rachel Andrews D.V.M.[1], Kylie Kavanagh B.Sc., V.M.S., M.V.S., M.P.H.[1], Daniel Bourland Ph.D.[1], David Hanbury Ph.D.[1], Ann M. Peiffer Ph.D.[1], Thomas Register Ph.D.[1], Ryne DeBo Ph.D.,[1] Kris Michalson, D.V.M., David Caudell D.V.M., Ph.D.[1], John Olson M.S., Benny Chen M.D., Gregory Sempowski Ph.D., and Nelson Chao M.D. [2]
Wake Forest School of Medicine, Winston-Salem, NC[1] and Duke University Medical Center, Durham, NC[2]

Introduction: Acute responses to radiation injury are the focus of most emergency medical response and mitigation efforts, but the major burden of radiation injury lies in delayed effects. These late and usually long-term effects of exposure on normal healthy tissues include cellular, molecular, and metabolic changes leading to organ dysfunction and failure; fibrosis; and neoplasia.

Methods: We present here the long-term adverse effects of single-dose whole-body exposures at 3.5-8.5 Gy in over 100 rhesus monkeys exposed at a median age of 4 years and observed for up to 13 years, in comparison to 38 non-irradiated controls. Some animals were exposed prior to puberty (<3.5 years of age), and the remainder as young adults (up to 10 years of age). Observations included an annual cycle clinical examinations, imaging (whole body CT and brain MRI), cognitive testing, hematology, clinical chemistry, and for those animals dying under observation, necropsy and histopathology.

Results: Major disease processes identified to date include (1) type II diabetes mellitus, sometimes with islet hyperplasia, amyloidosis, and increased peripheral insulin resistance; (2) myocardial fibrosis and reduced left ventricular diameter consistent with loss of myocardial elasticity; (3) immune compromise manifested as impaired vaccine responses, skin and wound infections, bronchopneumonia, pericarditis, and sepsis; (4) chronic pulmonary disease including pneumonitis, fibrosis, and epithelial dysplasia; (5) neoplasms including sarcomas, hematopoietic, epithelial, and neuroendocrine types; (6) early and later incipient focal MRI-detected brain lesions; (7) renal impairment, and (8) elevated circulating markers of inflammation and microbial translocation. Other stereotypical radiation effects (gonadal atrophy, cataracts) were predictably seen. Multiple disorders in the same animal were common, with diabetes being the most common co-morbid condition.

Conclusions: Our growing body of data indicates that a substantial burden of disease is present in long-term survivor non-human primates, including complex patterns of co-morbidity; metabolic and cardiac disease; injury of “high-dose” tissues such as brain at lower doses than anticipated; immunosuppression and inflammation; and pathologies including both loss and fibrous replacement of functional tissue, and cytoproliferative disorders including neoplasms. Comorbidities are often present in a given animal, necessitating an integrative approach.

Supported by NIH/NIAID U19 AI67798, NIH T32 OD010957, and DOD/CDMRP W81XWH-15-1-0574.

Radiation Research Society Annual Meeting, September 2018

Monocyte polarization in acute and delayed responses to total body irradiation in male rhesus monkeys

Kristofer T. Michalson, Andrew N. Macintyre, Gregory D. Sempowski, Gregory O. Dugan, J. Mark Cline, Thomas C. Register

Radiation induced fibrosis (RIF) is a debilitating, multi-organ, long term adverse effect of ionizing radiation exposure. Monocytes, as critical components of the innate immune system, may play a key role in the pathogenesis of RIF. Monocytes are classified as classical, intermediate, or non-classical phenotypes based upon their surface markers and other characteristics. Classical monocytes are linked to pro-inflammatory ("M1") macrophage responses, while intermediate and non-classical monocytes have been linked to pro-fibrotic ("M2") macrophage signaling and systemic pathologic fibrotic disorders. Monocyte polarization and individual phenotypic responses to TBI in relation to RIF is currently unclear.

We evaluated the effects of prior total body irradiation (TBI) on monocyte polarization in young adult (5.5 ± 0.4 yrs) male rhesus macaques. Subjects were 6 non-irradiated controls and 10 irradiated macaques exposed to a single dose of 4 Gy TBI. Total monocytes and monocyte subsets were quantified at baseline and regular intervals after irradiation from whole blood. Classical (CD14++, CD16-), intermediate (CD14++, CD16+), and non-classical (CD14+, CD16++) monocytes were sorted by FACS from positively selected CD14+ monocytes isolated from peripheral blood mononuclear cells before, 6 and 14 months after irradiation. Total monocytes were acutely depleted by TBI ($p<0.05$), but returned to baseline levels 28 days after irradiation and were not significantly different from controls thereafter. At 6 months post irradiation, monocyte polarization shifted towards lower classical (92% to 86%) and higher intermediate (7% to 12%) and non-classical monocyte subsets (0.6% to 2%) (ANOVA $p<0.01$) compared to baseline, with patterns returning to baseline by 14 months. No change in monocyte subsets was observed in the control animals. These data indicate that post-irradiation, circulating monocytes initially shifted towards intermediate and non-classical phenotypes before recovering towards normal, suggesting that monocyte programming may present a novel target opportunity for therapies to inhibit or prevent RIF.

Supported by NIH grants NIAID U19 AI067773 and U19 AI67798, R01 HL122393, T32 OD010957, and DOD W81XWH-15-1-0574

Long Term Follow-up of the Late Effects of Acute Radiation Exposure in Primates
Proposal Log Number PR141508

PI: J Mark Cline, DVM, PhD **Org:** Wake Forest Health Sciences **Award Amount:** $9,999,998

Study/Product Aim(s)

To study delayed effects of acute radiation exposure (DEARE) with a focus on our newly-described radiation-induced pathologies, through phenotypic and mechanistic studies, including:
1.Type 2 diabetes mellitus
2.Radiation-induced heart disease (RIHD)
3.Chronic immune impairment with restriction of the antigenic response repertoire; and
4.Radiation-specific genomic signatures underlying 1-3.

Approach

We will use unique nonhuman primate (NHP) resources, including a pre-existing long-term (10+ year) radiation-exposed survivor cohort and development of a prospective cohort allowing baseline pre-exposure assessments and 4 years of follow-up. Complementary immune, metabolic, and interventional studies to be done in mice. Priority will be given to pathways and strategies with high potential for translation to human exposures and outcomes.

Projects / Platforms	Project 1: Diabetes — Body composition, Redox Injury	Project 2: Radiation Induced Heart Disease — Cardiac function and biomarkers	Project 3: Immune Recovery — Thymopoiesis and immune function	Project 4: Genomic signatures — Genomic basis for observed injury
NHP Survivor cohort Long-term outcomes	✓	✓	✓	✓
NHP Prospective Cohort Baseline-controlled	✓	✓	✓	✓
Mouse Studies and Treatments	✓		✓	
NHP Study Archives Tncluding Treatments		✓		

Figure 1. Schematic overview of the matrix relationship between populations of irradiated animals studied and investigative approaches used.

Accomplishments: NHP and mouse irradiation studies under way. Data collection and analysis in progress. Methods development in progress for some novel outcomes, as planned. Initial publications and abstracts, data presented at national meetings.

Timeline and Cost

Activities / CY	15	16	17	18	19	20
Oversight/Core Primate Studies						
Proj 1 Diabetes						
Proj 2 Radiation/Heart Disease						
Proj 3 Immune Recovery						
Proj 4 Genomic sequencing and stem cell lines						
Estimated Budget ($K) *Based on budget period 09/30/15 – 09/29/20. Budget period in ( ) after dollar amounts.*	1	2	3	4	5	
	$2,150,541 (1)			$1,979,721 (4)		
	$1,975,657 (2)			$1,863,796 (5)		
	$2,030,283 (3)					

Updated: October 29, 2018

Goals/Milestones

CY15 Goal – Program/Project "Kickoff"
- ☑ Regulatory approvals, establishment of admin structure, scheduling/ planning
- ☑ Animal acquisition and NHP quarantine & sampling/analysis, both cohorts

CY16 Goals – Prospective NHP studies begin, preliminary results presented nationally
- ☑ Exome sequencing and IPSCs from NHP studies (in progress)
- ☑ Irradiation of NHP prospective cohort and post-irradiation sampling/analysis for cardiac, redox, tissue composition, RNA profiling, and biomarker studies; presentation of early results (in progress)
- ☑ Mouse radiation studies: classic model

CY17 Goal – Continued NHP and mouse studies
- ☑ Mouse radiation studies: secondary model development
- ☑ Continued analysis of NHP composition/biomarkers as above based on preliminary results; presentation of data

CY18 Goal – Continued NHP and mouse studies
- ☐ Mouse intervention study of HGH and IGF-1 (phenotypic)
- ☐ Continued analysis of NHP composition/biomarkers as above; publication
- ☐ Preliminary cell lineage data from NHPs presented nationally

CY19 Goal – Continued NHP and mouse studies
- ☐ Mouse intervention study of HGH and IGF-1 (functional)
- ☐ Primate studies as above continue; publication

CY20 Goal – Analysis and publication of results
- ☐ Mouse intervention study of HGH and IGF-1 (mechanistic)
- ☐ Necropsy of prospective cohort, analysis of terminal outcomes; publication

Comments/Challenges/ Issues/Concerns
- No changes to timeline at this time
- No changes in quarterly expenditures at this time

Budget Expenditure to Date

Projected Expenditure:
$2,150,541
GY 2015/2016
$1,975,657
GY 2017
$2,030,283
GY 2018